

University of Warwick institutional repository: <http://go.warwick.ac.uk/wrap>

A Thesis Submitted for the Degree of PhD at the University of Warwick

<http://go.warwick.ac.uk/wrap/35617>

This thesis is made available online and is protected by original copyright.

Please scroll down to view the document itself.

Please refer to the repository record for this item for information to help you to cite it. Our policy information is available from the repository home page.

Synthesis and characterisation of stereoregular cyclic poly(lactide)s

Matthew James Stanford, MChem(Hons)

A thesis submitted in partial fulfilment of the requirements for
the degree of Doctor of Philosophy in Chemistry

University of Warwick, Department of Chemistry

September 2010

Contents

Contents	ii
List of tables and figures	v
Acknowledgements	x
Publications	xi
Declaration	xii
Abstract	xiii
Abbreviations	xiv
Chapter 1: The synthesis of stereoregular, cyclic poly(lactide)	1
1.1 Introduction	2
1.2 Synthesis of stereoregular poly(lactide)	2
1.2.1 Anionic ROP	9
1.2.2 Coordination-insertion ROP	10
1.2.2.1 Tri- and tetra-dentate iminophenolato- and aminophenolato-(salen and salan) complexes	10
1.2.2.2 β -Diketiminato (BDI) complexes	19
1.2.2.3 Tetradentate amino(bis- and tris-phenolato) complexes	24
1.2.2.4 Miscellaneous ligands	28
1.2.3 Organocatalytic ROP	32
1.2.4 Conclusions and perspective	34
1.3 Cyclic polymers	35
1.3.1 Characterisation	36
1.3.2 Synthesis	38
1.3.2.1 Chain end reaction	39
1.3.2.2 Purification	42
1.3.2.3 Quantitative chain end conversion	43
1.3.2.4 Tethering	45
1.3.2.5 Intermediate examples	47
1.3.2.6 Catalyst cyclisation	49
1.3.2.7 Monomer controlled synthesis of cyclic polymers	56
1.3.2.8 Alternative routes	59
1.3.3 Complex architectures	60

1.3.4 Cyclic block copolymers	66
1.3.5 Properties/self assembly	68
1.3.6 Uses	73
1.4 References	75
Chapter 2: The one-pot synthesis of α,ω-chain end functional, stereoregular, poly(lactide)	85
2.1 Introduction	86
2.2 One pot α - and ω - chain end functionalisation	88
2.2.1 Aluminium salen/salan catalysts	88
2.2.2 Polymerisation and functionalisation procedure	91
2.2.3 Versatility of quench procedure	94
2.2.4 Telechelic and star shaped polymers	97
2.2.5 Synthesis of block copolymers	99
2.3 'Click' chemistry	107
2.3.1 Copper catalysed azide alkyne cycloaddition	107
2.3.2 Thiol-ene 'click' reaction	110
2.3.3 Thiol-ene 'click' chemistry on the ω - chain end	115
2.3.4 Telechelic and star shaped polymer	118
2.4 Conclusion	120
2.5 References	121
Chapter 3: The application of 'click' chemistry for the synthesis of cyclic poly(lactide)	126
3.1 Introduction	127
3.2 Cyclic poly(lactide)	129
3.2.1 Synthesis	129
3.2.2 Characterisation	131
3.2.3 Versatility of cyclisation	134
3.2.4 Organic catalysis of cyclic poly(lactide)	136
3.3 Cleavable cyclic poly(lactide)	138
3.3.1 Dithiol bridge cleavage	138
3.3.2 Diels-Alder bridge cleavage	145
3.4 Single point functionality	150
3.4.1 Benzyl functionality	150

3.4.2 ‘Click’ functionality	152
3.4.2.1 Sequential ‘click’ reactions	152
3.4.2.2 Cyclic polymer with ‘click’ functionality	158
3.5 Conclusion	162
3.6 References	163
Chapter 4: Complex architectures of cyclic poly(lactide)s	165
4.1 Introduction	166
4.2 One pot synthesis of multi-cyclic polymers	168
4.2.1 Cyclisations using trimethylolpropane tris-(3-mercaptopropionate)	169
4.2.2 Cyclisations using pentaerythritol tetrakis-(3-mercaptopropionate)	172
4.3 Cyclic PLA with a ‘click’ functional handle	176
4.4 Cyclic PLA as a macroinitiator	179
4.5 PEG- <i>b</i> -PLA block copolymers	183
4.5.1 PEG bearing thiol synthesis	183
4.5.2 PEG to cyclic PLA grafting	185
4.6 Poly(BLG- <i>co</i> -Cys) conjugations	188
4.7 Conclusions	193
4.8 References	194
Chapter 5: Experimental	196
5.1 General experimental details	197
5.1.1 Gel permeation chromatography (GPC)	198
5.1.2 Nuclear magnetic resonance (NMR)	198
5.1.3 Matrix-assisted laser desorption and ionisation time-of-flight mass spectrometry (MALDI-ToF MS)	199
5.1.4 Other techniques	199
5.2 Experimental details for chapter 2	200
5.3 Experimental details for chapter 3	205
5.4 Experimental details for chapter 4	210
5.5 References	212

List of tables and figures

Chapter 1

Figure 1.2.1 Microstructures for the stereocontrolled ROP of lactide from a) <i>rac</i> -lactide and b) <i>meso</i> -lactide.	4
Figure 1.2.2 Homonuclear decoupled proton NMR showing the different tetrads and their respective positions for <i>rac</i> -lactide a) ^1H NMR, b) ^{13}C NMR, and <i>meso</i> -lactide c) ^1H NMR, and d) ^{13}C NMR.	6
Figure 1.2.1.1 Anionic Polymerisation of lactide.	9
Figure 1.2.2.1 General mechanism for Coordination insertion ROP.	11
Figure 1.2.2.2 Tetradentate (imino- and amino-phenolato)aluminium complexes for stereoselective lactide ROP.	13
Figure 1.2.2.3 Tetradentate Schiff base aluminium complexes for stereoselective lactide ROP.	17
Figure 1.2.2.4 Tridentate Schiff base metal complexes for stereoselective lactide ROP.	19
Figure 1.2.2.5 (β -Diketiminato) metal complexes for catalysis of stereospecific lactide ROP	21
Figure 1.2.2.6 Tetradentate amino(bis- and tris- amino)phenolato complexes for stereospecific lactide ROP.	24
Figure 1.2.2.7 Miscellaneous catalysts for the stereocontrolled ROP of lactide.	30
Figure 1.2.3.1 Organic catalysts for the stereoregular ROP of lactide	32
Figure 1.3.2.1 Cyclisation of poly(ethylene glycol) using dichloromethane.	40
Figure 1.3.2.2 Thiol bridged reversible cycle formation	41
Figure 1.3.2.3 Copper catalysed ‘click’ chemistry in the synthesis of cyclic poly(styrene)	44
Figure 1.3.2.4 Electrostatic self-assembly in the synthesis of cyclic poly(tetrahydrofuran)	46
Figure 1.3.2.5 Zwitterionic polymerisation for the synthesis of cyclic poly(lactide)	48
Figure 1.3.2.6 Modified Grubbs catalyst allowing for ring opening metathesis polymerisation leading to cyclic poly(ethylene)	50
Figure 1.3.2.7 G2 dendritic monomer applied to REMP	51
Figure 1.3.2.8 Synthesis of cyclic poly(methyl acrylate)	54
Figure 1.3.2.9 Cyclic thiocarbamate initiator for the synthesis of poly(sulphide)s	55
Figure 1.3.2.10 Cyclic poly(oxyepichlorohydrin oxymaloyl) from the acid catalysed polymerisation of maleic anhydride and epichlorohydrin.	57
Figure 1.3.2.11 Thermodynamically controlled ring cross over polymerisation	58

Figure 1.3.2.12 Cyclic poly(ferrocenylsilane) oligomers.	59
Figure 1.3.3.1 Tin based catalysis in the synthesis of cyclic poly(caprolactone)	61
Figure 1.3.3.2 Synthesis of a doubly fused tricyclic loop poly(tetrahydrofuran).	63
Figure 1.3.3.3 Poly(caprolactone)- <i>b</i> -poly(styrene) block copolymers with complex architectures.	65
Figure 1.3.4.1 Tin catalyst in the synthesis of cyclic block copolymers of caprolactone and lactide.	67
Figure 1.3.5.1 Cyclisation of poly(N-isopropylacrylamide)	70
Figure 1.3.5.2 Self assembly of cyclic brushes with a poly(chloroethylvinyl ether) backbone	71
Figure 1.3.5.3 Self-assembly of cyclic poly(ethylene oxide) with a hexa- <i>p</i> -phenylene block	72
Chapter 2	
Figure 2.2.1.1 Aluminum complexes applied as catalysts in the stereoregular ROP of lactide	90
Figure 2.2.2.1 <i>In situ</i> functionalisation of the ω -chain end of heterotactic PLA. i) IPA, n eq. <i>rac</i> -lactide, toluene, 70 °C, 4 h; ii) <i>in situ</i> addition of anthranoyl chloride, 70 °C, 120 h.	92
Figure 2.2.2.2 ¹ H NMR spectrum of anthracene functionalised PLA (heterotactic stereochemistry not shown)	93
Figure 2.2.2.3 MALDI ToF MS of anthracene functionalised PLA	94
Table 2.1 Preparation of ω -chain end functionalised poly(lactide)s	96
Figure 2.2.4.1 Acid chlorides that were applied for ω -chain end functionalisation. a) acetyl chloride; b) hexanoyl chloride; c) benzoyl chloride; d) isonicotinoyl chloride; e) anthranoyl chloride; f) isobutyroyl chloride; g) pivaloyl chloride; h) hexynoyl chloride	95
Figure 2.2.4.2 Synthesis of telechelic and star shaped PLA	97
Figure 2.2.4.3 MALDI-ToF MS analysis of 1,1,1-tris(hydroxymethyl)ethane initiated star polymer	98
Figure 2.2.5.1 Synthesis of acid chloride functional polyethylene glycol. i) 50 eq. succinyl chloride, CH ₂ Cl ₂ , 16 h, and subsequent application in the quenching of PLA polymerisation.	99
Figure 2.2.5.2 Synthesis of RAFT chain transfer agent acid chloride, 4 .	100
Figure 2.2.5.3 MALDI-ToF MS analysis of RAFT chain transfer agent bearing PLA	101
Figure 2.2.5.4 Synthesis and subsequent degradation of PLA- <i>b</i> -PS. i) IPA, <i>rac</i> -lactide, toluene, 70 °C, 2 h; ii) 4 , toluene, 70 °C, 120 h; iii) Styrene, toluene, 16 h, 120 °C; iv) TBD, MeOH, toluene, 16 h, 110 °C.	102
Figure 2.2.5.5 Synthesis of RAFT chain transfer agent bearing telechelic and star shaped PLA. i) 1 , <i>rac</i> -lactide, toluene, 70 °C, 2 h; ii) 4 , toluene, 70 °C, 120 h	103

Table 2.2. GPC data for synthesis and degradation of multi-arm stars	104
Figure 2.2.5.6 GPC traces for a) 3-arm heterotactic PLA star-shaped polymer b) 3-arm (heterotacticPLA)- <i>b</i> -PS star-shaped polymer c) PS after degradation of poly(ester).	105
Table 2.3 Degradation conditions for ω - functional PLA	107
Figure 2.3.1.1 The application of CuAAC chemistry for chain end functionalisation. i) IPA, <i>rac</i> -lactide, toluene, 70 °C, 2 h; ii) hexynoyl chloride, toluene, 70 °C iii) azido triethylene glycol, CuI, NEt ₃ , THF, 25 °C, 7 days.	109
Figure 2.3.1.2 ¹ H NMR demonstrating ‘click’ conjugation with; azido triethylene glycol, CuI, TEA, THF, 7 days, RT (azido triethylene glycol (Integrals: resonance a = 20; b = 0.4))	110
Figure 2.3.2.1 Synthesis of alcohol bearing protected maleimide functionality, 5	112
Table 2.4 ‘Click’ conjugation of thiols to maleimide-functional PLAs	113
Figure 2.3.2.2 ¹ H NMR analysis demonstrating quantitative ‘click’ conjugation with thiophenol (Integrals: resonance a = 20; c = 2.4; d = 6.0)	114
Figure 2.3.2.3 MALDI –ToF MS analysis demonstrating complete conjugation of thiophenol to polymer chain end	115
Figure 2.3.3.1 Synthesis of maleimide functional acid chloride, 6	117
Figure 2.3.3.2 Synthesis of poly(lactide) bearing ω - chain end maleimide functionalisation. i) IPA, <i>rac</i> -lactide, toluene, 70 °C, 2 h; ii) toluene, 70 °C, 120 h; iii) heat; iv) thiophenol, NEt ₃ , RT, 2 h	118
Figure 2.3.4.1 Synthesis of maleimide bearing telechelic and star shaped PLA. i) 1 , <i>rac</i> -lactide, toluene, 70 °C, 2 h; ii) 6 , toluene, 70 °C, 120 h; iii) heat	119
Table 2.5 Click functionalisation of the PLA ω -chain end	120
Chapter 3	
Figure 3.2.1.1 Cyclisation of the stereoregular PLA. i) 5 , Al salen, toluene. 70 °C, 4 h; then in situ addition of 6 , 70 °C, 120 h; ii) Vacuum, 100 °C, 24 h; iii) 1eq. ethanedithiol, CH ₂ Cl ₂ , NEt ₃ , Na ₂ S ₂ O ₅	130
Figure 3.2.2.1 MALDI-ToF MS of (i) the linear and (ii) the cyclic polymer	132
Figure 3.2.2.2 ² H NMR of linear (top) and cyclic polymers (bottom) (Isotactic polymer used for simplicity)	133
Figure 3.2.2.3 GPC traces of polymer chain before, grey (left) and after, black (right) cyclisation.	134
Table 3.1 Preparation of a range of cyclic poly(lactides)	135
Figure 3.2.4.1 Synthesis of maleimide functional telechelic polymer <i>via</i> organic catalysis. i) 5 , thiourea, (-)-sparteine, CH ₂ Cl ₂ , 30 mins; ii) 6 , NEt ₃ , CH ₂ Cl ₂ , 24 h; iii) heat, 24 h	137
Figure 3.3.1.1 Synthesis and cleaving of dithiol bridged cyclic PLA. i) 1eq. 1,2-ethanedithiol, CH ₂ Cl ₂ , NEt ₃ , Na ₂ S ₂ O ₅ ; ii) ⁿ Bu ₃ P, CH ₂ Cl ₂	140

or ⁿ Bu ₃ P, NEt ₃ , <i>N</i> -methylmaleimide, CH ₂ Cl ₂ or ⁿ Bu ₃ P, NEt ₃ , <i>N</i> -(1-pyrenyl)maleimide, CH ₂ Cl ₂	
Figure 3.3.1.2 MALDI-ToF MS of linear polymers before and after cleavage of dithiol bridge with ⁿ Bu ₃ P, NEt ₃ and <i>N</i> -methylmaleimide	142
Figure 3.3.1.3 MALDI-ToF MS of cyclic polymers before and after cleavage of dithiol bridge with ⁿ Bu ₃ P, NEt ₃ and <i>N</i> -methylmaleimide	143
Table 3.2 Linear and cyclic polymer cleaving with <i>N</i> -(1-pyrenyl)maleimide trapping	144
Figure 3.3.2.1 Synthesis of heat cleavable diol initiator, 7 . i) toluene, reflux, 16 h	145
Figure 3.3.2.2 MALDI-ToF MS of linear diels alder bridged polymer recorded under high laser power (small distribution at M _w = ~3000 corresponds to complete polymer).	146
Figure 3.3.2.3 MALDI-ToF MS of cyclic diels alder bridged polymer under high laser power.	147
Figure 3.3.2.4 MALDI-ToF MS of linear diels alder bridged polymer cleaved at 200 °C in microwave.	149
Figure 3.4.1.1 Benzyl functional diol initiator, 8 . i) 2,2-dimethoxypropane, PTSA, Acetone, 16 h; ii) DCC, CH ₂ Cl ₂ , 4h; then benzyl alcohol, DCC, DMAP, CH ₂ Cl ₂ , 16 h; iii) DOWEX H ⁺ resin, CH ₂ Cl ₂ , 16 h	150
Figure 3.4.1.2 Benzyl functional cyclic polymer synthesis. i) 1eq ethane dithiol, CH ₂ Cl ₂ , NEt ₃ , Na ₂ S ₂ O ₅	151
Figure 3.4.2.1 Sequential ‘click’ reactions with alkene and alkyne functionalities. i) 10 eq. NEt ₃ , 10 eq. DDT, CH ₂ Cl ₂ , 0.5 h; ii) 10 eq. benzyl thiol, DMPP, CH ₂ Cl ₂ , 2 h; iii) 10 eq. NEt ₃ , 10 eq. DDT, CH ₂ Cl ₂ , 0.5 h; iv) 20 eq. benzyl thiol, DMPP, CH ₂ Cl ₂ , 24 h	154
Table 3.3 Sequential α- and ω-chain end conjugation	155
Figure 3.4.2.2 MALDI-ToF MS analysis of dodecanethiol conjugation, showing only single addition to maleimide chain end.	156
Figure 3.4.2.3 MALDI-ToF MS analysis of thiophenol conjugation to alkyne functional linear polymer, showing exactly two additions	157
Figure 3.4.2.4 Diol initiator synthesis bearing ‘click’ functional handles, 9 & 10 . i) 2,2-dimethoxypropane, PTSA, Acetone, 16 h; ii) DCC, CH ₂ Cl ₂ , 4h; then allyl alcohol, DCC, DMAP, CH ₂ Cl ₂ , 16 h; iii) DOWEX H ⁺ resin, CH ₂ Cl ₂ , 16 h; iv) 2,2-dimethoxypropane, PTSA, Acetone, 16 h; v) DCC, CH ₂ Cl ₂ , 4h; then propargyl alcohol, DCC, DMAP, CH ₂ Cl ₂ , 16 h; iii) DOWEX H ⁺ resin, CH ₂ Cl ₂ , 16 h	158
Table 3.4 Single point Michael addition to cyclic PLA	159
Figure 3.4.2.5 Incorporation and ‘click’ chemistry of a single point functionality onto cyclic PLA. i) 1eq ethane dithiol, CH ₂ Cl ₂ , NEt ₃ , Na ₂ S ₂ O ₅ ; ii) 10 eq. benzyl thiol, DMPP, CH ₂ Cl ₂ , 4 h	160
Figure 3.4.2.6 MALDI-ToF MS of benzyl thiol conjugation to alkene functional, cyclic poly(lactide)	161

Chapter 4

Figure 4.1.1 Cyclic polymer architectures, a) cyclic; b) ‘tadpole’ shaped; c) tadpole; d) ‘theta’ shaped; e) ‘Doubly fused bicyclic’ structure; f) spirocyclic; g) ‘handcuff’ shaped; h) backbone linked; i) enchain; j) enchain with linkers; k) ‘quatrefoil’ shaped.	167
Figure 4.2.1.1 One pot synthesis of ‘handcuff’ shaped poly(lactide); i) 0.67 eq Trimethylolpropane tris-(3-mercaptopropionate), CH ₂ Cl ₂ , NEt ₃ , Na ₂ S ₂ O ₅ .	170
Figure 4.2.1.2 MALDI-ToF MS of the ‘handcuff’ shaped poly(lactide).	171
Figure 4.2.2.1 One pot synthesis of spirocyclic poly(lactide); i) 0.5 eq. Pentaerythritol tetrakis-(3-mercaptopropionate), CH ₂ Cl ₂ , NEt ₃ , Na ₂ S ₂ O ₅ .	174
Figure 4.2.2.2 MALDI-ToF MS of the spirocyclic poly(lactide).	175
Figure 4.3.1 Alkene bearing linear and cyclic poly(lactide) for thiol-ene conjugations	177
Figure 4.3.2 Conjugations were carried out with a) 1,3-Propanedithiol, b) Trimethylolpropane tris-(3-mercaptopropionate) c) Pentaerythritol tetrakis-(3-mercaptopropionate).	178
Table 4.1 Preparation of a range of linear and cyclic poly(lactide) stars	178
Figure 4.4.1 Thioglycerol conjugation to cyclic polymer. i) 1eq. ethane dithiol, CH ₂ Cl ₂ , NEt ₃ , Na ₂ S ₂ O ₅ ; ii) 10 eq. thioglycerol, DMPP, CH ₂ Cl ₂ , 4 h.	181
Figure 4.4.2 Thioglycerol chain extension. i) <i>rac</i> -lactide, Al salen, toluene, 70 °C, 4 h.	182
Figure 4.5.1.1 Synthesis of PEG bearing thiol chain ends, i) 20 eq. 3-thiopropionic acid, DCC, CH ₂ Cl ₂ , DMAP, 48 h.	184
Table 4.2 Preparation of a range of thiol bearing PEG chains	184
Table 4.3 Cyclic PLA- <i>b</i> -PEG conjugations	186
Figure 4.5.2.1 PEG- <i>b</i> -PLA cyclic and linear conjugations. i) linear PLA, Figure 4.3.1 , DMPP, CH ₂ Cl ₂ , 48 h; ii) cyclic PLA, Figure 4.3.1 , DMPP, CH ₂ Cl ₂ , 48 h	187
Figure 4.6.1 Deprotection of the poly(BLG- <i>co</i> -tBMLC) to poly(BLG- <i>co</i> -Cys)	189
Figure 4.6.2 Conjugation of the linear and cyclic polymers to poly(BLG- <i>co</i> -Cys). i) linear PLA, Figure 4.3.1 , DMPP, CH ₂ Cl ₂ , 48 h; ii) cyclic PLA, Figure 4.3.1 , DMPP, CH ₂ Cl ₂ , 48 h	190
Table 4.4 Poly(BLG- <i>co</i> -Cys)- <i>b</i> -PLA conjugations	191

Acknowledgements

Without the eternal support of my new wife Joanne I would not have completed my PhD, and therefore it is with great pleasure that I thank her for being next to me throughout.

I am enormously grateful to have shared my entire PhD with Ryan Pounder and for every moan in the car and grumpy day in the lab I thank him for always being there, even though I suspect he didn't always want to be.

Without the help of Andrew Dove none of this work would have been possible, I am appreciative for his advice and ideas.

Publications

The following publications have arisen from the work in this thesis:

Chapter 1:

‘Stereocontrolled ring opening polymerisation of lactide’

Stanford, M. J.; Dove, A. P. *Chem. Soc. Rev.* **2010**, 39, 486-494

Chapter 2:

‘Metal free thiol-maleimide ‘Click’ reaction as a mild functionalisation strategy for degradable polymers’

Pounder, R. J.; Stanford, M. J.; Brooks, P.; Richards, S. P.; Dove, A. P. *Chem. Commun.* **2008**, 5158-5160

‘One-pot synthesis of α,ω -chain end functional, stereoregular, star shaped poly(lactide)’

Stanford, M. J.; Dove, A. P. *Macromolecules* **2009**, 42, 141-147

Chapter 3:

‘Synthesis of stereoregular cyclic poly(lactide)s via ‘thiol-ene’ click chemistry’

Stanford, M.J.; Pflughaupt, R.J.; Dove, A.P., *Macromolecules*, **2010**, 43, 6538 - 6541.

Declaration

I hereby declare that this thesis consists of my own work and has not previously been submitted for any degree at any institution. Initial investigations into the behaviour of the maleimide on a polymer chain were carried out in collaboration with Ryan Pounder.

Where other sources of information have been used, they have been acknowledged and referenced.

Signature.....

Abstract

Poly(lactide)s is a biocompatible and biodegradable polymer available from renewable feed stocks and has therefore received a great deal of attention in recent years. Although significant research has been carried out examining its properties, architectural differences have received little attention. Notably, cyclic polymers are known to have strikingly different properties from their linear counterparts. This research will examine possible new routes for the synthesis of cyclic poly(lactide)s.

Abbreviations

CH ₂ Cl ₂	Dichloromethane
CMC	Critical micelle concentration
CuAAC	Copper catalysed azide alkyne cycloaddition
DCC	Dicyclohexylcarbodiimide
DDT	Dodecanethiol
DMPP	Dimethylphenyl phosphine
GPC	Gel permeation chromatography
<i>i</i> PA	Isopropanol
MALDI-ToF MS	Matrix Assisted Laser Desorption Ionisation – Time of Flight Mass Spectrometry
MeOH	Methanol
MS	Mass Spectroscopy
MTC	2,2-bis(hydroxymethyl)propionic acid
NEt ₃	Triethylamine
NHC	N-Heterocyclic carbene
NMR	Nuclear Magnetic Resonance
PDI	Poly Dispersity Index
PEG	Poly ethylene glycol
PLA	Poly(lactide)
PTSA	Paratoluenesulphonic acid
RAFT	Reversible addition fragmentation chain transfer
REMP	Ring expansion metathesis polymerisation
ROMP	Ring opening metathesis polymerisation

ROP	Ring opening polymerisation
TBD	1,5,7-Triazabicyclo[4.4.0]dec-5-ene
T _g	Glass transition temperature
THF	Tetrahydrofuran
T _m	Melting point

Chapter 1: The synthesis of stereoregular, cyclic poly(lactide)

1.1 Introduction

This thesis centres around one specific goal; the synthesis of cyclic, stereoregular poly(lactide). For the purposes of examining the current literature in this area it is worth addressing the areas of stereocontrol and cyclic polymerisations separately. These two areas will be the subjects of Chapter 1.

1.2 Synthesis of stereoregular poly(lactide)

Poly(lactic acid) (PLA), a renewable, biocompatible and biodegradable polymer, has received a significant amount of interest from both research and industry over recent years.¹ The physical properties of PLA make it a viable alternative to more common petrochemically-derived polymeric materials as well as being suitable for more specialised applications in the pharmaceutical and microelectronics industries.² However, control of the microstructure is imperative, as this has been demonstrated to significantly affect the physical properties of the polymer in bulk. Polymerisation of lactide is commonly achieved through two different processes, polycondensation reactions and ring opening polymerisation. Control over the microstructure is realised exclusively by the ring-opening polymerisation of lactide (the cyclic dimer of lactic acid) compared to polycondensation reactions. Ring

opening polymerisation (ROP) allows far greater control during the polymerisation and therefore results in more regular polymer chains. This regularity leads to lower polydispersity (PDI), higher molecular weight and high levels of chain-end fidelity in comparison to poly condensation reactions.

Through the use of ROP it is also possible to control the stereoselectivity of the polymerisation, allowing control of the tacticity of the polymer chain. This is possible through the application of enantiomerically controlled feedstocks. Lactide has two stereocentres and therefore there are four available forms; *DD*-, *LL*-, *rac*- (a 50:50 mixture of *DD*- and *LL*-) and *meso*-lactide (*DL*-). In the absence of epimerisation, the stereocontrolled polymerisation of *rac*- and *meso*- lactide can result in a range of polymer microstructures, **Figure 1.2.1**. This is described as the tacticity of the polymer and the ring opening polymerisation of *meso*-lactide can potentially lead to either syndiotactic PLA (alternating *S* and *R* stereocentres i.e. -*SRSRSR*-) or heterotactic PLA in which the stereocentres doubly alternate i.e. -*SSRRSSRR*-. ROP of *rac*-lactide can also lead to heterotactic PLA by alternating insertion of *D*- and *L*-lactide enantiomers as well as ‘isotactic’ polymers.

The amount of stereoerrors that occur on the polymer chain can vary depending on the level of control provided by the catalyst, although this is only obvious in isotactic polymer, where a variety of possible outcomes are possible. A racemic catalyst system with no errors will result in distinct polymer chains of PLLA and PDLA, whereas a single error, or a non-racemic catalyst, will result in a stereoblock copolymer, most likely with a tapered central block. If the catalyst system makes a large number of stereoerrors, or there is chain transfer occurring, then a multiblock polymer can be synthesised, these possibilities are shown in **Figure 1.2.1**.

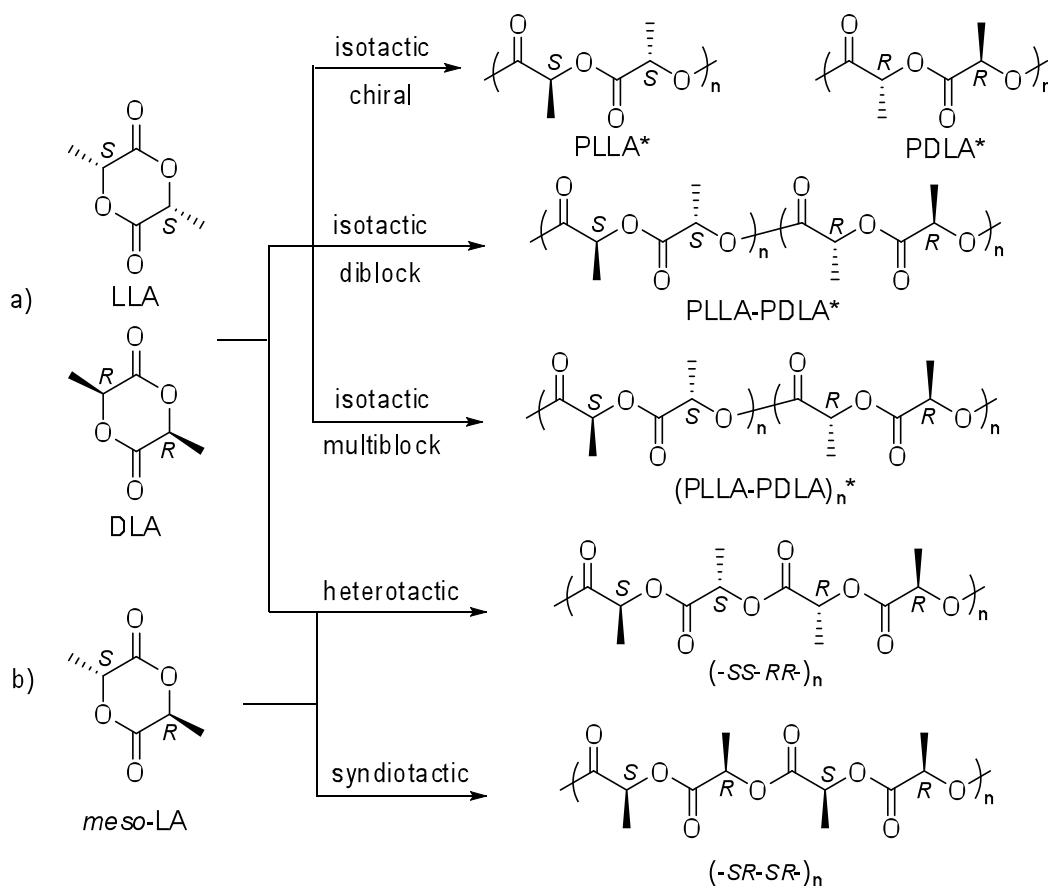


Figure 1.2.1 Microstructures for the stereocontrolled ROP of lactide from a) *rac*-lactide and b) *meso*-lactide.

Characterisation of the microstructure has been a particular challenge in the identification of the polymer tacticity and therefore the discovery of new stereoregular catalytic systems. Initially, the optical activity of the polymer was used on the basis that in PLLA of $M_w > 6000$, α_D^{22} remains constant at 142° ,^{3,4} enabling the identification of isotactic systems, at least at low monomer conversion. More recently, Munson *et al.* demonstrated that the tacticity of the polymer can be

determined from ^{13}C NMR and homonuclear decoupled ^1H NMR analysis, **figure 1.2.2.**⁵ In order to decouple the effect of splitting between the methyl and methine protons, homonuclear decoupling of the methyl signal is carried out resulting in singlet resonances in the methine region ($\delta = 5.15\text{--}5.25$ ppm). Adaptation of the Bovey formalism such that '*i*' describes an iso and '*s*' a syndio relationship between adjacent stereocentres (Note, this is sometimes *m/meso* and *r/racemic*) provides a method for describing the tacticities of the polymer. At the tetrad level this is a three letter sequence such that a chain of pure poly(*L*-lactide) will have a repeating tetrad of *LLLL* which would be represented by *iii* whereas a pure heterotactic PLA would contain tetrads of both *LLDD* and *LDDL*, or *isi* and *sis*, respectively. It is worthy of note that in the absence of epimerisation and transesterification the ROP of *rac*- and *meso*-lactide results in different possible tetrad sequences, **figure 1.2.2.**

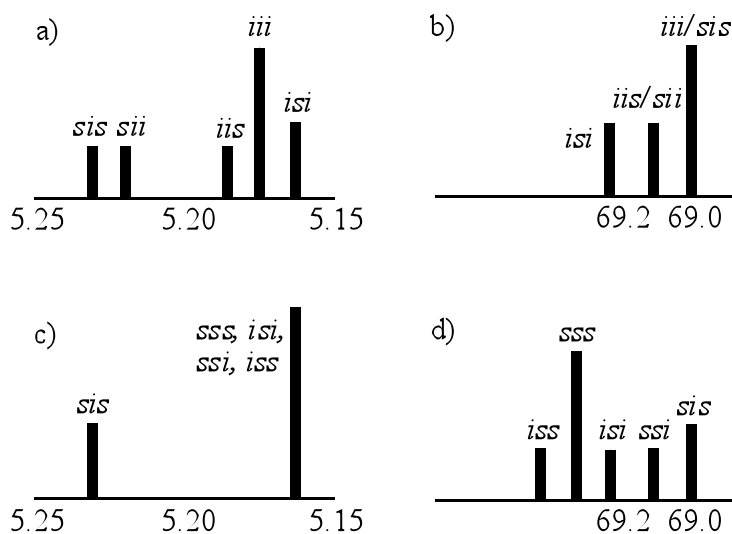


Figure 1.2.2 Homonuclear decoupled proton NMR showing the different tetrads and their respective positions for polymer from *rac*-lactide a) ^1H NMR, b) ^{13}C NMR, and *meso*-lactide c) ^1H NMR, and d) ^{13}C NMR.

The degree of stereoregularity of lactide is expressed as P_r or P_m , representing the probability of racemic or mesomeric enchainment respectively (the probability of forming a new *racemic* (syndiotactic) or *meso* (isotactic) diad). It is possible to calculate this from the deconvoluted ^1H NMR spectra,^{6,7} (see reference for calculation and an explanation of the kinetics involved in stereocontrol). In this text it is these P_r or P_m values that are referred to, to determine the ability to synthesise stereoregular PLA for a particular catalyst (described as $P_r = x$, or $P_m = x$). It is important to note that P_r or $P_m = 0.50$ describes a completely atactic polymer and $P_r = 1.00/P_m = 0.00$ or $P_m = 1.00/P_r = 0.00$ being a perfect heterotactic or isotactic polymer respectively.

Control of the polymer tacticity has a significant impact on the physical properties of the polymer in bulk. Differences have been shown in polymer melting (T_m) and glass transition (T_g) temperatures. Indeed, heterotactic PLA displays a T_m of 130 °C and no observable T_g , whereas enantiopure PLLA possesses a T_m of 180 °C and a T_g of ~50 °C.

Recent studies of stereoregular PLA have also shown that when pure PLLA and PDLA are mixed they form a stereocomplex that results in an increase in the melting point.⁸ This increase is most significant in a 1:1 mix of polymer chains and is *ca.* 50 °C. Stereocomplexation can also be observed in highly stereoblock copolymers and therefore can be accessed through the application of *rac*-lactide as a feedstock. The formation of the stereocomplex is related to the increase in crystallinity when the opposite chains of PLLA and PDLA come together and form a much more stable structure than pure chains of either enantiopure component.

Polymerisation of lactide into the polymer chain can proceed *via* several different mechanisms including anionic, *pseudo*-anionic (general base catalysis), coordination-insertion ROP and a monomer-activated mechanism. In all cases, stereocontrol is maintained by two mechanisms; chain end control and enantiomorphic site control.

Chain end control is demonstrated when the chirality of the propagating chain-end bound to the catalyst determines the chirality of the next monomer to be inserted, and is generally associated with hindered but achiral catalyst systems. Enantiomorphic site control is demonstrated when the chirality of the catalyst dictates the chirality of the next insertion.

There are a large number of catalysts systems that have been studied for the ROP of lactide; organic, enzymatic, traditional anionic or metal based.¹ Metal based catalysts are by far the most widely studied and have the most examples of stereocontrolled ROP. Recently more attention has been applied to the area of organic catalysis, possibly due to the benefits that these catalysts have, namely cost, stability and availability. However, there are still very few examples of stereocontrol using organic catalysts, and none have been shown to work at ambient temperatures or above. Enzymatic catalysis using lipases is predominantly slow for the ROP of lactide and has not been shown to allow stereocontrol of the polymer and will receive no further discussion herein.

A large range of metal-based catalysts from across the periodic table, show some level of stereocontrol for the ROP of lactide. However, due to recent advances in the field allowing for superbly high levels of control, only examples that show significantly more than a bias towards stereocontrolled polymer will be discussed, particularly in areas which have received a great deal of attention. In order to be concise, only catalysts with P_r or $P_m \geq 0.7$ will be discussed in detail.

1.2.1 Anionic ROP

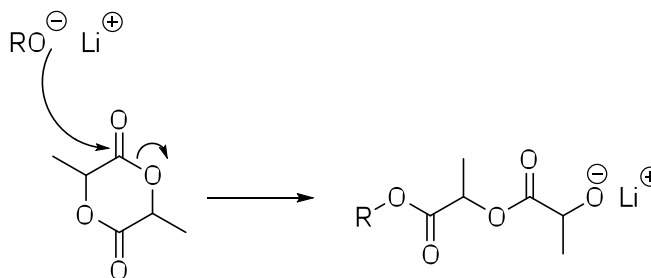


Figure 1.2.1.1 Anionic polymerisation of lactide.

A range of anionic polymerisation techniques for the ROP of lactide exist,⁹ but only lithium species have successfully been applied to give significant stereocontrol in the polymerisation of *rac*-lactide. The mechanism of anionic ROP is based around the attack of an anion on the lactide ring causing acyl bond cleavage and the subsequent formation of the alkoxide anion that leads to propagation, **Figure 1.2.1.1**.

Lithium *tert*-butoxide has been observed to produce heterotactic (referred to as disyndiotactic in these reports) with P_r determined to be 0.76 in a polymerisation carried out at room temperature.¹⁰ The level of stereocontrol is significantly increased when the polymerisation is carried out at -20 °C, $P_r = 0.94$, although transesterification reactions at both temperatures result in loss of stereocontrol at increased reaction times.¹¹ With no significant hindrance surrounding the lithium

this suggests a chain end control process is apparent, although no mechanism is proposed in this research.

More recently butyllithium has been employed in the synthesis of heterotactic polymer, in much the same way as the alkoxide, producing a polymer at 20 °C where $P_r = 0.72$.¹² In an analogous experiment, polymerisation using magnesium *tert*-butoxide in identical conditions has been shown to produce slightly less heterotactic bias ($P_r = 0.63$). However, in contrast to lithium *tert*-butoxide lowering the temperature in either of the above cases does not improve stereocontrol.

1.2.2 Coordination-insertion ROP

1.2.2.1 Tri- and tetra-dentate iminophenolato- and aminophenolato- (salen and salan) complexes

Metal salts and coordination complexes that operate by a coordination-insertion mechanism dominate the metal-mediated ROP of lactide. The mechanism of coordination insertion polymerisation involves a metal centre onto which the lactide can coordinate through its carbonyl oxygen; a step that has been shown to be particularly important in stereocontrol. Attack from the alkoxide chain end to the

activated carbonyl carbon and subsequent ring-opening results in the formation of a new chain-extended metal alkoxide species in which the close proximity of the carbonyl group is postulated to stabilise the propagating species through coordination back to the metal centre as a lactate, **Figure 1.2.2.1**.

A hindered metal, either from a ligand system or the growing polymer chain, can cause significant difference in the rates of insertion between the different enantiomers of lactide, and therefore stereocontrol can be exerted.

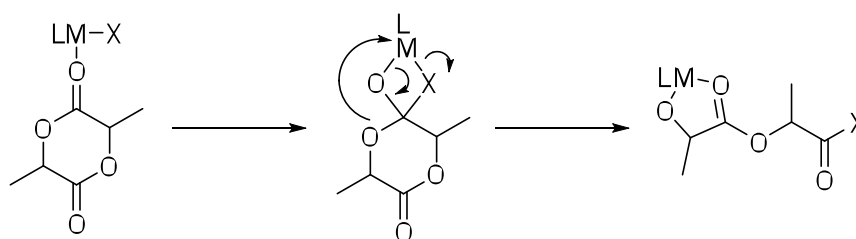


Figure 1.2.2.1 General mechanism for Coordination insertion ROP.

The application of tetradentate salicaldimine (salen) aluminium complexes in the stereocontrolled ROP of lactide is an area that has received a great deal of attention. Commonly employed at 70 °C in solution, a range of ligand substituents have been tested and all of the possible microstructures have been achieved. Initial work in 1993 by Spassky *et al.* employed a single (+)-enantiomer of a chiral aluminium complex to synthesise stereoregular PLA, (+)i **Figure 1.2.2.2**.¹³ At low conversion it was identified that the growing polymer chain consisted of almost exclusively *D*-

lactide (up to 88% enantiomeric enrichment at 19% conversion), although at higher conversion both enantiomers of the monomer were incorporated. An increase in the melting point of these polymers was observed when high conversion was reached, this suggests that stereocomplexation was occurring and indicating a tapered stereoblock microstructure was present.^{14,15} This catalyst was later shown by Coates *et al.* to produce syndiotactic PLA from *meso*-lactide.¹⁶

Smith, Baker and coworkers later identified that through the application of a racemic catalyst system it was possible to produce PLA that would also demonstrate stereocomplexation behaviour.¹⁷ This catalytic system was considered to be producing pure PDLA and PLLA from the different catalyst enantiomers. However, Coates *et al.* demonstrated that chains of isotactic stereoblock were actually being synthesised from the racemic.¹⁸ Each block was determined to contain on average of 11 lactide monomer units that co-crystallised to give a solid with melting point 179 °C.

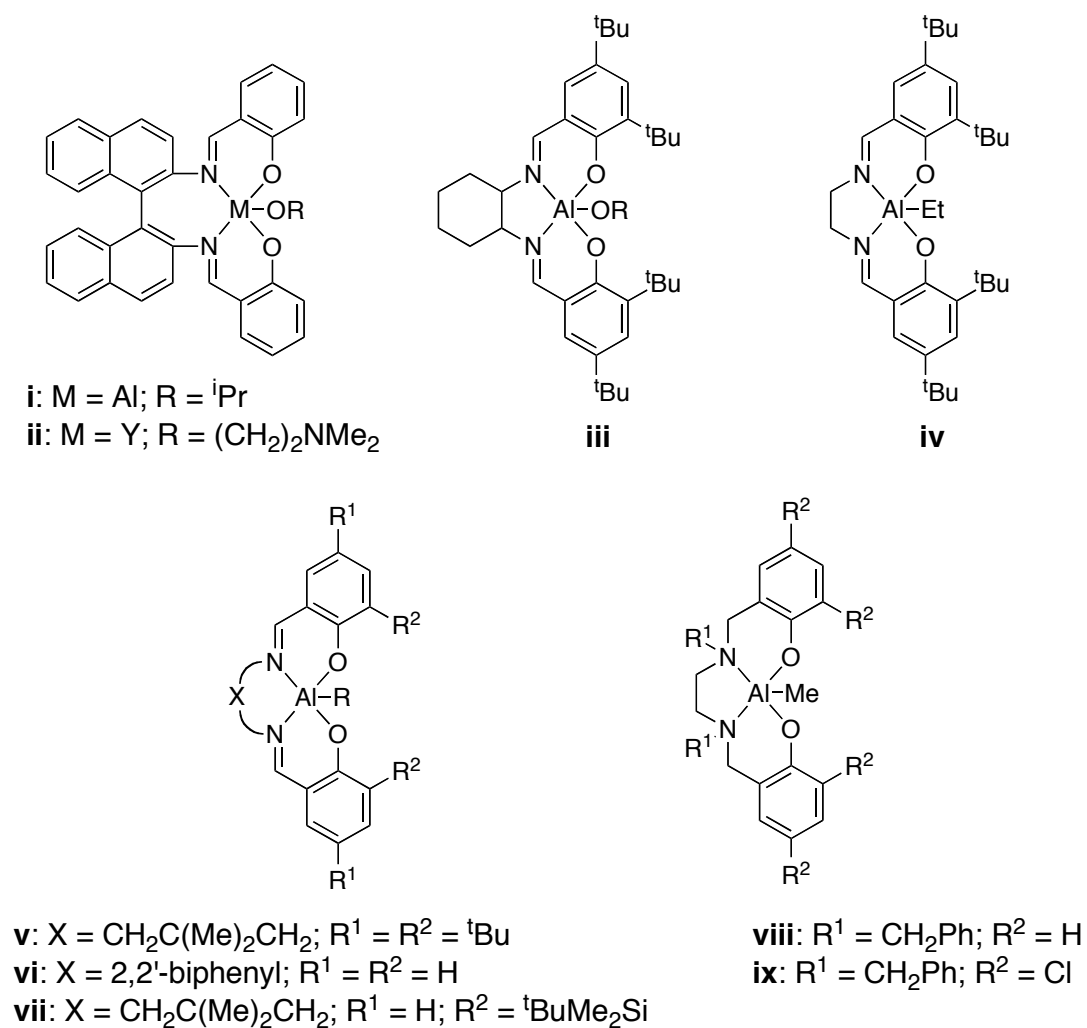


Figure 1.2.2.2 Tetradentate (imino- and amino-phenolato)aluminium complexes for stereoselective lactide ROP.

Both of these catalyst systems were postulated to be demonstrating enantiomorphic site control due to the large chiral ligands that were being employed. However, assigning the mechanism by which these chiral catalysts impart stereocontrol can be problematic and often involves more complex intermediates than the general

mechanism. It has been recognised that the ligand chirality, polymer chain end and even the solvent can all play a role in the stereocontrol.¹⁹ Subtle changes in the backbone of the salen ligands have been postulated to result in the complex adopting different stereoisomers in response to a chiral chain end, greatly influencing the outcome of the stereocontrol.

Majerska and Duda who, through the application of a ligand exchange mechanism, were able to synthesise a true PLLA-PDLA stereoblock copolymer, employed a similar system to that of Spassky. This mechanism involved adding the different enantiomers of the catalyst at 0 % and 50 % lactide conversion, which, through chain transfer, allowed for the synthesis of a stereoblock copolymer. The polymer synthesised in this way had a melting point of 210 °C, showing stereocomplexation behaviour very similar to that of a 50:50 mixture of pure PLLA and PDLA.²⁰

Feijen *et al.* have employed a similar catalyst that is much more simply derived, **Figure 1.2.2.2**, being based around the cyclohexyl backbone, commercially available, Jacobsen's ligand, **iii** (both *R,R*- and *rac*- derivatives).^{21,22} In this work, with *R,R*-**iii** they were able to observe kinetic differences between the *L*- and *D*-lactide that resulted in high levels of isotactic enchainment, $P_m = 0.93$. Importantly these catalysts could, for the first time, be employed under melt conditions of 130 °C and still retain high levels of stereocontrol ($P_m = 0.88$). Recent studies have shown that other (salen) aluminium catalysts also provide high levels of stereocontrol in melt conditions of 130 °C, a practical feature that allows for decreased reaction times and overcomes issues of solubility.²³

The chirality of this Jacobsen type catalyst has been shown to exert minimal control during the initial ring-opening event, and the solvent significantly influences this

step; such that an opposite enantiomer is inserted in chloroform and toluene.²⁴ This suggests that the high levels of stereocontrol are exerted by a chain end control mechanism. Through the application of enantiomerically pure catalyst it is apparent that errors resulting in a stereoblock copolymer over pure chains are not a result of chain transfer but of stereoerrors during the chain end control mechanism. Transesterification and epimerisation in this system are both very low, with a small amount of the former being observable after significantly increased reaction times. This is apparent throughout the work on salen/salan aluminium complexes and it suggests that errors are a result of insertion errors rather than chain transfer.

Achiral catalysts were shown by Nomura *et al.* to synthesise stereoregular PLA with a $P_r = 0.81$.²⁵ It is suggested that these achiral catalysts, **iv Figure 1.2.2.2**, produce stereoregular polymers *via* a chain end control mechanism. The stereocontrol is achieved through the application of phenyl substituents, *t*-butyl groups in this case, that considerably increase the steric bulk at the metal centre. This reduces the rate of the polymerisation, but increases the energy barrier to lactide coordination to the metal, and therefore chain end control can be exerted.

Nomura *et al.* have more recently demonstrated that it is possible to employ melt polymerisation temperatures of up to 210 °C while still maintaining control of stereoselectivity, catalyst **v, Figure 1.2.2.2** ($P_r = 0.98$ with *meso*-lactide).²⁶ At this temperature rates are significantly increased, but it was possible to determine that the backbone of the metal complex plays an important role in activity even at these high temperatures.

Probably the most significant advance in the practical application of these catalysts was the work of Gibson *et al.* between 2004 and 2006, with extensive examination

of the effect the ligand has on the kinetics and stereocontrol of the polymerisation.^{27,28} A range of salan/salen, **v - ix**, **Figure 1.2.2.2**, catalysts differing in their steric and electronic properties were developed and applied to the polymerisation of *rac*-lactide. The phenoxy substituents were found to play an important role in both the rate and selectivity of the polymerisation. Electron withdrawing groups generally increased the rate of the polymerisation, while sterically encumbering groups in the *ortho* position resulted in slower rates but increased selectivity. Stereocontrol was generally improved through increasing the length of the backbone, possibly due to the ease with which sterically hindered process, like monomer approach, could be incorporated. This range of catalysts allows a range of tacticities from $P_r = 0.96$ to $P_m = 0.88$ with a salan and a salen complex respectively. Chen and coworkers, further demonstrated the importance of this linker in the polymerisation process with extended ligand backbones to achieve ($P_m = 0.90$).²⁹

Coates *et al.* have been able to employ yttrium based salan ligands and demonstrated that they have no effect on stereocontrol.³⁰ An identical catalyst with an aluminium centre does, however, provide stereocontrol ($P_m = 0.96$) although no reason for this difference is given. The polymer synthesised from *rac*-lactide is inherently isotactic, although no stereocomplexation is observed in this case. This is explained *via* a polymer exchange mechanism where the growing polymer chain switches between catalysts in the racemic mixture creating stereo-multiblock copolymers that cannot undergo stereocomplexation. Cui and coworkers were able to polymerise *rac*-lactide with modest heteroselectivity ($P_r = 0.69$) with both salen and salan based yttrium complexes.³¹

The large amount of research in this area has resulted in a significant library of catalysts with a broad array of ligand structures, thus allowing a complete range of polymer microstructures to be synthesised. Salen/salan aluminium based complexes also have the advantage that the active species, the aluminium alkoxide, can be generated *in situ* from the aluminium ethyl/methyl and an alcohol. Although not broadly acknowledged with research groups each preferring the application of a single alcohol, recent reports have shown that this facilitates control of the α -chain end of the polymer.³²

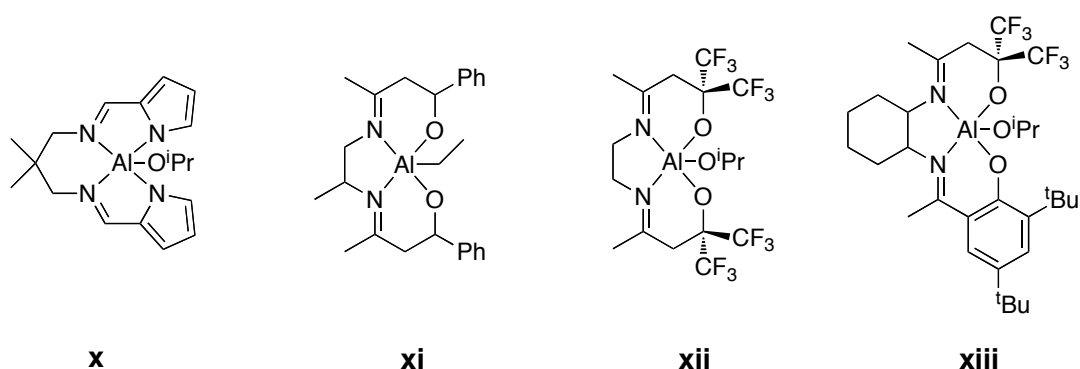


Figure 1.2.2.3 Tetradentate Schiff base aluminium complexes for stereoselective lactide ROP.

Several other tetradentate and tridentate Schiff base ligands have also been applied as catalysts for lactide ROP. Achiral bis(pyrroline) Schiff base aluminium alkoxides, **x** **Figure 1.2.2.3**, mediate a moderately isospecific ROP of *rac*-lactide ($P_m = 0.75$).³³ Notably, the ROP of *meso*-lactide using these catalysts demonstrated very little stereocontrol ($P_r = 0.59$), with no correlation being observed between ligand substituents and stereocontrol. Enolic tetradentate Schiff base

aluminium catalysts, **xi Figure 1.2.2.3**, have also been employed in the polymerisation of *rac*-lactide, resulting in stereocontrol ($P_m = 0.80$).³⁴ Carpentier *et al.* employed a similar system in which electron withdrawing trifluoromethyl groups were located adjacent to the alkoxides, **xii Figure 1.2.2.3**.³⁵ No differences in polymer tacticity were observed when either chiral or achiral ligands were applied suggesting that stereocontrol is again determined by a chain end control mechanism ($P_m = 0.83$ - 0.87 under melt conditions of 120 - 140 °C). Carpentier *et al.* also examined the application of a mixed fluororous alkoxy-phenolate Schiff base ligand, **xiii Figure 1.2.2.3**, that also led to isotactic PLA at 60 °C in toluene solution ($P_m = 0.81$).³⁶

Tridentate Schiff base ligands (NNO) with hindered substituents, **xiv Figure 1.2.2.4**, have been demonstrated to give high levels of stereocontrol with zinc at -55 °C ($P_r = 0.91$).³⁷ ^1H NMR studies of these compounds suggest the presence of both monomeric and dimeric species in solution at room temperature, at least in the less hindered variants ($P_r = 0.59$ - 0.65). A similar system has also been shown in the solid state to form large crown-like macrocycles, although it is unclear if these species are involved in the solution polymerisation ($P_r = 0.75$).³⁸ Calcium based analogues of this system, **xv Figure 1.2.2.4**, have also been shown to allow stereocontrol in THF at -33 °C ($P_r = 0.73$).³⁹ Mehrkhodavandi *et al.* have employed a diaminocyclohexylane indium catalyst that forms a dimeric initiating species through a single bridging ethoxido and chlorido ligand, **xvi Figure 1.2.2.4**.⁴⁰ The mechanism is thought to proceed *via* an equilibrium between the monomeric and dimeric forms of the catalyst and it has been shown to give modest stereocontrol to the polymer chain ($P_r = 0.6$ - 0.7).

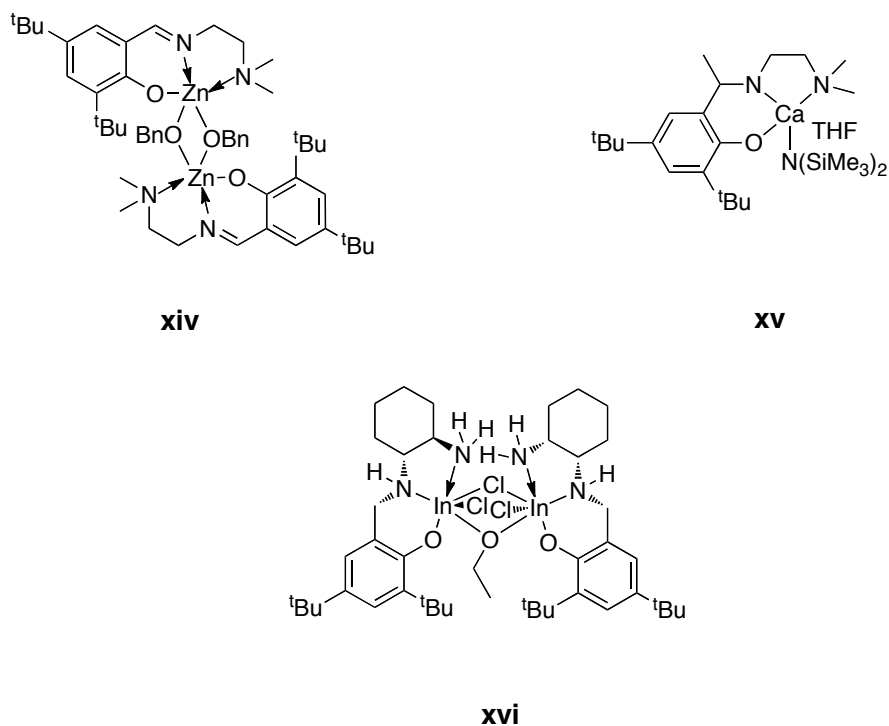


Figure 1.2.2.4 Tridentate Schiff base metal complexes for stereoselective lactide ROP.

1.2.2.2 β -Diketiminato (BDI) complexes

(β -Diketiminato) metal complexes have not been as broadly researched as the salen/salan based complexes but since their initial reports in 1999 they have shown impressive control of the stereoregular ROP of lactide.⁴¹ The research of Coates *et*

al. using zinc complexes has defined this particular area since their initial communication, demonstrating that catalyst **xvii**, **Figure 1.2.2.5**, could produce heterotactic PLA from *rac*-lactide with a $P_r = 0.94$ when employed at ambient temperature. The activity of these catalysts is extremely high, with a polymerisation of target DP = 200 complete within 20 minutes at room temperature. Interestingly these species have been shown to form dimeric, and trimeric in some cases, structures in the solid state although it not discussed whether this is the case in solution.

Initiation using these species has been shown to occur with alkoxide, acetate, alkyl, lactate and amide species although only alkoxide and lactate afforded controlled polymers with narrow PDI due to its fast incorporation onto the polymer chain end. These initiators are also analogous to the putative chain end of the growing polymer, meaning that the rates of initiation and propagation will be similar, an important factor in maintaining control of the polymerisation.

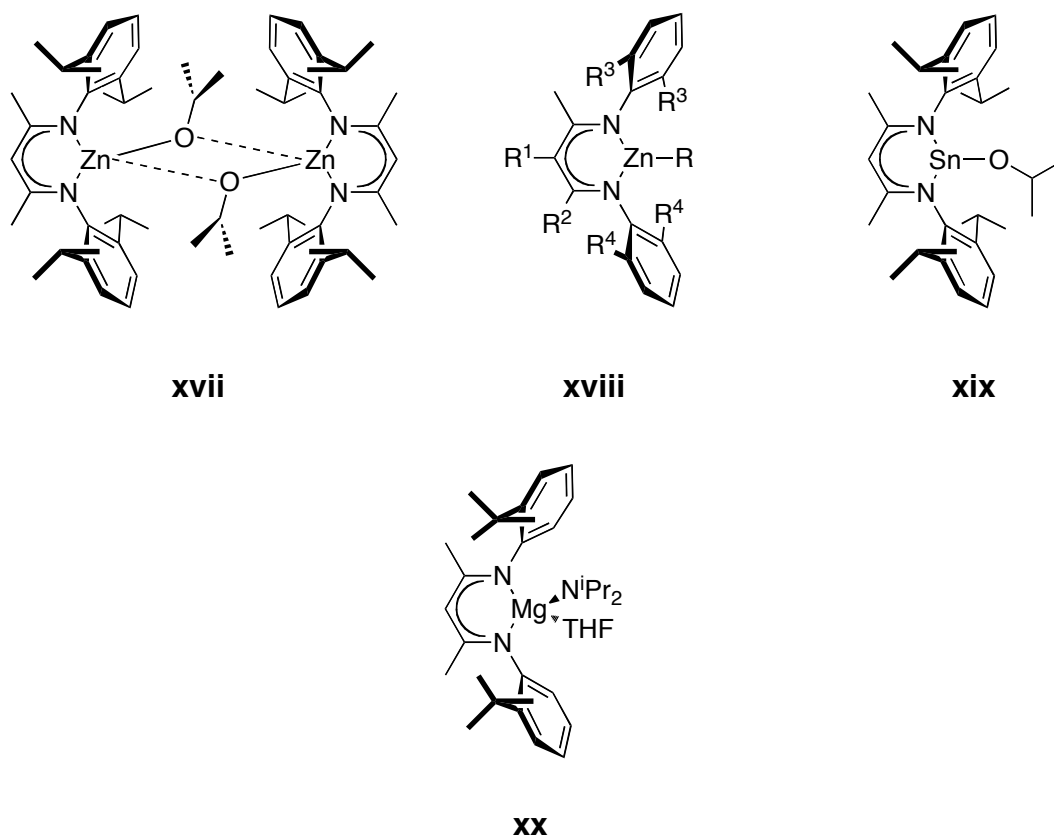


Figure 1.2.2.5 (β-Diketiminato) metal complexes for catalysis of stereospecific lactide ROP.

Subsequent research by Coates and coworkers has shown that control of the substituents in the on the BDI system controls not only the levels of stereocontrol but also the rate of the polymerisation.⁴² Alteration of the *ortho*- substituents on the aromatic rings of the ligand to less hindered ethyl and *n*-propyl groups results in decreased rate and stereocontrol.⁴³ These results suggest that the mechanism of stereocontrol is through the chain end of the polymer, and indeed the stability of the bidentate zinc lactate species has been shown to be very high. BDI zinc catalysts

have also been shown to be active catalysts for a range of other polymerisation reactions, with further implications of ligand alterations being examined.⁴⁴

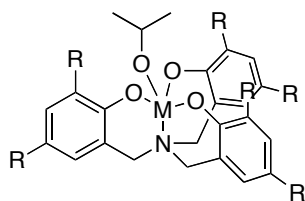
β -Diketiminato complexes based on tin(II) and magnesium have also demonstrated notable levels of stereocontrol in lactide ROP. The first and only known example of stereoregular tin controlled polymerisation is using this ligand system, **xix** **Figure 1.2.2.5**, although little more than a heterotactic bias is shown ($P_r = 0.70$).⁴⁵ This is believed to be related to the stereochemically active lone pair on the tin.⁴⁶ Stereocontrol is only observed for (β -Diketiminato) Mg complexes when carried out in THF, otherwise identical conditions in both CH_2Cl_2 and benzene results in atactic polymer, **xx**, **Figure 1.2.2.5**, ($P_r = \sim 0.9$).^{47,48} These results are a direct contrast to otherwise identical zinc complexes that exhibit control in all three solvent systems.

Through low temperature ^1H NMR studies Chisholm and co-workers observed notable differences between the zinc and magnesium complexes in the binding of THF to the metal centre. In the case of zinc, THF was rapidly dissociated into solution and even at -80°C , rapid exchange was observed. In the analogous magnesium complexes both free and bound THF were observed at low temperature with the maintenance of a high level of symmetry above and below the plane of the BDI backbone. This led the authors to postulate that the incorporation of the THF into the active magnesium catalytic species generates a more coordinately hindered metal centre that is more discriminatory to the incoming lactide.⁴⁹ Attempts to achieve the same level of steric hindrance through the incorporation of an ether into the ligand set results in no improvement of stereocontrol in CH_2Cl_2 ($P_r = 0.49$), although in THF competition between the ether and the solvent is observed, along

with high levels of stereocontrol ($P_r = 0.85$).

Computational studies have shown that the BDI ligand shows stereocontrol through the chain end of the polymer.⁵⁰ The approach of the monomer is of particular interest as both electrostatic and stereoelectric interactions govern it, a theme that is possibly common across all lactide catalysts. However, in the case of magnesium, the rate determining, and stereocontrol determining, step is in fact the minimisation of the steric interactions for a transition state during the ring opening of a ligated monomer.

1.2.2.3 Tetradentate amino(bis- and tris-phenolato) complexes

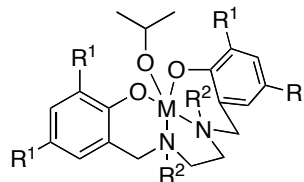


xxi: M = Ti; R = ^tBu

xxii: M = Zr; R = ^tBu

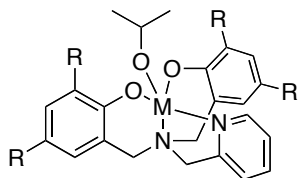
xxiii: M = Hf; R = ^tBu

xxiv: M = Ge; R = Me

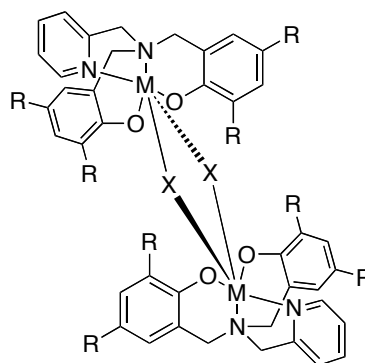


xxv: M = Ti, Zr, Hf; R¹ = Me, ^tBu; R² = Me

xxvi: M = Zr; R¹ = R² = Me

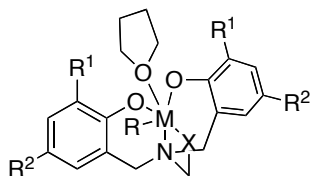


xxvii: M = Ti, Zr, Hf; R = Me, ^tBu, C(Me)₂Ph



xxviii: M = Y, Sm, La, Nd; X = BH₄, Cl

xxix: M = Y; X = BH₄



xxx: M = Y; R = N(SiHMe₂)₂; R¹ = R² = C(Me)₂Ph; X = OMe

Figure 1.2.2.6 Tetradentate amino(bis- and tris- amino)phenolato complexes for stereospecific lactide ROP.

A wide range of tetradentate amine(bisphenolato) and amino(trisphenolato) metal complexes have been employed in the stereocontrolled ROP of lactide.⁵¹ The metals of group 4 have been studied through the application of titanium, zirconium, and hafnium as well as germanium. These catalysts, **xxi** - **xxiv**, **Figure 1.2.2.6**, have been employed in melt at 130 °C and in solution at ambient temperature, and produce similar levels of stereocontrol under both sets of conditions (from **Figure 1.2.2.6** - **xxii** (Zr): $P_r = 0.96$; **xxiii** (Hf): $P_r = 0.88$; **xxiv** (Ge): $P_r = 0.80$). Mechanistically it is interesting to study the metals from a single group, as it provides an interesting insight into the metals involvement in the reaction. For example, unlike other group IV metals, titanium provides no stereocontrol whatsoever, producing atactic polymer ($P_r = 0.50$). It is postulated that this is caused by the chelation of the growing polymer chain being less favoured, leading to a large amount of chain transfer and poor stereocontrol. Zirconium and hafnium have much more comparable stereocontrol, producing heterotactic PLA from *rac*-lactide with $P_r = 0.96$ and $P_r = 0.88$ in the melt respectively ($P_r = 0.98$ and 0.97 respectively in solution polymerisation at ambient temperature). Importantly this research was the first example of fast polymerisations in bulk with stereocontrol being possible at high levels of conversion, making it particularly interesting for use in industry.

Davison *et al.* further demonstrate that upon the application of diamine-(bisphenolate) ligands around group IV metal centres (**xxv** - **xxvi** **Figure 1.2.2.6**) a reduction in the levels of stereocontrol is observed such that a maximum $P_m = 0.75$ was obtained with complex **5**.⁵² This difference is attributed to the structural differences in the catalysts. Ligands of the type **xxv** or **xxvi** can form C_2 symmetric

chiral complexes, whereas catalysts of type (c) form nonchiral C_S symmetric complexes. The mechanism at work here must be that of enantiomorphic site control, as demonstrated by these results, despite the use of a nonchiral ligand.

Davidson *et al.* also demonstrated the first and only instance of a single site germanium catalyst for the ROP of lactide using this ligand, **xxiv Figure 1.2.2.6**.⁵³

This catalyst is employed in bulk polymerisations at 130 °C and produces heterotactic PLA ($P_r = 0.78 - 0.82$). The mechanism for this catalyst is identified as involving several particularly complex steps, with a low energetic barrier to inversion of the stereochemistry at the metal centre.

Mountford *et al.* have employed a range of rare earth metals with diaminobis(phenoxide) ligands to form dimeric borohydride complexes.⁵⁴ An yttrium compound gave the highest heterotactic enrichment, $P_r = 0.87$, complex **xxvii Figure 1.2.2.6**. The identical complexes of yttrium, samarium and neodymium are all dimeric, at least in the solid state, and when the polymerisation is carried out in THF all produce heterotactic enrichment to some degree (Yttrium $P_r = 0.87$, Samarium $P_r = 0.72$, and neodymium $P_r = 0.64$).

A similar, achiral, tetradentate alkoxy-amino-bis(phenolate) ligand, **xxx, Figure 1.2.2.6**, has been used to synthesise heterotactic PLA from *rac*-lactide with a variety of group III metals.⁵⁵ Carpentier and coworkers have explored the use of lanthanum, yttrium and neodymium with varying degrees of success. Yttrium has proved to give the greatest stereocontrol with P_r of up to 0.9 possible with tailoring of the ligand system, initiating species and solvent. Indeed the need to carry out polymerisations in THF is shown by a reduction of P_r from 0.8 to 0.6 in moving to toluene as a solvent. The significantly decreased stereocontrol of lanthanum and

neodymium when compared to yttrium strongly suggests that the metal centre has a direct influence in the polymerisation process. The ionic radius of the metal centre is believed to be an influence here; presumably the small size of yttrium gives better selectivity during the approach of the monomer. It has also been suggested that group 3 metal isopropoxides can become aggregated, at least to dimers, a process that may be involved in the lactide coordination process.⁵⁶

The steric bulk of the substituents on the aromatic rings, in particular the *ortho*-position, significantly affect the stereocontrol.⁵⁷ Increasing the steric hindrance of these groups also reduces the rate of polymerisation as would be expected, although these catalysts are extremely fast, completing a DP = 200 polymer in 20 minutes at room temperature, so the reduced rate is insignificant. Polymerisation of *meso*-lactide results in modestly syndiotactic polymer ($P_r = 0.76$), indicative of a chain end control mechanism.

In an analogous fashion to the (salen/salan)aluminium catalysts, the metal alkoxide is commonly derived *in situ*. Altering the ligand that is lost upon chelation of the alcohol, in this case *iso*-propanol, also affects the stereocontrol with $-N(SiMe_3)_2$ being particularly ineffective. Recently, Carpentier *et al.* have employed this *in situ* alkoxide generation to show that these catalysts are capable of immortal lactide polymerisation.⁵⁸ This allows a single catalytic species to produce up to 50 polymer chains through the application of 50 equivalents of alcohol with respect to catalyst. The PLA synthesised in this manner still shows heterotactic microstructure ($P_r = 0.9$) as well as demonstrating a high level of control over the polymerisation (PDI = 1.08).

1.2.2.4 Miscellaneous ligands

A range of other catalytic metal complexes that demonstrate stereocontrolled ROP but do not fit into the broad categories outlined above. Although each area has not received a great deal of research in the ROP of lactide, they are of significant interest due to their high levels of stereocontrol.

Okuda and coworkers have reported the use of complexes of the type **xxxi** - **xxxiv**, **Figure 1.2.2.7**, to show highly heterotactic selectivity for the ROP of PLA from *rac*-lactide at room temperature ($P_r = 0.67 - 0.96$).⁵⁹ A range of dithia-alkanediyl-bridged bisphenolato (OSSO)-type ligands are reported with varying activity and selectivity, based around the length of the S-S spacer unit. More flexible thiolate linkers provided the highest heteroselectivities in combination with sterically bulky *o*-phenoxy substituents (From **Figure 1.2.2.7** - **xxxi**: $P_r = 0.96$; **xxxii**: $P_r = 0.94$; **xxxiii**: $P_r = 0.93$; **xxxiv**: $P_r = 0.94$). A new mechanism involving the dynamic monomer recognition is proposed to control stereoselectivity based on the fluxionality of the ancillary ligand. This interconversion of the ligand configuration is significantly different from the commonly known mechanism for chain end control and is currently an area for further investigation. These complexes have also been demonstrated to give stereoregular polymer when employed with yttrium and lutetium.⁶⁰ Increase in the heteroselectivity was observed by increasing the bulk of the bis(phenolato) ligands, although a more significant effect is again observed by changing the bridging moiety. Only a C3 or C4 bridge allows

fluxionality for interconversion of the ligand framework. This mechanism is coined as “a dynamic enantiomorphic site control” mechanism.

Metal complexes bearing trispyrazolyl- and trisindazolylborate ligands **xxxv**, **Figure 1.2.2.7**, have been applied to a range of metals in the research of Chisholm *et al.*⁶¹ Although these ligands give only modest stereocontrol with zinc and magnesium, (Zn shows no enantiomeric preference, Mg demonstrates a slight propensity to form syndiotactic polymer from *meso*-lactide) calcium centered complexes have produced highly heterotactic polymer ($P_r > 0.9$). The calcium species is also significantly more reactive than either the magnesium or zinc, completing DP = 100 polymerisation of *rac*-lactide in 1 min compared to 1 h and 6 days respectively for Mg and Zn respectively. These catalysts also demonstrate anomalous behaviour in copolymerisations of 1:1 *meso:rac*-lactide. The zinc catalyst, despite its modest stereocontrol, preferentially polymerises *L*-lactide from this mixture in comparison to *meso*-lactide for the other two systems. This behaviour suggests that the stereocontrol is from an enantiomorphic site controlled mechanism imposed by the achiral catalyst.⁶²

(Trisphenolate)titanium alkoxide complexes, **xxxv** **Figure 1.2.2.7**, have been employed in the heteroselective polymerisation of *rac*-lactide by Hofmeister and coworkers.⁶³ Despite significantly higher heteroselectivity than previous titanium catalysts ($P_r = 0.82$), an induction period of up to 30 minutes was observed using these catalysts. This was attributed to the steric bulk of the *para*-substituent interfering with conformational isomerisation of the trisphenolate ligand.

A series of bis(thiophosphonic amido)yttrium catalysts, **xxxvi**, **Figure 1.2.2.7**, have been employed in the ROP of *rac*-lactide by Williams and coworkers.⁶⁴ These

catalysts have rather modest activity with polymerisations at room temperature taking in the order of a few days, however they demonstrate a significant heterotactic bias (xxxvi, **Figure 1.2.2.7** - $P_r = 0.79$). It is interesting to note that these catalysts heavily transesterify the polymer chain, inevitably scrambling the stereochemistry, and if this could be controlled would be capable of higher levels of stereocontrol.

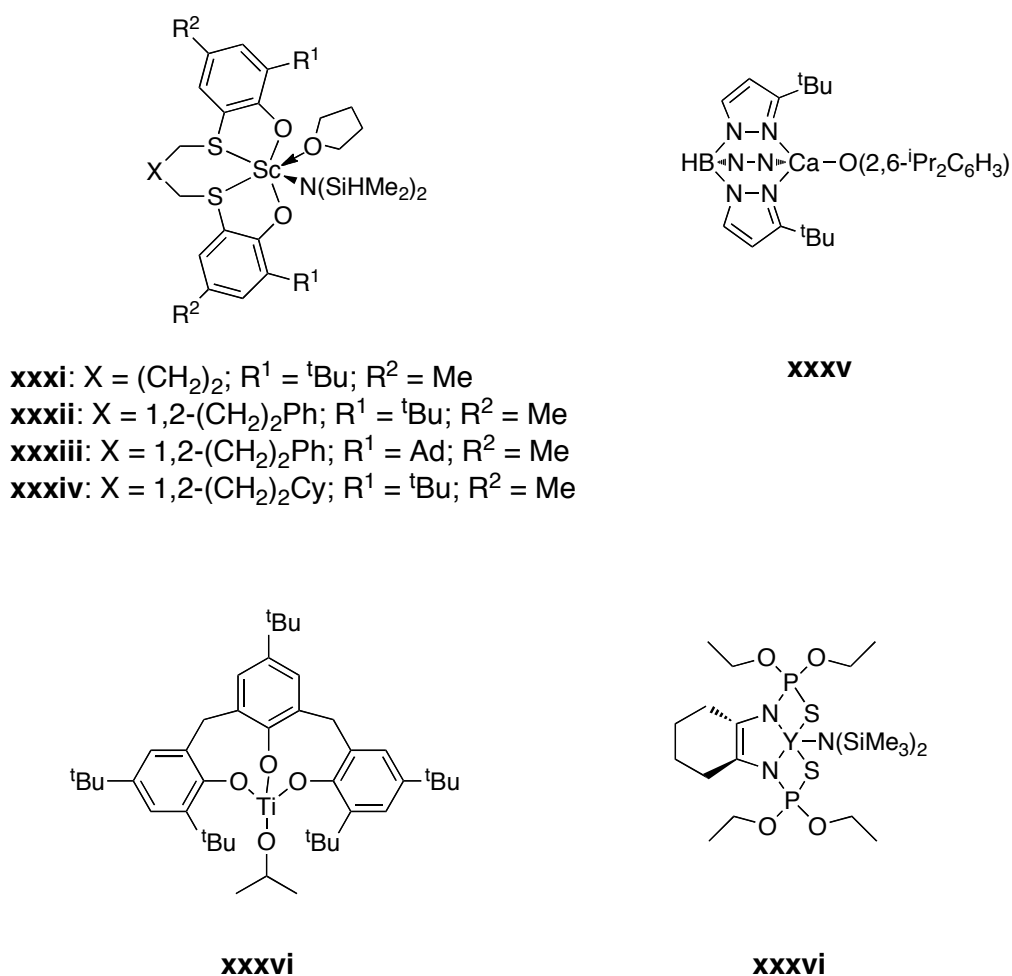


Figure 1.2.2.7 Miscellaneous catalysts for the stereocontrolled ROP of lactide.

Interestingly, metal salts without the support of bulky or chiral ligands have recently been shown to mediate the stereospecific ROP of lactide. Alkoxychloridotitanium(IV) complexes of the general formula $\text{TiCl}_x(\text{O}^i\text{Pr})_{4-x}$ provide moderate levels of stereocontrol.⁶⁵ In both solution polymerisation, 70 °C, and bulk polymerisation, 130 °C, it was observed that low levels of heterotacticity were present ($P_r = \sim 0.7$). It was noted that with an increased number of chlorine ligands, greater levels of stereocontrol were observed.

A recent investigation by Hillmyer *et al.* has also employed indium to access stereocontrolled polymerisation.⁶⁶ Through the combination of indium(III) chloride and NEt_3 it was possible to form heterotactic PLA through the application of *rac*-lactide and benzyl alcohol ($P_r = 0.9$). The polymerisation allows high levels of control although transesterification is shown to occur at long reaction times. Interestingly stereocontrol was shown only to be possible with *rac*- and not *meso*-lactide. This is possibly a result of the formation of complex species for initiation or because both stereocentres are involved in chain end control. This is a particularly simple catalytic system, although the exact mechanism for the polymerisation and stereocontrol is not understood at this stage.

1.2.3 Organocatalytic ROP

Recent interest in organic catalysts for the ROP of lactide has shown that it is possible to achieve very high levels of control over the polymerisation. However, despite the number of catalysts identified only two examples have been shown to allow for stereocontrol of the polymer, and both of these have been at significantly reduced temperatures. Stereocontrol is only achieved at low temperatures, this is believed in all these cases to be a reflection of the steric hindrance of the active site, although increased strength of hydrogen bonds at this temperature should not be ruled out.

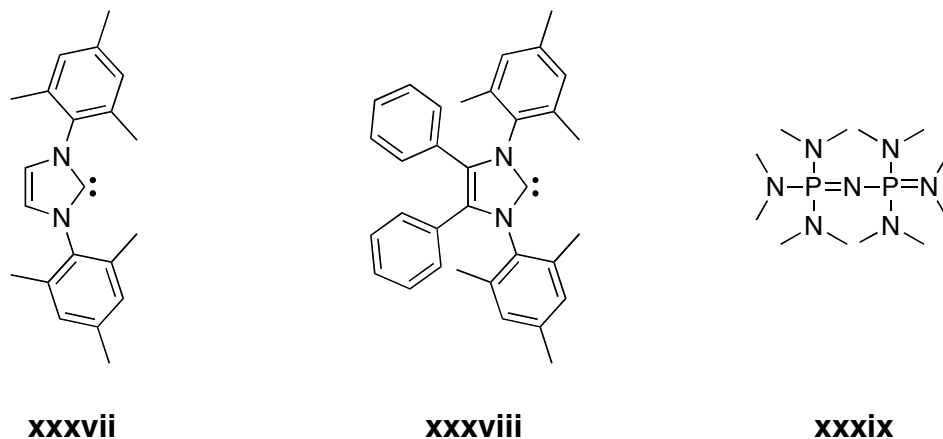


Figure 1.2.3.1 Organic catalysts for the stereoregular ROP of lactide.

Hillmyer, Tolman and coworkers demonstrated the application of IMes NHC, **xxvii** **Figure 1.2.3.1**, at -20 °C in dichloromethane shows a preference for isotacticity ($P_m = 0.75$).⁶⁷ This discovery occurred during work involving the IMes NHC as a ligand for a dimeric zinc complex, but was nevertheless the first reported case of stereoregular polymer synthesised using an organic catalyst. Waymouth, Hedrick and coworkers were able to advance on this work, showing that, despite being synthetically challenging, the application of sterically encumbered NHCs, **xxviii**, **Figure 1.2.3.1**, for the synthesis of isotactic poly(lactide) with $P_m = 0.9$ at -78 °C.⁶⁸ Initial results suggested that enantiomorphic site control was an important factor in the stereocontrol due to the chirality of the catalyst. However, the catalyst showed no improvement in stereoregularity when employed in a racemic mixture suggesting that steric congestion of the active site, and therefore chain end control, was the mechanism of stereocontrol. It was also possible to synthesise heterotactic PLA ($P_m = 0.83$) from *meso*-lactide using these catalytic systems.

Dimeric phosphazene bases, **xxix**, **Figure 1.2.3.1**, have recently been demonstrated by Wade *et al.* to produce highly stereoregular isotactic PLA ($P_m = 0.95$).⁶⁹ Application of this sterically encumbered catalyst at -75 °C was required to achieve this stereocontrol, but such is the reactivity of these species that, even at this low temperature, a PLA of DP 100 is complete within 3 hours. Phosphazene bases are believed to polymerise PLA through an activated alcohol mechanism, demonstrated by the ¹H NMR shift of the hydroxyl proton. A chain end control with stereoerror mechanism is suggested to predominate the polymerisation, presumably through the hindrance of the catalytic site by the bulky catalyst.

Levels of transesterification in these catalytic systems have previously been shown to be incredibly low, with hugely increased reaction times required to see any significant broadening of the PDI.

1.2.4 Conclusions and perspective

Significant advances in the stereocontrolled ROP of lactide have been made over the last decade. Through judicious choice of the metal–ligand system high levels of iso- or heterospecificity can be targeted. Future developments will undoubtedly look to further develop the range of stereospecific catalyst species to develop greater water tolerance, increased selectivity towards alcoholic initiators and propagating species over water, lower cost, recoverability and lowered toxicity. While metal-free catalysts demonstrate many of these attributes, the development of catalysts that display high levels of stereoselectivity at ambient temperature will also be important.

1.3 Cyclic Polymers

As well as microstructure, it is also possible to control the physical properties of the polymer chain by accurate and quantitative control of the polymer architecture. Although there are a near infinite range of possible architectures for even a simple polymer chain they can broadly be divided into three categories; linear (including telechelic), star shaped (including dendritic and branched polymers), and cyclic polymers (including multiple cycles, rotaxanes and catenates). Although there has been a large amount of interest in the field of polymer architecture in these first two categories, very little research has been carried out on cyclic polymers. This is exemplified by a SciFinder search suggesting there are 50 times fewer hits for ‘cyclic polymers’ compared to ‘star polymers’. Recently, there has been increased interest in cyclic polymers, largely because of improved synthetic techniques, and several reviews have been written about them.^{70,71}

One possibility why very little research has been directed at cyclic polymers, is due to the difficulty encountered during the synthesis of these structures. Indeed, research has shown that once the polymer chain reaches high molecular weight the possibility of forming cyclic product by ring closing is greatly reduced.⁷² That is not to suggest that ring closing high molecular weight polymers is not possible, indeed there are many reports of cyclic polymer being produced as the by-product of reactions, but that the amount of linear, and other architectural impurities will become greater than the amount of cyclised product.

Despite the difficulty in their synthesis, cyclic polymers are of particular interest as they have been shown to provide significantly different physical properties and behaviour to that of their linear counterparts. Differences in melting temperature, T_g , viscosity and crystallisation behaviour have all been identified in cyclic structures when compared to similar linear polymers.⁷³ With this diversity of physical properties accessible through the application of cyclic polymers it is no wonder that current interest is directed at overcoming the inherent problems with their synthesis.

1.3.1 Characterisation

The characterisation of cyclic polymers is an area of particular interest as it is an important factor in demonstrating that cyclic product has been synthesized during a reaction. Proving the presence of pure cyclic polymer, and showing the structure of it, is a particularly interesting challenge. As yet there is very little evidence that can be gained without the comparison to an otherwise identical linear counterpart of the cyclic polymer. In the case of comparison, it is possible to examine the MALDI-ToF MS, ^1H and ^{13}C NMR, and GPC of the polymers. If the reaction producing the cycle is accompanied by a shift in molecular weight or alteration of NMR signals, then this analysis becomes a simple technique for the identification of the reaction, although in itself this is not evidence for the cyclisation. MALDI-ToF MS analysis will also reveal a change in molecular weight due to a leaving group, or additional

moieties added, from the cyclisation step. These techniques are limited by a problem, as at high molecular weight the NMR signals will become minute and shifts in molecular weight less significant and therefore much harder to identify.

In comparison to the limitations of MALDI-ToF MS and NMR, GPC data is of vital importance in the identification of complete cyclisation, and provides a unique tool for examining purity. In all cases cyclic polymers have, in comparison to their linear counterparts, a reduced hydrodynamic volume caused by the reduced freedom of the chain. As GPC is a measure of hydrodynamic volume and not molecular weight, a decrease in the apparent M_n and M_w of the polymer would be observed in the case of a cyclic product. This particular phenomenon is therefore diagnostic of the presence of cyclic polymers and also provides an insight into the level of linear impurity, as it will generally provide a distinct and separate peak by GPC if it is present. It is also possible to examine the more complex structures that are possible based around cyclic polymers, however due to the complexity of the system very pure materials would be required.⁷⁴

Intrinsic viscosity measurements can also be used to determine if the polymer is cyclic in comparison to its linear counterpart. However, as other architectural or functionality changes can affect the viscosity of the polymer, this is, again, not in itself evidence for the cyclisation being complete. It is also important to note that viscosity measurements on low molecular weight polymers are particularly challenging to achieve, and this may therefore be unsuitable for a large number of cyclic polymer syntheses.

It has also been reported that cyclisation of the polymer can cause an increase in the glass transition temperature of the resultant polymer.⁷⁵ Unfortunately, there has not

been a large amount of non-theoretical research into this topic and the nature of polymers means that it is not always possible to examine this particular phenomenon.

Finally, a recent report by Grubbs and coworkers has demonstrated that if you can generate a cyclic polymer that is both large and rigid enough it is possible to observe it *via* microscopy techniques.⁷⁶ This was achieved through a G2 dendritic type monomer and a degree of polymerisation of around 2000, and although this is not necessarily possible for a lot of cyclic polymer syntheses, it is a significant step forward in the characterisation of cyclic polymers.

1.3.2 Synthesis

Cyclic polymers can be synthesized, largely, in one of two ways; firstly, the synthesis of a linear polymer followed by the reaction of the chain ends, and secondly, through the application of a catalyst which predominantly forms cyclic polymer products. Some unique synthetic techniques also exist but, to remain concise, only the advantages and disadvantages of these two main techniques will be the focus here.

1.3.2.1 Chain end Reaction

Cyclisation of the polymer chain through tethering the chain ends directly opposes the probability of the chain ends meeting in solution. For this reason alone cyclisation *via* this method has not been reported to produce any cyclic polymers with a molecular weight of greater than 40,000 g.mol⁻¹, a problem that can only overcome through the use of higher, or *pseudo*-higher, dilutions. An example of how this would be possible has been applied recently through the application of micelle formation.⁷⁷ Using self-assembly to produce micelles it was possible to effectively contain the vast majority of alkyne chain ends inside the micelle rendering them inaccessible for ‘click’ chemistry with the azide chain ends on the outside of the micelle. The slow transfer of chains between micelles allowed for CuAAC cyclisation to occur in the bulk solution at extremely low dilutions despite the overall concentration of the polymer in solution being significantly higher (CMC was determined to be 1.02 x 10⁻² g/L). In this example cyclic PMEO₂MA-*b*-POEGMA block copolymers with a molecular weight of up to 15,000 g.mol⁻¹ were synthesised.

Despite the shortcomings involved in techniques that have to overcome the probability of chain ends meeting, this is a synthetic route that has received a great deal of attention due the comparative ease with which it can be complete; in many cases very little additional synthesis is required to perform the cyclisation. It is important to note here, that any techniques employed must give complete chain end

fidelity at each stage of the polymer synthesis, thus reducing linear impurities, and therefore some polymerisation techniques are inappropriate for this method.

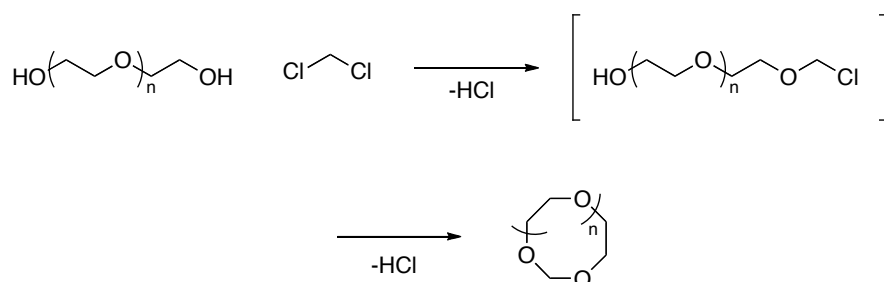


Figure 1.3.2.1 Cyclisation of poly(ethylene glycol) using dichloromethane.

The earliest report of cyclising polymer chains in this was that of Booth *et al.*, demonstrating that PEG and PEG-*b*-oxybutlene were cyclised *via* the reaction of the chain ends with CH_2Cl_2 (**Figure 1.3.2.1**).⁷⁸ The yields that were achieved using this reaction ranged from 30 – 80 %, and rigorous purification was required in order to obtain pure cyclic product by GPC analysis. Booth and coworkers later demonstrated that through the introduction of a non-solvent for the polymer chain during the cyclisation step, in this case hexane for poly(oxyethylene)s, yields of cyclic product could be improved.⁷⁹ It was postulated that this was because of the coiling effect that would be induced in the polymer chain by the non-solvent, effectively reducing the distance between the polymer chain ends. Purification was

still required in this case but higher molecular weight polymers could be achieved, up to $\sim 40,000 \text{ g.mol}^{-1}$ compared to $\sim 15,000 \text{ g.mol}^{-1}$ without the non-solvent present.

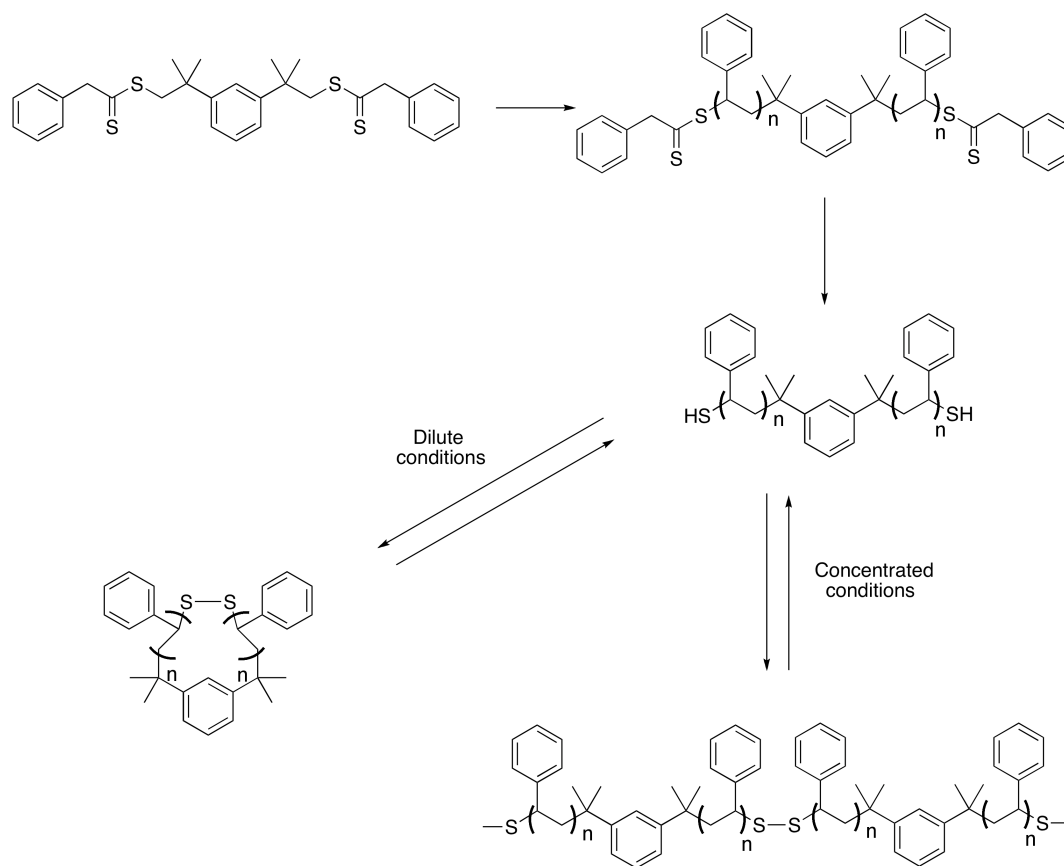


Figure 1.3.2.2 Thiol bridged reversible cycle formation.

In a more recent report Monteiro *et al.* were able to increase the yield of their cyclisation using a slow injection technique.⁸⁰ They were able to synthesise 50-100 mg of cyclic polymer over a period of three days with around 80% purity. The increased reaction time in this case was due to the cyclisation step being the

formation of a dithiol bridge, a relatively slow reaction. Employing poly(styrene) with both α - and ω - thiol functionality, synthesised *via* a reversible addition fragmentation chain transfer (RAFT) polymerisation method, enabled the formation of monocyclic product (**Figure 1.3.2.2**). At higher concentrations multiblock copolymers were observed. Interestingly, this reaction is reversible so it was possible to return to the linear polymer in both cases.

1.3.2.2 Purification

In all of the reports discussed so far, one of the main problems is the large amount of linear impurity that is encountered during the procedure. It is known to be the case that the linear impurity will tend to be of higher molecular weight than the cycle due to the decreased likelihood of the cyclisation occurring. This difference has allowed Semlyen and coworkers to use preparative GPC to purify the product, where the reduced freedom of the cyclic product combined with its lower molecular weight completely separates it from the reduced retention time of the linear impurities (normally multiple joined chains, hence the increased molecular weight). However, various other methods have been demonstrated to allow for purification of the cyclic polymer.

Fractional crystallisation of the polymer has proven to work on several occasions, but is particularly laborious, in many cases requiring many crystallisations for a

small amount of impurity to be removed. This technique highlights the differences in the physical properties of the cyclic and linear properties.

Interestingly, several recent reports have employed the use of rotaxane formation to purify the polymer. Huang and coworkers employed the known inclusion complex of β -cyclodextrin with poly(ethylene glycol) to purify their cyclic polymer.⁸¹ A similar technique to this has been employed recently by Grubbs *et al.* who used the formation of the rotaxane in much the same way, but used a crown ether attached to a solid support.⁸² Although this report was not of a chain end based cyclisation technique, this purification method enabled them to remove up to 30% impurity of linear polymer simply by a single pass of the polymer solution through the solid support.

1.3.2.3 Quantitative chain end conversion

In spite of the range of purification techniques that are available, in the ideal cyclisation procedure little or no purification would be required. Indeed, cyclisation techniques have been improved significantly since the initial research of Booth and Semlyen, and more recent techniques have allowed for near quantitative synthesis of cyclic product.

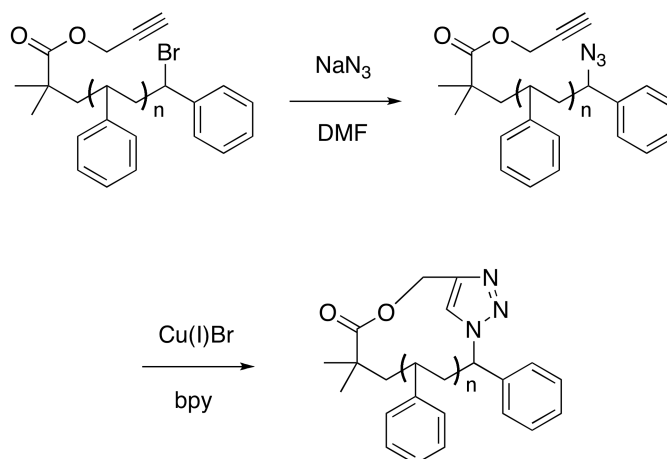


Figure 1.3.2.3 Copper catalysed ‘click’ chemistry in the synthesis of cyclic poly(styrene).

The recent increase in interest in ‘click’ type reactions in polymer chemistry has provided a particularly fast and quantitative group of reactions that are particularly useful in the synthesis of cyclic polymers. Grayson *et al.* have employed the copper catalysed azide-alkyne cycloaddition (CuAAC) reaction in the synthesis of cyclic poly(styrene) using *pseudo* high dilution techniques, involving overnight drop wise addition (**Figure 1.3.2.3**).⁸³ Due to the speed of this ‘click’ reaction, it was possible to achieve higher levels of purity in the cyclic polymers than those examples that had gone before, in fact the cyclisation was deemed to be quantitative. Conversion of the chain end was also simple, reaction of the Br bearing chain end from the polymerisation with NaN_3 . Despite previous reports concerning low chain end fidelity with radical polymerisation, this was not found to be a problem. Proof of cyclisation could be determined by $^1\text{H-NMR}$, GPC, MALDI-ToF and, in this case,

IR. Grayson and coworkers have also extended this methodology to the synthesis of cyclic block copolymers, poly(methyl methacrylate)-*b*-poly(styrene) cyclic block copolymer with molecular weight up to $\sim 10,000 \text{ g.mol}^{-1}$.⁸⁴ Two recent reports have demonstrated the use of CuAAC reactions in the cyclisation of poly(δ -valerolactone) and poly(ϵ -caprolactone).^{85,86}

1.3.2.4 Tethering

In order to overcome the unfavourable situation of the polymer chain ends having to encounter each other in solution, techniques have been developed to reduce the mobility of the polymers. One way of achieving this is to tether the polymer to a surface, therefore generating a situation where the freedom of the polymer is reduced and chain ends are held together.

Semlyen *et al.* have employed a technique similar to this to effectively reduce the distance between chain ends and favour cyclic product, through the application of a polymer support from which the polymers are grown.^{87,88} By tethering the polymers using ionic bonding that were able to increase the percentage yield of cyclic polymer synthesised. Purification was still required and this was carried out *via* preparative GPC with yields in the order of $\sim 20 \%$, and molecular weights up to $3,000 \text{ g.mol}^{-1}$ observed. This procedure was also thought to be applicable in the synthesis of catenates, through the addition of both small and polymeric cycles to the solution during the polymerisation.⁸⁹ However, with small cycles no catenates

were observed and with polymeric cycles characterisation of the products was too complicated to determine if catenated products were present in large quantities. It is likely that this technique would certainly not have resulted in these complex architectures exclusively, but a purely statistical mix of products.

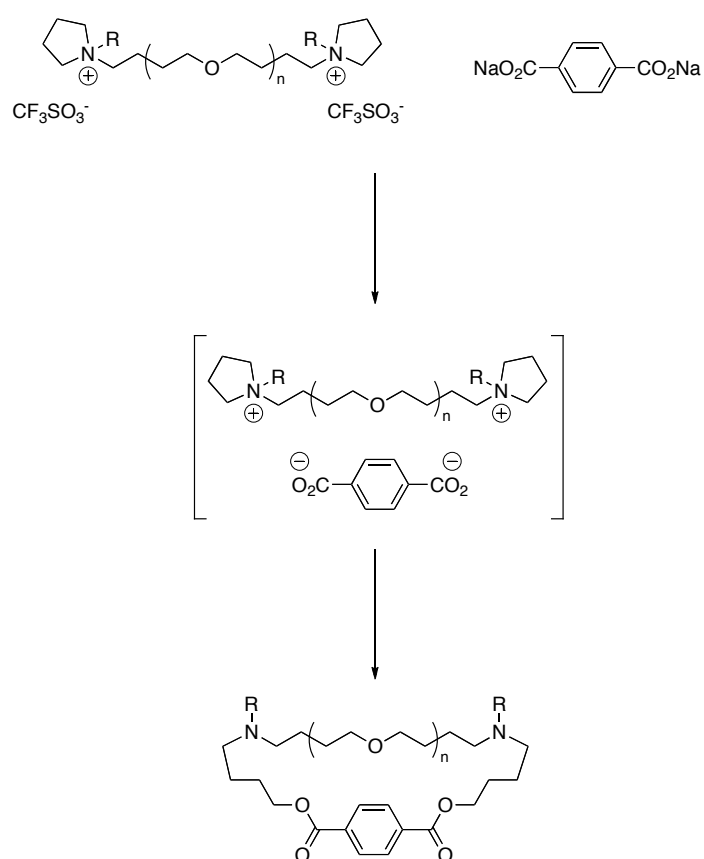


Figure 1.3.2.4 Electrostatic self-assembly in the synthesis of cyclic poly(tetrahydrofuran).

Using a not dissimilar process, Tezuka *et al.* have employed an electrostatic self assembly to allow for post polymerisation modification in the synthesis of cyclic poly(tetrahydrofuran) (**Figure 1.3.2.4**).⁹⁰ Using moderately dilute conditions (0.2 g/L) it was possible to selectively produce the cyclic product. The amount of anion could be controlled through repeated washing of the polymer solution with a water solution of the salt, guaranteeing an equal amount of polymer and counterion. Cyclisation was carried out *via* the temperature initiated, quantitative ring-opening of the pyrrolidinium salt end groups. A range of anions and solvents were examined that enabled a range of cyclic polymers, however, THF was notably better than other solvents. This is a novel approach to reducing the mobility of the chain ends prior to covalent cyclisation and enables a simple approach to achieving equimolar quantities of reactants.

1.3.2.5 Intermediate examples

In a similar fashion to these tethering examples, if it is possible to bring both ends of the polymer chain together using the catalyst then this will render it almost impossible to form anything other than cyclic product. Waymouth *et al.* were able to achieve this using a zwitterionic species in the polymerisation of lactide (**Figure 1.3.2.5**).⁹¹ In the absence of an alcohol initiator, *N*-heterocyclic carbenes (NHCs) form a cationic species at the α -chain end of the polymer. It is proposed that this forms a cyclic zwitterion with the putative polymer chain end allowing the further

insertion of monomer units without breaking the interaction between α - and ω -chain ends. When no more lactide is present cyclisation is completed by a back biting step resulting in a pure poly(lactide) cycle. This mechanism allows for high molecular weight but with slightly reduced control over the polymerisation resulting in broadened PDI compared to that of NHC initiated linear poly(lactide) (1.30 for cyclic poly(lactide) and 1.10 for linear poly(lactide)). Computational studies have shown that faster propagation than initiation allows for the control that these polymerisations exhibit despite being so rapid.⁹²

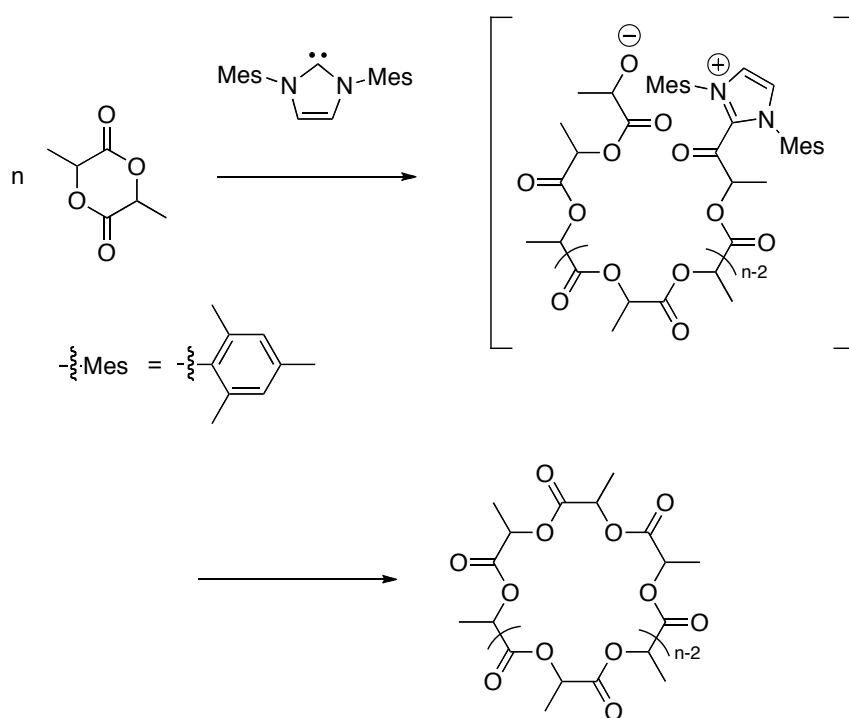


Figure 1.3.2.5 Zwitterionic polymerisation for the synthesis of cyclic poly(lactide).

In an analogous fashion Waymouth and coworkers were also able to employ a similar system using 1,3-dimethylsilylimidazol-2-ylidene to polymerise β -lactones *via* a cyclic initiator formed during the first turnover of the polymerisation.⁹³ This system can be employed alongside both functional lactones and lactide to produce complex cyclic polymers with molecular weights in the range 7,000 g.mol⁻¹ to 26,000 g.mol⁻¹ while maintaining a very low PDI (< 1.3). This system requires the addition of CS₂ to complete the cyclisation step due to the lack of a wholly zwitterionic polymerisation and therefore no back biting mechanism. A mechanistic study of this reaction implicates a novel mechanism involving the reversible opening of the spirocyclic imidazolidines.

A similar system with imadazole-based catalysts has been employed by Kricheldorf *et al.* with a zwitterionic polymerisation species that ring opens and backbites throughout the polymerisation. It is proposed that the mechanism for this reaction is kinetically controlled step growth polycondensation.⁹⁴ High levels of transesterification are observed in this polymerisation procedure as well as intensive racemisation; however, despite this no linear products are observed.

1.3.2.6 Catalyst cyclisation

Although synthetically more complicated, a catalyst system that has both ends of the polymer chain permanently attached allows for the optimum route to cyclic polymers. Using this technique means that the entropically challenging step of

bringing the chain ends together is not required and improves on the control issues evident in tethered and zwitterionic systems. These systems would completely remove the requirement for a high dilution step and in theory should completely remove the possibility of linear impurities.

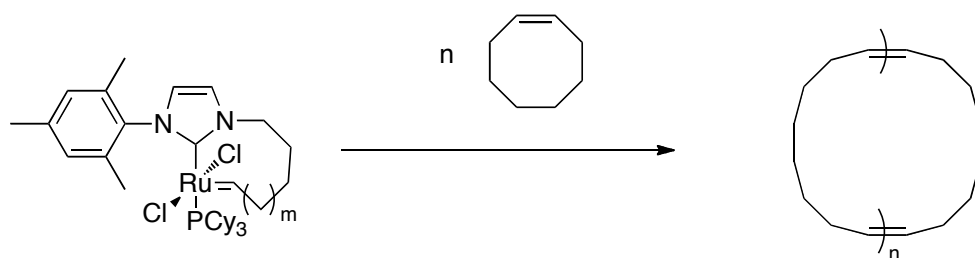


Figure 1.3.2.6 Modified Grubbs catalyst allowing for ring expansion metathesis polymerisation leading to cyclic poly(ethylene).

Grubbs and coworkers reported synthesising cyclic polymers in this way in 2002.⁹⁵ Through the application of the cyclic initiator, (**Figure 1.3.2.6**), it was possible to polymerise cyclooctene to produce exclusively cyclic polymers, a process that would come to be referred to as ring expansion metathesis polymerisation (REMP). In this report the polymers were hydrogenated to form cyclic poly(ethylene) that could be compared to linear polymers prepared in exactly the same way using a non-cyclic catalyst. Important analysis of these polymers involved the cleaving of the linear and cyclic polymers, *via* one 1,2-diol unit per polymer chain, and resulted in a decrease and increase in the molecular weight by GPC respectively. The

mechanism of this reaction is equilibrium driven giving, as expected from earlier research, a PDI of around 2.

The catalytic system reported by Grubbs et al. has been employed with a range of monomers including cyclooctadiene and 1,5,9-cyclododecatriene,⁹⁶ and more recently a range of highly functional and dendritic alkenes.⁹⁷ In some of these later cases, linear impurities could be observed during analysis and it was identified that linear polymers were exclusively the result of linear impurities in the monomer feedstocks. These linear impurities would result in a non-cyclic species being formed during the polymerisation, an error that cannot be readily corrected. Increasing the purity of the monomer allowed for higher molecular weights and narrower PDis to be obtained.

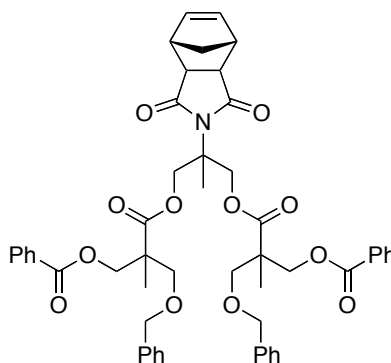


Figure 1.3.2.7 G2 dendritic monomer applied to REMP.

REMP with a dendritic monomer results in a polymer that is observable by AFM as a distinct doughnut shape, (**Figure 1.3.2.7**). In this case the size of the monomer

results in a rigid structure, although despite this inherent steric challenge, high molecular weights were achievable during the polymerisation (up to $\sim 5,000,000$ g.mol⁻¹). Further monomer additions after completing polymerisation resulted in no further growth, suggesting both that no catalyst is retained within the polymer structure and that thermodynamic equilibrium of ring sizes is not taking place, i.e. the polymerisation is purely kinetically controlled.

Grubbs and coworkers have carried out a large amount of work examining how the structure of the catalysts effects the kinetics and mechanism of the REMP.^{98,99} The findings of these studies show that the length of the linker between NHC and Ru can change the rate at which the catalyst releases from the system, shorter being a quicker release, but this in turn effects the rate of polymerisation, shorter being a slower rate. Alterations to the NHC substituents have also been shown to affect the rate of polymerisation, with saturation of the NHC backbone shown to increase polymerisation efficiency. Although the equilibrium determines the upper molecular weight of the polymers that were synthesised, with one catalyst it was possible to achieve molecular weights of 60 - 120 kg.mol⁻¹ for poly(olefin)s.

Using a similar system based on a tin catalyst, Kricheldorf *et al.* have been able to synthesise polyester based cyclic polymers. In their initial reports the cyclic product contains a bridging O-Sn-O bond from the spirocyclic tin initiator because no permanent cyclisation step is carried out.^{100,101} However, it is possible to quench the polymerisation using an acid chloride, possibly allowing for the synthesis of a cycle using a difunctional acid chloride, although this is carried out at high concentrations in initial reports.¹⁰² In an extension to this work, using the same polymerisation technique as Albertsson before,¹⁰³ Kricheldorf *et al.* were able to

generate tin-containing cycles that could be permanently cyclised using succinyl chloride.¹⁰⁴ These polymers showed a small amount of linear impurities by ¹H-NMR, possibly the reason for the broad PDis. Kricheldorf and coworkers proposed the “Inverse Ruggli-Ziegler Dilution Method” and they were the first to acknowledge that the impurities are probably higher molecular weight due to the decreased chance of cyclisation as previously mentioned.

In a similar fashion Osakada *et al.* used a palladium initiator for the cyclic polymerisation of 2-alkoxy-1-methylenecyclopropanes.¹⁰⁵ Two different catalyst structures were observed being inclusive of one or two palladiums in the cyclic initiating species. This resulted in cyclic polymers of 15,000 g.mol⁻¹ and 29,000 g.mol⁻¹ respectively and could be an issue in using a metal catalyst in this way. No reaction to complete cyclisation and remove the palladium was carried out in this example. The polyhomologation of boracyclanes can also be tailored for the synthesis of cyclic polymers, as demonstrated by Shea *et al.* in the synthesis of cyclic poly(methylene) ketones.¹⁰⁶

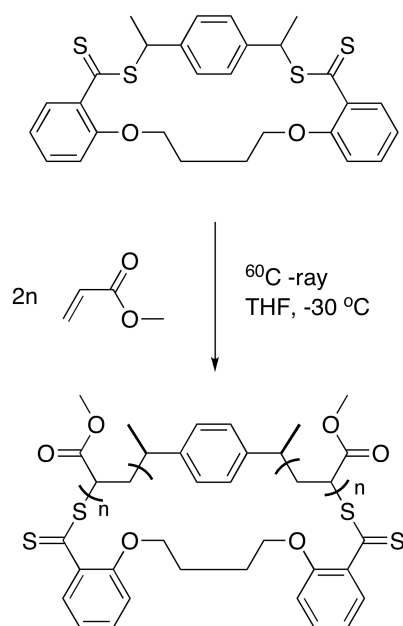


Figure 1.3.2.8 Synthesis of cyclic poly(methyl acrylate).

A cyclic initiator can also be applied in organic catalysis to form cyclic polymers as demonstrated by the work of Pan *et al.*, who used the cyclic initiator (**Figure 1.3.2.8**) to form cyclic poly(methyl acrylate).¹⁰⁷ Polymerisation at $-30\text{ }^{\circ}\text{C}$ was required to achieve controlled cycle formation due to the nature of radical polymerisations. At this temperature the reduced diffusion rate of the polymer results in repetitive monomer insertion without complex propagation and termination steps.

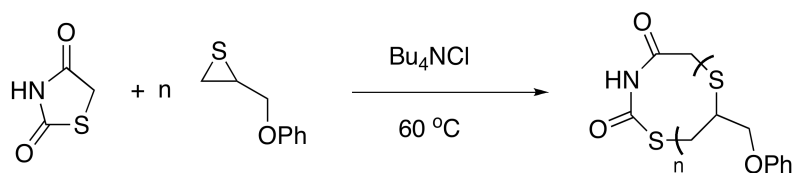


Figure 1.3.2.9 Cyclic thiocarbamate initiator for the synthesis of poly(sulphide)s.

Kudo *et al.* were able to employ a cyclic version of their previously identified thiocarbamate initiator to form cyclic analogues via a ring expansion polymerisation similar to that of Grubbs and coworkers (**Figure 1.3.2.9**).¹⁰⁸ Again, to maintain the cyclic nature of the initiating species cyclic monomers are required; thiiranes, in this case phenoxypropylenesulphide, were used to produce cyclic poly(sulphide)s. At low molecular weight very controlled polymers are observed, but as the molecular weight increases significant increases in the PDI occur such that a polymer with molecular weight of 4,200 g.mol⁻¹ has a PDI of 4.5. In an extension of this work it was possible to target higher molecular weights using a smaller initiator,¹⁰⁹ although it is possible that monomer purity is the limiting factor in both cases, as observed by Grubbs and coworkers.

1.3.2.7 Monomer controlled synthesis of cyclic polymers

Judicious choice of monomer can also be used to generate cyclic polymers, indeed simply a clean polycondensation reaction of a linear monomer would exclusively yield cyclic end products at 100% conversion.¹¹⁰ However, controlling the polymerisation can be more challenging using polycondensation techniques and therefore cyclic monomers offer a preferential option. Using cyclic monomers, from a high purity monomer feedstock, with no initiator has been shown to result in the synthesis of cyclic polymers. On many occasions this can be as a side product to the intended procedure, but there are several examples that specifically target such cyclic polymers.

Endo *et al.* have shown that the thermally induced polymerisation of cyclic disulphides, 1,2-dithiane and lipoic acid, results in the formation of an interlinked cyclic, or polycatenane, structure.¹¹¹ Evidence for this complex structure is gained from the photodecomposition of the polymer resulting in the dithiol bonds breaking and then reforming, and as a result becoming untangled. GPC analysis reveals a significant decrease in molecular weight over the first 4 h after which no further reduction is observed ($t = 0 \text{ h } M_n = \sim 1,000,000 \text{ g.mol}^{-1}$, $t = 4 \text{ h } M_n = \sim 8,000 \text{ g.mol}^{-1}$ and $t = 6 \text{ h } M_n = \sim 8,000 \text{ g.mol}^{-1}$). Physical characteristics also confirm this, with the elastic modulus of the material being high due to the presence of the physically linked ‘net like’ structure.

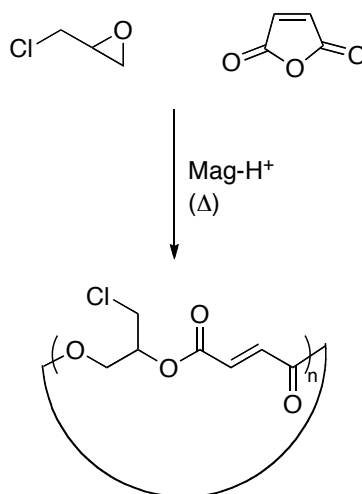


Figure 1.3.2.10 Cyclic poly(oxyepichlorohydrin oxymaloyl) from the acid catalysed polymerisation of maleic anhydride and epichlorohydrin.

Ferrarhi and coworkers were able to synthesise cyclic poly(oxyepichlorohydrin oxymaloyl) simply from the acid catalysed polymerisation of maleic anhydride and epichlorohydrin (**Figure 1.3.2.10**).¹¹² This is achieved through the application of acid catalyst to this polycondensation, and resulted in lower than 50 % yield of polymer with low M_n and high PDI ($M_n = \sim 1,000 \text{ g.mol}^{-1}$, PDI = ~ 5.0).

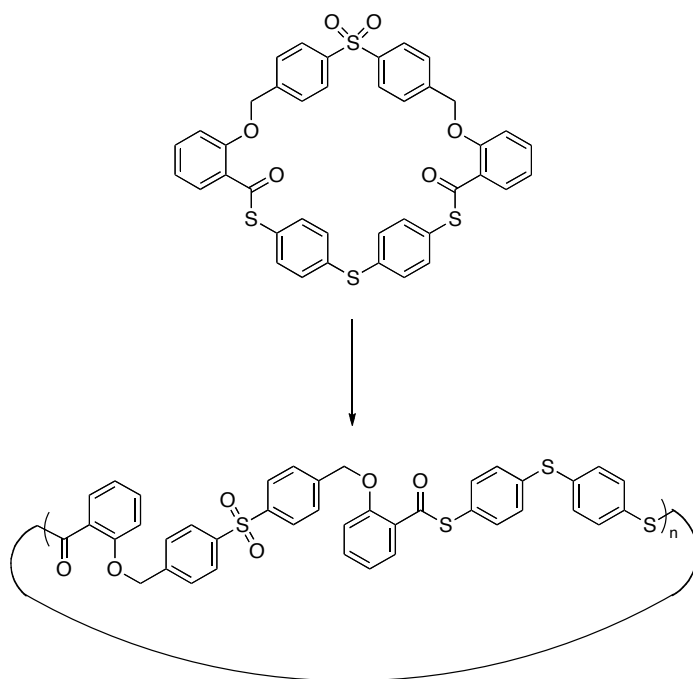


Figure 1.3.2.11 Thermodynamically controlled ring cross over polymerisation.

Nishikubo *et al.* have demonstrated the synthesis of cyclic polymers from the thermodynamically controlled ring crossover reaction of a cyclic dithioester monomer (**Figure 1.3.2.11**).¹¹³ The thioester forms a dynamic covalent bond in the presence of quaternary onium salts as catalysts leading to cyclic polymer product of molecular weights up to $3,500 \text{ g.mol}^{-1}$ with a PDI of 1.7.

1.3.2.8 Alternative routes

There are other routes to cyclic polymers, although generally very low in molecular weight due to the difficulties that have already been discussed. Manners *et al.* were able to synthesise cyclic oligomers of poly(ferrocenylsilanes) using 4,4'-dimethyl-2,2'-bipyridine (Me_2bpy) (**Figure 1.3.2.12**).¹¹⁴ The reaction initially produced a small amount (24 %) of polymeric structure, with a molecular weight of $11,900 \text{ g.mol}^{-1}$ and PDI 2.1, which MALDI-ToF MS analysis revealed was a mixture of products although clearly cyclic. From this reaction it was possible to isolate the oligomers, where $x = 2 - 6$, and the crystal structure of these showed conclusively that they were cyclic. At a lower temperature a larger proportion of the cyclic polymeric structure was formed (54 % compared to cyclic oligomers) with higher molecular weight, $M_n = 28,400 \text{ g.mol}^{-1}$, and narrower poly dispersity, PDI = 1.4, demonstrating the application of this technique in cyclic polymer synthesis.

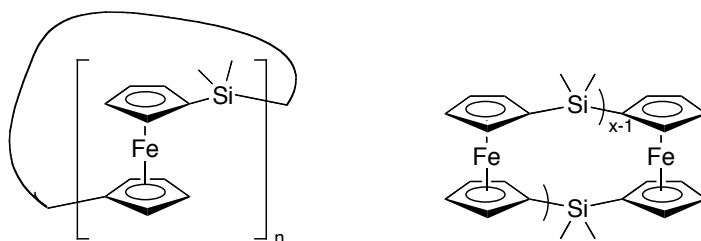


Figure 1.3.2.12 Cyclic poly(ferrocenylsilane) oligomers.

Semlyen and coworkers have shown that ring-chain equilibrium reactions under dilute conditions can be used in the synthesis of a range of cyclic polymers.¹¹⁵ The simple procedure of preparing a high mass linear polymers of tetraethylene glycol or 1,10-decandiol with a dimethyl ester, using dibutyltin oxide catalyst, followed by refluxing in chlorobenzene with further catalyst forms cyclic oligomers of $DP < 10$. It was possible to form oligomeric cycles with very little linear impurity, although a small amount could be identified in most examples.

1.3.3 Complex architectures

As has been examined in the syntheses given already, a significant change to the physical properties of the polymer are observed after the transition from a linear to a cyclic structure. It is interesting to see, therefore, that there are a few examples where more complex architectures have been synthesised, resulting in different alterations to the physical properties. Tadpole-shaped polymers have an interesting combination of both a cyclic and linear section and there are several syntheses for this type of structure. Huang *et al.* have synthesised such a structure, using cyclic poly(ethylene glycol) as a macroinitiator for the polymerisation of styrene to form multiple side chains.^{116,117} The cyclisation was carried out under *pseudo* dilute conditions in THF/heptane, to reduce the hydrodynamic volume of the polymer; TsCl and base were used to complete the cyclisation in both cases, although a slightly different approach was used to polymerise the poly(styrene). This polymer

could be applied in the extraction of dyes from a water phase, although the self-assembly of the structures involved was not considered.

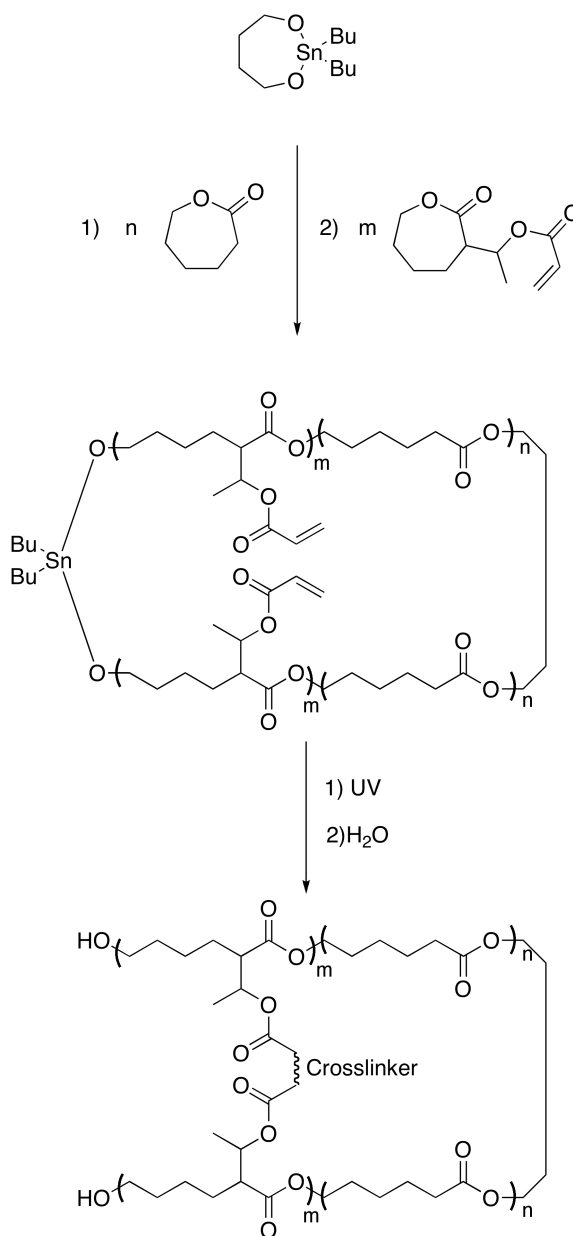


Figure 1.3.3.1 Tin based catalysis in the synthesis of cyclic poly(caprolactone).

Jérôme *et al.* were able to employ a system similar to that previously discussed of Kricheldorf *et al.* to synthesise more complex structures due to the nature of their cyclisation step (**Figure 1.3.3.1**).^{118,119} By incorporating a small amount of cross linkable monomer, α -(1-acryloyloxyethyl)- ϵ -caprolactone, as a secondary block to main poly(lactide), it was possible to photo-crosslink the polymer whilst keeping the tin catalyst in position at the ω -chain end. It was therefore possible to continue polymerisation resulting in a two-tailed tadpole like structure. It was possible to achieve this in relatively concentrated conditions, although it would be possible for crosslinking to occur between the cycles in very concentrated conditions.

The synthesis of linked cyclic structures has also been examined, with a large range of architectures possible. Tezuka *et al.* have demonstrated that using a similar technique to that previously described, employing a quadruply charged species in the electrostatic self-assembly enabled the synthesis of double cyclic, or 8 shaped, polymer.¹²⁰ In this example a poly(styrene) with α - and ω - functional *N*-methylpyrrolidinium salts was subjected to the heat treatment in the presence of a tetracarboxylate anion. GPC analysis of the resultant the structure reveals a molecular weight significantly higher than the linear analogue but lower than twice it (such that $M_n(\text{Bicycle})/M_n(\text{Linear}) = 1.52$).

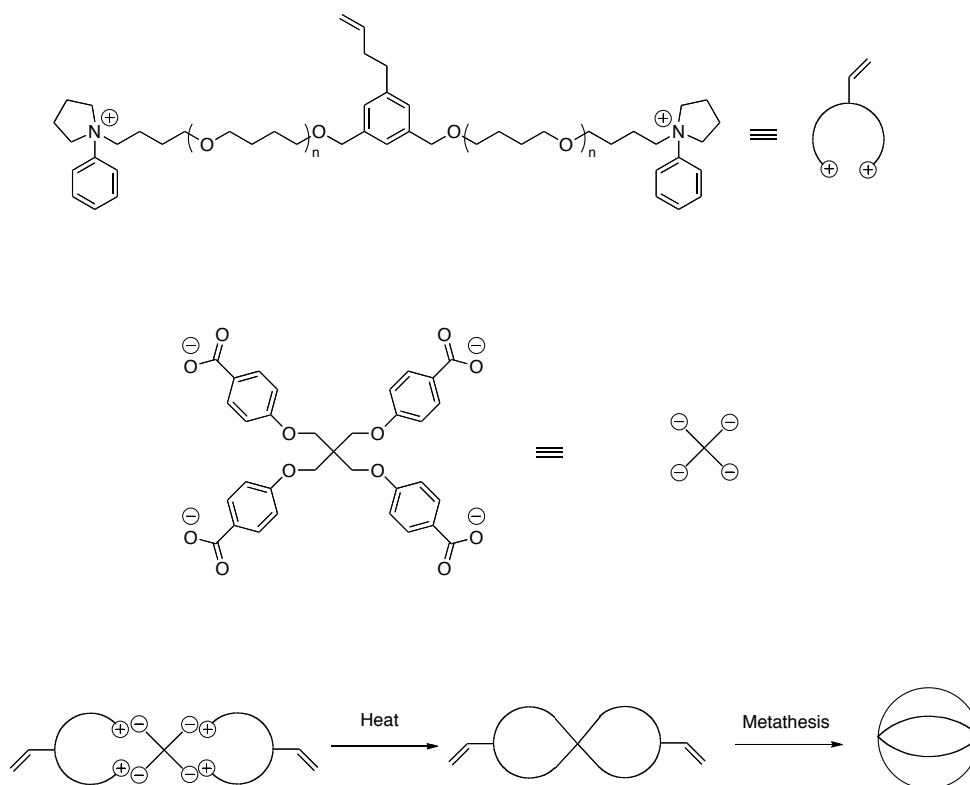


Figure 1.3.3.2 Synthesis of a doubly fused tricyclic loop poly(tetrahydrofuran).

Tezuka and coworkers have also been able to synthesise a doubly fused tricyclic loop polymer (**Figure 1.3.3.2**).¹²¹ Through the use of an initiator containing an allyl functionality that becomes the centre of the polymer chain they were able to complete a cyclisation step *via* Grubbs catalysed metathesis. After this second cyclisation step the molecular weight by GPC can be seen to decrease, 7,800 g.mol⁻¹ to 7,000 g.mol⁻¹, in a similar fashion to what is seen upon cyclisation of a linear precursor. The metathesis reaction is carried out under dilute conditions to

avoid intermolecular reactions occurring, with ^1H NMR analysis showing that this is the case.

Liu *et al.* have reported the synthesis of quatrefoil-shaped star-cyclic poly(styrene) containing a polyhedral oligomeric silsesquioxane (POSS) core.¹²² The synthesis of a poly(styrene) star bearing 8 terminal azide groups enabled them to, under high dilution conditions, use a difunctional propargyl ether to form the quatrefoil structure. DSC analysis revealed that the T_g of the star-cyclic structure was higher than that of the star-linear structure as had previously been identified for cyclic *versus* linear polymers. Liu and coworkers have also recently synthesised macrocycle-terminated core-cross-linked star polymers of molecular weight up to $450,000 \text{ g.mol}^{-1}$.¹²³ Through the application of CuAAC cyclisation, in a similar procedure to Grayson *et al.*, and post-cyclisation polymerisation they were able to synthesise tadpole shaped polymers of poly(styrene). Core cross-linking was carried out *via* ATRP polymerisation with divinylbenzene. The number of arms per polymer star varies from between 20 to 80 depending on the molecular weight of the tadpole polymer, steric hindrance being evident during the star formation.

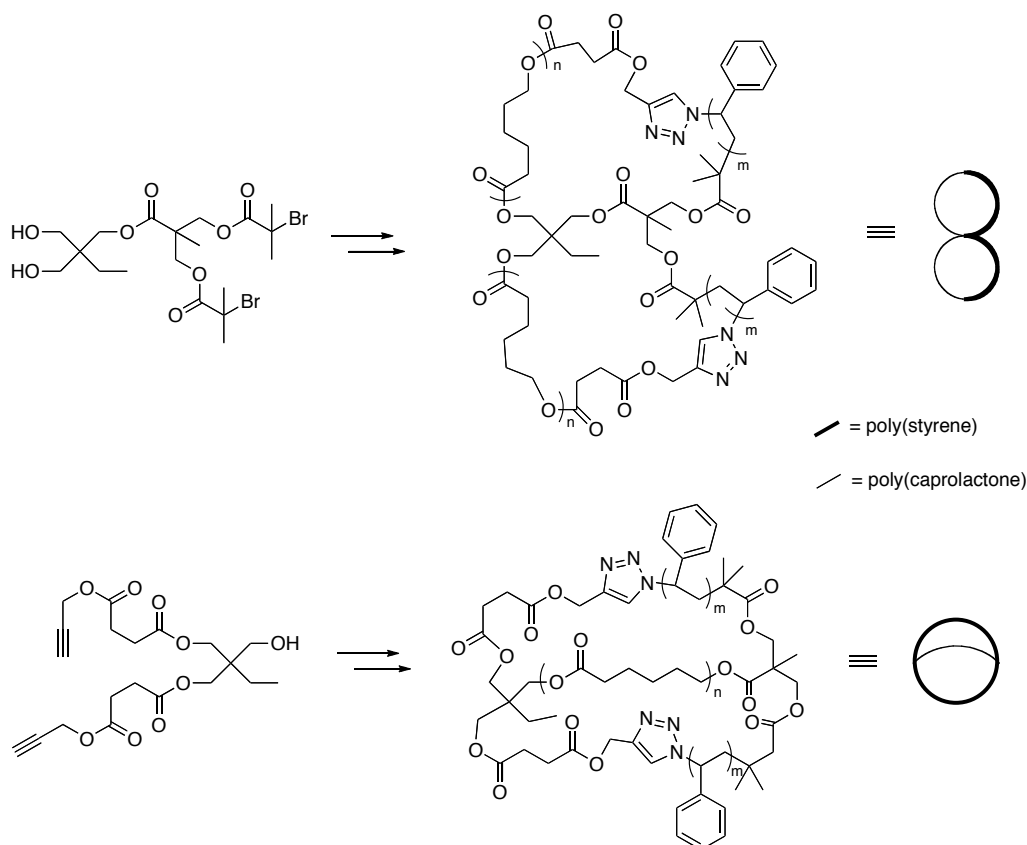


Figure 1.3.3.3 Poly(caprolactone)-*b*-poly(styrene) block copolymers with complex architectures.

Pan and coworkers have synthesised a block copolymer bicycle containing poly(caprolactone) and poly(styrene) (**Figure 1.3.3.3**).¹²⁴ Through the application of an initiator for two mechanistically distinct polymerisations followed by judicious choice of chain end modification they were able to perform ‘click’ chemistry between the poly(caprolactone) and poly(styrene) ω -chain ends exclusively. Using a not dissimilar approach they have also been able to form a

theta shaped structure with a poly(caprolactone) bridging a cyclic poly(styrene) (**Figure 1.3.3.3**).¹²⁵

Cyclic polymers have been grafted to a linear chain by Hemery *et al.*, resulting in well defined multicyclic poly(styrene) structures (molecular weights up to 87,000 g.mol⁻¹).¹²⁶ Cyclisation was carried out as they had previously reported in the literature using 1,3-bis(1-phenylethylenyl)benzene to couple a two-ended dianionic poly(styrene).¹²⁷ Purity of the cyclic product was not examined and it was believed to be a mixture of linear and cyclic polymer, both of which were grafted to a linear poly(styrene) resulting in a complex structure but maintaining a narrow PDI.

1.3.4 Cyclic block copolymers

Block copolymers have recently become an area of great interest in polymer chemistry due to their ability to self-assemble to form complex 3 dimensional structures. Cyclic block copolymers would therefore be of interest due to the influence that the constrained nature of the polymers would have on self-assembly. The synthesis of cyclic block copolymers is largely similar to those techniques that have already been covered, and indeed several examples have already been mentioned, but several recent examples show the versatility that can now be incorporated into these architectures.

Tezuka *et al.* were able to synthesise both AB and ABA cyclic block copolymers via ATRP, where A and B were poly(methyl acrylate)/poly(n-butyl acrylate) and

poly(*n*-butyl acrylate)/poly(ethylene oxide) respectively.¹²⁸ Cyclisation was carried out with end group modification using allyltributylstannane followed by the metathesis reaction between allyl chain ends. High dilution procedures were required and molecular weights of up to 9000 g.mol⁻¹ (PDI ~1.3) were observed. ATRP is a well-understood polymerisation so this technique should be applicable to a range of block copolymers.

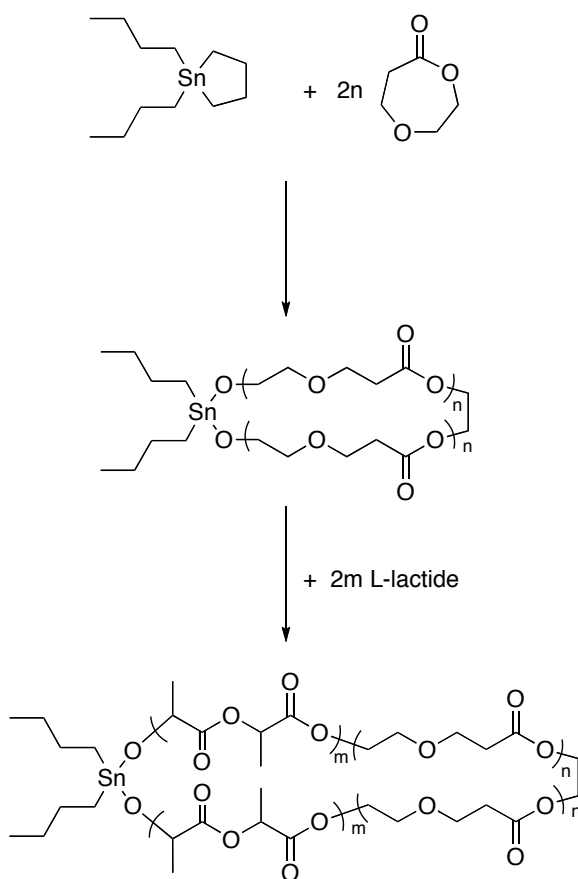


Figure 1.3.4.1 Tin catalyst in the synthesis of cyclic block copolymers of caprolactone and lactide.

Using a tin catalyst as previously discussed, Kricheldorf *et al.* were able to synthesise cyclic poly(lactide)-*b*-poly(caprolactone) structures (**Figure 1.3.4.1**).¹²⁹ It is also possible to synthesise block copolymers using the organic system proposed by Pan *et al.* but using poly(methyl acrylate) as an initiator.¹⁰⁷ In this way they were able to form cyclic poly(methyl acrylate)-*b*-poly(N-isopropylacrylamide) structures with controlled molecular weights and PDis.

1.3.5 Properties/self assembly

The properties of the cyclic polymers themselves can vary greatly dependant on the polymer itself, so logically they have to be compared to the linear version of the same molecular weight polymer. Early work did not generally cover the physical properties in enough detail to make a definite comparison between the forms, but recently this has become a staple procedure for proving that the polymer is indeed cyclic. Physical properties are seen to vary due to the reduced freedom imposed on the polymer chain by the fact that it is cyclic.

The self-assembly of cyclic polymer structures is of particular interest as the confined nature of the polymers results in different behaviour to that seen in linear polymers. Borsali and coworkers have studied the effect on micelle morphology

for linear versus cyclic poly(styrene)-*b*-poly(isoprene) copolymers self assembled in heptane.¹³⁰ It was identified that for otherwise identical polymers the linear version self-assembled into the classical spherical shape, where as the cyclic copolymer forms a giant wormlike structure. The difference between linear and cyclic polymers is believed to be due to the ‘double constraint effect’, where the polymer has a loop in both the shell and the core. No comparison is made between the cyclic polymer and a block copolymer of half the molecular weight, which may be more comparable to the behaviour of the cyclic polymer.

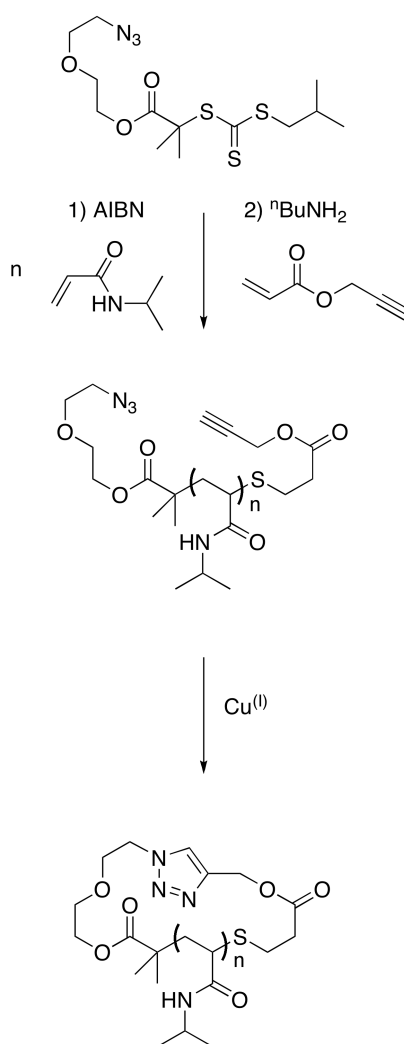


Figure 1.3.5.1 Cyclisation of poly(N-isopropylacrylamide).

Winnik *et al.* have examined the effect that the cyclic topology of polymers have on the phase separation of poly(N-isopropylacrylamide), poly(NIPAM) (**Figure 1.3.5.1**).¹³¹ Cyclisation was carried out using a similar technique to that of Grayson *et al.* using CuAAC for ring closing. For the three chain lengths that were examined, the phase separation in aqueous conditions takes place over a much

wider range of temperatures for the cyclic polymer compared to the linear. The reason for this is believed to be due to partial inhibition of the polymer chains behaving cooperatively during the coil-to-globule collapse. Although this is thought to be due to the packing of the chain segments being affected by the cyclic topology, it is also possible that these differences are caused by the tethering group itself; further analysis is underway to determine if this is the case.

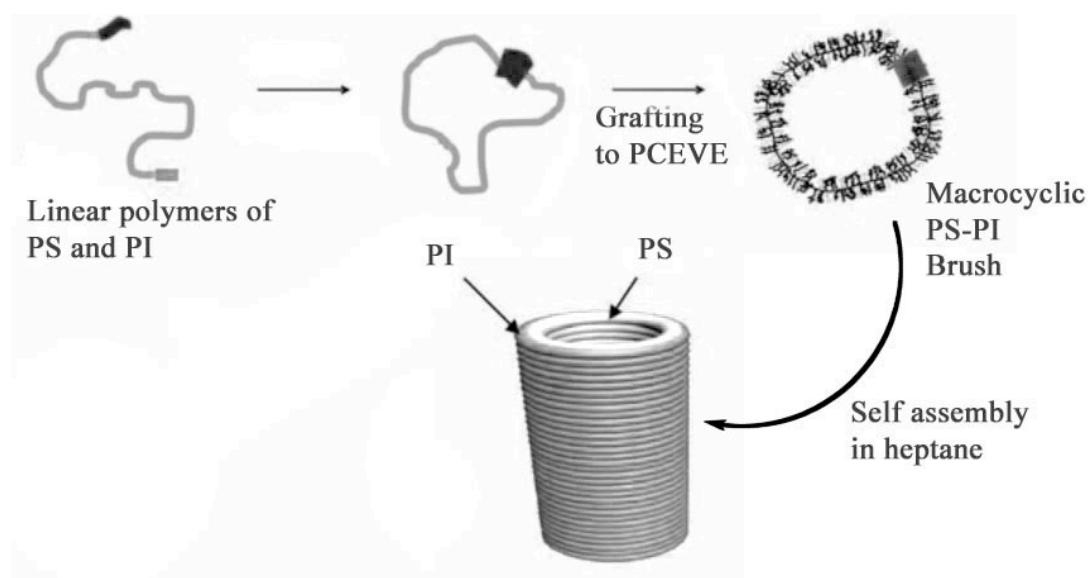


Figure 1.3.5.2 Self assembly of cyclic brushes with a poly(chloroethylvinyl ether) backbone.¹³²

Deffieux *et al.* have examined the self assembly of ABC triblock copolymers where the backbone was substituted poly(chloroethylvinyl ether).¹³² Using this backbone

to functionalise with randomly distributed poly(styrene) and poly(isoprene) branches results in a brush like cyclic polymer. After self assembly in a selective solvent for poly(isoprene) it was possible to form tubular structures that could be examined *via* microscopy techniques (**Figure 1.3.5.2**). Individual polymer structures are observable by AFM, and it is believed that together these form clusters, and therefore tubes during the solvent evaporation. It has recently been shown that this procedure can also be carried out to provide a very powerful method to investigate the structure and topology of macromolecules by directly imaging them under AFM.¹³³ It is demonstrated to be possible to synthesise and image a range of more complex architectures including catenates and trefoil knots (a cyclic polymer which has twisted to form knots).

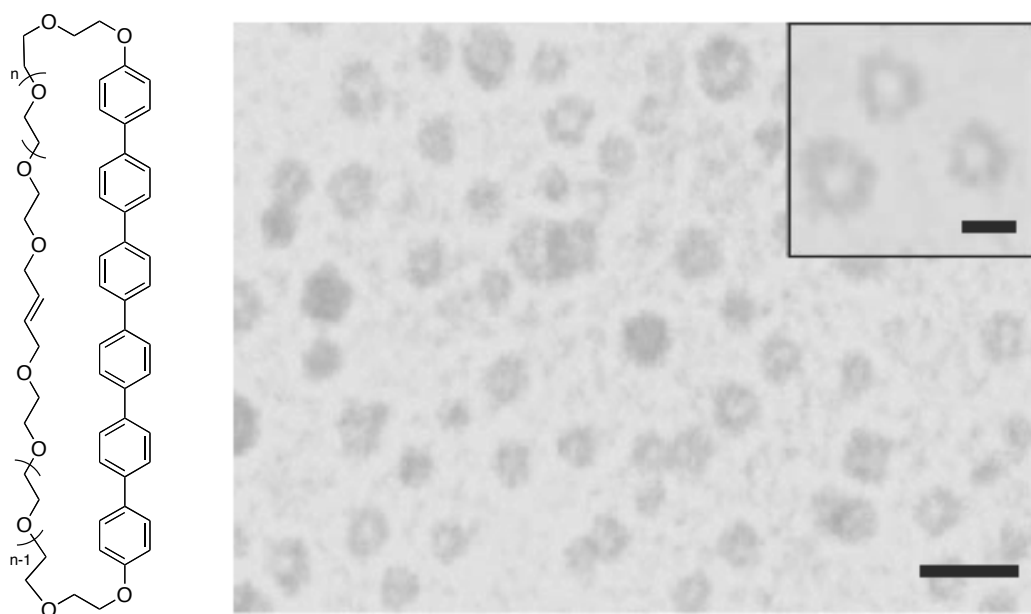


Figure 1.3.5.3 Self-assembly of cyclic poly(ethylene oxide) with a hexa-*p*-phenylene block in solution. The scale bar represents 20 nm and 5 nm (inset).¹³⁴

Another example is the work of Lee *et al.* where the incorporation of a stiff rod-like building block into an amphiphilic molecular architecture leads to self-assembly.¹³⁴ The cyclic polymers, consisting of poly(ethylene oxide) and hexa-*p*-phenylene ($M_n = 2000 - 2,500 \text{ g.mol}^{-1}$), were synthesised by a ring closing metathesis reaction in highly dilute conditions (0.005 M). In this case the self-assembly was driven by the strong interactions between the rigid poly-aromatic systems and resulted in the formation of barrel-like structures as depicted in (**Figure 1.3.5.3**). It is important to note that these structures are formed both in bulk and in solution making them of particular interest in a variety of well-defined organic nanostructures with biological functions.

1.3.6 Uses

As yet there is not a significant amount of research into applications for cyclic polymers. The costs of production coupled with the small quantities that can be generated by a large number of the synthetic routes make them unpractical in an industrial environment. However, recent research by Szoka *et al.* has revealed that polymer topology, cyclic versus linear, plays an important role in blood circulation time of a polymer.¹³⁵ In this case the cyclic block copolymer of α -chloro- ϵ -caprolactone and ϵ -caprolactone showed an increased half-life over its linear

counterpart. The longer t_{half} of the cyclic polymer may provide an interesting opportunity for the application of cyclic polymers in drug delivery.

1.4 References

- ¹ a) Dove, A.P., *Chem. Commun.*, **2008**, 6446. b) Dechy-Cabaret, O.; Martin-Vaca, B.; Borissou, D., *Chem. Rev.*, **2004**, *104*, 6147.
- ² a) Drumright, R.E.; Gruber, P.R.; Henton, D.E., *Adv. Mater.*, **2000**, *12*, 1841. b) Auras, R.; Harte, B.; Selke, S., *Macromol. Biosci.*, **2004**, *4*, 835. c) Uhrich, K.E.; Cannizzaro, S.M.; Langer, R.S.; Shakesheff, K.M., *Chem. Rev.*, **1999**, *99*, 3181.
- ³ Ovitt, T.M.; Coates, G.W., *J. Am. Chem. Soc.*, **1999**, *121*, 4072.
- ⁴ Chisholm, M.H.; Eilerts, N.W.; Huffman, J.C.; Iyer, S.S.; Pacold, M.; Phomphrai, K., *J. Am. Chem. Soc.*, **2000**, *122*, 11845.
- ⁵ Zell, M.T.; Padden, B.E.; Paterick, A.J.; Thakur, K.A.M.; Kean, R.T.; Hillmyer, M.A.; Munson, E.J., *Macromolecules*, **2002**, *35*, 7700.
- ⁶ Belleney, J.; Wisniewski, M.; Le Borgne, A., *Eur. Polym. J.*, **2004**, *40*, 523.
- ⁷ Coudane, J.; Ustariz, C.; Schwach, G.; Vert, M., *J. Polym. Sci. A: Polym. Chem.*, **1997**, *35*, 1651.
- ⁸ Fukushima, K.; Kimura, Y., *Polym. Int.*, **2006**, *55*, 626.
- ⁹ Ko, B-T.; Lin, C-C., *J. Am. Chem. Soc.*, **2001**, *123*, 7973.
- ¹⁰ Kasperczyk, J.E., *Macromolecules*, **1995**, *28*, 3937.
- ¹¹ Bero, M.; Dobrzyński, P.; Kasperczyk, J., *J. Polym. Sci. A: Polym. Chem.*, **1999**, *37*, 4038.
- ¹² Bero, M.; Kasperczyk, J., *Polymer*, **2000**, *41*, 391.

- ¹³ Leborgne, A.; Vincens, V.; Joulgard, M.; Spassky, N., *Makromol. Chem., Macromol. Symp.*, **1993**, 73, 37.
- ¹⁴ Spassky, N.; Wisniewski, M.; Pluta, C.; Le Borgne, A., *Macromol. Chem. Phys.*, **1996**, 197, 2627.
- ¹⁵ Wisniewski, M.; Le Borgne, A.; Spassky, N.; *Macromol. Chem. Phys.*, **1997**, 198, 1227.
- ¹⁶ Ovitt, T.M.; Coates, G.W., *J. Am. Chem. Soc.*, **1999**, 121, 4072.
- ¹⁷ Radano, C.P.; Baker, G.L.; Smith III, M.R., *J. Am. Chem. Soc.*, **2000**, 122, 1552.
- ¹⁸ Ovitt, T.M.; Coates, G.W., *J. Polym. Sci. A: Polym. Chem.*, **2000**, 38, 4686.
- ¹⁹ Chisholm, M.H.; Patmore, N.J.; Zhou, Z., *Chem. Commun.*, **2005**, 127.
- ²⁰ Majerska, K.; Duda, A., *J. Am. Chem. Soc.*, **2004**, 126, 1026.
- ²¹ Zhong, Z.; Dijkstra, P.J.; Feijen, J., *Angew. Chem. Int. Ed.*, **2002**, 41, 4510.
- ²² Zhong, Z.; Dijkstra, P.J.; Feijen, J., *J. Am. Chem. Soc.*, **2003**, 125, 11291.
- ²³ Du, H.; Pang, X.; Yu, H.; Zhuang, X.; Chen, X.; Cui, D.; Wang, X.; Jing, X.; *Macromolecules*, **2007**, 40, 1904.
- ²⁴ Chisholm, M.H.; Galluci, J.C.; Quisenberry, K.T.; Zhou, Z., *Inorg Chem.*, **2008**, 47, 2613.
- ²⁵ Nomura, N.; Ishii, R.; Akakura, M.; Aoi, K., *J. Am. Chem. Soc.*, **2002**, 124, 5938.
- ²⁶ Nomura, N.; Ishii, R.; Yamamoto, Y.; Kondo, T., *Chem. Eur. J.*, **2007**, 13, 4433.
- ²⁷ Hormnirun, P.; Marshall, E.L.; Gibson, V.C.; White, A.J.P.; Williams, D.J., *J. Am. Chem. Soc.*, **2004**, 126, 2688.
- ²⁸ Hormnirun, P.; Marshall, E.L.; Gibson, V.C.; Pugh, R.I.; White, A.J.P., *Proc. Natl. Acad. Sci.*, **2006**, 103, 15343.

- ²⁹ Tang, Z.; Chen, X.; Pang, X.; Yang, Y.; Zhang, X.; Jing, X., *Biomacromolecules*, **2004**, 5, 965.
- ³⁰ Ovitt, T.M.; Coates, G.W., *J. Am. Chem. Soc.*, **2002**, 124, 1316.
- ³¹ Liu, X.; Shang, X.; Tang, T.; Hu, N.; Pei, F.; Cui, D.; Chen, X.; Jing, X.; *Organometallics*, **2007**, 26, 2747.
- ³² Stanford, M.J.; Dove, A.P., *Macromolecules*, **2009**, 42, 141.
- ³³ Du, H.; Velders, A.H.; Dijkstra, P.J.; Zhong, Z.; Chen, X.; Feijen, J., *Macromolecules*, **2009**, 42, 1058.
- ³⁴ Pang, X.; Chen, X.; Du, H.; Wang, X.; Jing, X., *J. Organomet. Chem.*, **2007**, 692, 5605.
- ³⁵ Bouyahi, M.; Grunova, E.; Marquet, N.; Kirillov, E.; Thomas, C.M.; Roisnel, T.; Carpentier, J.-F., *Organometallics*, **2008**, 27, 5815.
- ³⁶ Alaaeddine, A.; Thomas, C.M.; Roisnel, T.; Carpentier, J.-F., *Organometallics*, **2009**, 28, 1469.
- ³⁷ Chen, H-Y.; Tang, H-Y.; Lin, C-C., *Macromolecules*, **2006**, 39, 3745.
- ³⁸ Pang, X.; Chen, X.; Zhuang, X.; Jing, X., *J. Polym. Sci. A: Polym. Chem.*, **2008**, 46, 643.
- ³⁹ Darensbourg, D.J.; Choi, W.; Karroonnirun, O.; Bhuvanesh, N., *Macromolecules*, **2008**, 41, 3493.
- ⁴⁰ Douglas, A.F.; Patrick, B.O.; Mehrkhodavandi, P., *Angew. Chem. Int. Ed.*, **2008**, 47, 2290.
- ⁴¹ Cheng, M.; Attygalle, A.B.; Lobkovsky, E.B.; Coates, G.W., *J. Am. Chem. Soc.*, **1999**, 121, 11583.

- ⁴² Allen, S.D.; Moore, D.R.; Lobkovsky, E.B.; Coates, G.W., *J. Organomet. Chem.*, **2003**, 137.
- ⁴³ Chamberlain, B.M.; Cheng, M.; Moore, D.R.; Ovitt, T.M.; Lobkovsky, E.B.; Coates, G.W., *J. Am. Chem. Soc.*, **2001**, 123, 3229.
- ⁴⁴ Jeske, R.C.; Rowley, J.M.; Coates, G.W., *Angew. Chem. Int. Ed.*, **2008**, 47, 6041.
- ⁴⁵ Dove, A.P.; Gibson, V.C.; Marshall, E.L.; White, A.J.P.; Williams, D.J., *Chem Commun.*, **2001**, 283.
- ⁴⁶ Dove, A.P.; Gibson, V.C.; Marshall, E.L.; Rzepa, H.S.; White, A.L.P.; Williams, D.J., *J. Am. Chem. Soc.*, **2006**, 128, 9834.
- ⁴⁷ Chisholm, M.H.; Gallucci, J.; Phomphrai, K., *Inorg. Chem.*, **2002**, 41, 2785.
- ⁴⁸ Chisholm, M.H.; Phomphrai, K., *Inorganica Chimica Acta*, **2003**, 350, 121.
- ⁴⁹ Chisholm, M.H.; Gallucci, J.; Phomphrai, K., *Inorg. Chem.*, **2005**, 44, 8004.
- ⁵⁰ Marshall, E.L.; Gibson, V.C.; Rzepa, H.S., *J. Am. Chem. Soc.*, **2005**, 127, 6048.
- ⁵¹ Chmura, A.J.; Davidson, M.G.; Frankis, C.J.; Jones, M.D.; Lunn, M.D., *Chem. Commun.*, **2008**, 1293.
- ⁵² Chmura, A.J.; Davidson, M.G.; Jones, M.D.; Lunn, M.D.; Mahon, M.F.; Johnson, A.F.; Khunkamchoo, P.; Roberts, S.L.; Wong, S.S.F., *Macromolecules*, **2006**, 39, 7250.
- ⁵³ Chmura, A.J.; Chuck, C.J.; Davidson, M.G.; Jones, M.D.; Lunn, M.D.; Bull, S.D.; Mahon, M.F., *Angew. Chem. Int. Ed.*, **2007**, 46, 2280.
- ⁵⁴ Bonnet, F.; Cowley, A.R.; Mountford, P., *Inorg. Chem.*, **2005**, 44, 9046.
- ⁵⁵ Cai, C-X.; Amgoune, A.; Lehmann, C.W.; Carpentier, J-F., *Chem. Commun.*, **2004**, 330.

- ⁵⁶ Ma, H.; Okuda, J., *Macromolecules*, **2005**, 38, 2665.
- ⁵⁷ Amgoune, A.; Thomas, C.M.; Roisnel, T.; Carpentier, J-F., *Chem. Eur. J.*, **2006**, 12, 169.
- ⁵⁸ Amgoune, A.; Thomas, C.M.; Carpentier, J-F., *Macromol. Rapid. Commun.*, **2007**, 28, 693.
- ⁵⁹ Ma, H.; Spaniol, T.P.; Okuda, J., *Angew. Chem. Int. Ed.*, **2006**, 45, 7818.
- ⁶⁰ Ma, H.; Spaniol, T.P.; Okuda, J., *Inorg. Chem.*, **2008**, 47, 3328.
- ⁶¹ Chisholm, M.H.; Galluci, J.; Phomphrai, K., *Chem. Commun.*, **2003**, 48.
- ⁶² Chisholm, M.H.; Eilerts, N.W.; Huffman, J.C.; Iyer, S.S.; Pacold, M.; Phomphrai, K., *J. Am. Chem. Soc.*, **2000**, 122, 11845.
- ⁶³ Russell, S.K.; Gamble, C.L.; Gibbins, K.J.; Juhl, K.C.S.; Mitchell III, W.S.; Tumas, A.J.; Hofmeister, G.E., *Macromolecules*, **2005**, 38, 10336.
- ⁶⁴ Hodgson, L.M.; Platel, R.H.; White, A.J.P.; Williams, C.K., *Macromolecules*, **2008**, 41, 8603.
- ⁶⁵ Kim, Y.; Jnaneshwara, G.K.; Verkade, J.G., *Inorg. Chem.*, **2003**, 42, 1437.
- ⁶⁶ Pietrangelo, A.; Hillmyer, M.A.; Tolman, W.B., *Chem. Commun.*, **2009**, 2736.
- ⁶⁷ Jensen, T.R.; Breyfogle, L.E.; Hillmyer, M.A.; Tolman, W.B., *Chem. Commun.*, **2004**, 2504.
- ⁶⁸ Dove, A.P.; Li, H.; Pratt, R.C.; Lohmeijer, B.G.G.; Culkin, D.A.; Waymouth, R.M.; Hedrick, J.L., *Chem. Commun.*, **2006**, 2881.
- ⁶⁹ Zhang, L.; Nederberg, F.; Messman, J.M.; Pratt, R.C.; Hedrick, J.L.; Wade, C.G., *J. Am. Chem. Soc.*, **2007**, 129, 12610.

- ⁷⁰ Hadjichristidis, N.; Pitsikalis, M.; Pispas, S.; Iatrou, H., *Chem. Rev.*, **2001**, *101*, 3747.
- ⁷¹ Laurent, B.A.; Grayson, S.M., *Chem. Soc. Rev.*, **2009**, *38*, 2202.
- ⁷² Jacobsen, H.; Stockmayer, W.H., *J. Chem. Phys.*, **1950**, *14*, 1600.
- ⁷³ Semlyen, J.A., *Cyclic Polymers*, Kluwer Academic, Dordrecht, The Netherlands, 2nd edn, 2000.
- ⁷⁴ Gorbunov, A.A.; Vakhrushev, A. V.; *Polymer*, **2004**, *45*, 6761.
- ⁷⁵ (a) Liu, H.; Wilén, C.-E.; Shi, W.; *Macromol. Theory Simul.*, **2002**, *11*, 459. (b) Liu, H.; Wilén, C.-E., *J. Polym. Sci., Part B: Polym. Phys.*, **2004**, *42*, 1235. (c) Wang, X.; Liu, H.; Qiu, L., *Mater. Lett.*, **2007**, *61*, 2350.
- ⁷⁶ Boydston, A.J.; Holcombe, T.W.; Unruh, D.A.; Fréchet, J.M.J.; Grubbs, R.H., *J. Am. Chem. Soc.*, **2009**, *131*, 5388.
- ⁷⁷ Ge, Z.; Zhou, Y.; Xu, J.; Liu, H.; Chen, D.; Liu, S., *J. Am. Chem. Soc.*, **2009**, *131*, 1628.
- ⁷⁸ Yan, Z.-G.; Yng, Z.; Price, C.; Booth, C., *Makromol. Chem., Rapid Commun.*, **1993**, *14*, 725.
- ⁷⁹ Yu, G.-E.; Sinnathamby, P.; Price, C.; Booth, C., *Chem. Commun.*, **1996**, 31.
- ⁸⁰ Whittaker, M.R.; Goh, Y.-K.; Gemici, H.; Legge, T.H.; Perrier, S.; Monteiro, M.J., *Macromolecules*, **2006**, *39*, 9028.
- ⁸¹ Pang, X.; Wang, G.; Jia, Z.; Liu, C.; Huang, J., *J. Polym. Sci. Part A: Polym. Chem.*, **2007**, *45*, 5824.
- ⁸² Boydston, A.J.; Grubbs, R.H., unpublished results.
- ⁸³ Laurent, B.A.; Grayson, S.M., *J. Am. Chem. Soc.*, **2006**, *128*, 4238.

- ⁸⁴ Eugene, D.M.; Grayson, S.M., *Macromolecules*, **2008**, *41*, 5082.
- ⁸⁵ Misaka, H.; Kakuchi, R.; Zhang, C.; Sakai, R.; Satoh, T.; Kakuchi, T., *Macromolecules*, **2009**, *42*, 5091.
- ⁸⁶ Hoskins, J.N.; Grayson, S.M., *Macromolecules*, **2009**, *42*, 6406.
- ⁸⁷ Wood, B.R.; Hodge, P.; Semlyen, J.A., *Polymer*, **1993**, *34*, 3052.
- ⁸⁸ Wood, B.R.; Hodge, P.; Semlyen, J.A., *Polymer*, **1993**, *34*, 3059.
- ⁸⁹ Wood, B.R.; Semlyen, J.A., *Polymer*, **1994**, *35*, 1542.
- ⁹⁰ Oike, H.; Mouri, T.; Tezuka, Y., *Macromolecules*, **2001**, *34*, 6592.
- ⁹¹ Culkin, D.A.; Jeong, W.; Csihony, S.; Gomez, E.D.; Balsara, N.P.; Hedrick, J.L.; Waymouth, R.M., *Angew. Chem. Int. Ed.*, **2007**, *46*, 2627.
- ⁹² Jeong, W.; Shin, E.J.; Culkin, D.A.; Hedrick, J.L.; Waymouth, R.M., *J. Am. Chem. Soc.*, **2009**, *131*, 4884.
- ⁹³ Jeong, W.; Hedrick, J.L.; Waymouth, R.M., *J. Am. Chem. Soc.*, **2007**, *129*, 8414.
- ⁹⁴ Kricheldorf, H.R.; Lomadze, N.; Schwarz, G., *Macromolecules*, **2008**, *41*, 7812.
- ⁹⁵ Bielawski, C.W.; Benitez, D.; Grubbs, R.H., *Science*, **2002**, *297*, 2041.
- ⁹⁶ Bielawski, C.W.; Benitez, D.; Grubbs, R.H., *J. Am. Chem. Soc.*, **2003**, *125*, 8424.
- ⁹⁷ Boydston, A.J.; Holcombe, T.W.; Unruh, D.A.; Fréchet, J.M.J.; Grubbs, R.H., *J. Am. Chem. Soc.*, **2009**, *131*, 5388.
- ⁹⁸ Boydston, A.J.; Xia, Y.; Kornfield, J.A.; Gorodetskaya, I.A.; Grubbs, R.H.; *J. Am. Chem. Soc.*, **2008**, *130*, 12775.
- ⁹⁹ Xia, Y.; Boydston, A.J.; Yao, Y.; Kornfield, J.A.; Gorodetskaya, I.A.; Spiess, H.W.; Grubbs, R.H., *J. Am. Chem. Soc.*, **2009**, *131*, 2670.
- ¹⁰⁰ Kricheldorf, H.R.; Lee, S.-R., *Macromolecules*, **1995**, *28*, 6718.

- ¹⁰¹ Kricheldorf, H.R.; Lee, S.-R., *Macromolecules*, **1996**, 29, 8689.
- ¹⁰² Kricheldorf, H.R.; Langanke, D., *Macromol. Chem. Phys.*, **1999**, 200, 1183.
- ¹⁰³ Stridsberg, K.; Albertsson, A.-C., *J. Polym. Sci. Part A: Polym. Chem.*, **2000**, 38, 1774.
- ¹⁰⁴ Kricheldorf, H.R.; Langanke, D.; Stricker, A.; Räder, H.J., *Macromol. Chem. Phys.*, **2002**, 203, 405.
- ¹⁰⁵ Takeuchi, D.; Inoue, A.; Osakada, K.; Kobayashi, M.; Yamaguchi, K., *Organometallics*, **2006**, 25, 4062.
- ¹⁰⁶ Shea, K.J.; Lee, S.Y.; Busch, B.B., *J. Org. Chem.*, **1998**, 63, 5746.
- ¹⁰⁷ He, T.; Zheng, G.-H.; Pan, C.-y., *Macromolecules*, **2003**, 36, 5960.
- ¹⁰⁸ Kudo, H.; Makino, S.; Kameyama, A.; Nishikubo, T., *Macromolecules*, **2005**, 38, 5964.
- ¹⁰⁹ Kudo, H.; Sato, M.; Wakai, R.; Iwamoto, T.; Nishikubo, T., *Macromolecules*, **2008**, 41, 521.
- ¹¹⁰ Kricheldorf, H.R., *Macromolecules*, **2003**, 36, 2302.
- ¹¹¹ Endo, K.; Yamanaka, T., *Macromolecules*, **2006**, 39, 4038.
- ¹¹² Ferrahi, M. I.; Belbachir, M., *J. Appl. Polym. Sci.*, **2006**, 12, 1240.
- ¹¹³ Kudo, H.; Makino, S.; Nishikubo, T., *J. Polym. Sci. Part A: Polym. Chem.*, **2007**, 45, 680.
- ¹¹⁴ Chan, W. Y.; Lough, A. J.; Manners, I., *Angew. Chem. Int. Ed.*, **2007**, 46, 9069.
- ¹¹⁵ Hamilton, S.C.; Semlyen, J.A.; Haddleton, D.M., *Polymer*, **1998**, 39, 3241.
- ¹¹⁶ Pang, X.; Wang, G.; Jia, Z.; Liu, C.; Huang, J., *J. Polym. Sci. Part A: Polym. Chem.*, **2007**, 45, 5824.

- ¹¹⁷ Jia, Z.; Fu, Q.; Huang, J., *Macromolecules*, **2006**, *39*, 5190.
- ¹¹⁸ Li, H.; Debuigne, A.; Jérôme, R.; Lecomte, P., *Angew. Chem. Int. Ed.*, **2006**, *45*, 2264.
- ¹¹⁹ Li, H.; Jérôme, R.; Lecomte, P., *Polymer*, **2006**, *47*, 8406.
- ¹²⁰ Oike, H.; Hamada, M.; Eguchi, S.; Danda, Y.; Tezuka, Y., *Macromolecules*, **2001**, *34*, 2776.
- ¹²¹ Tezuka, Y.; Fujiyama, K., *J. Am. Chem. Soc.*, **2005**, *127*, 6266.
- ¹²² Ge, Z.; Wang, D.; Zhou, Y.; Liu, H.; Liu, S., *Macromolecules*, **2009**, *42*, 2903.
- ¹²³ Peng, Y.; Liu, H.; Zhang, X.; Liu, S.; Li, Y., *Macromolecules*, **2009**, *42*, 6457.
- ¹²⁴ Shi, G.-Y.; Yang, L.-P.; Pan, C.-Y., *J. Polym. Chem. Sci.: Part A: Polym. Chem.*, **2008**, *46*, 6496.
- ¹²⁵ Shi, G.-Y.; Pan, C.-Y., *J. Polym. Chem. Sci.: Part A: Polym. Chem.*, **2009**, *47*, 2620.
- ¹²⁶ Lepoittevin, B.; Hemery, P., *J. Polym. Chem. Sci.: Part A: Polym. Chem.*, **2001**, *39*, 2723.
- ¹²⁷ Lepoittevin, B.; Dourges, M. A.; Masure, M.; Hermery, P.; Baran, K.; Cramail, H., *Macromolecules*, **2000**, *33*, 8218.
- ¹²⁸ Adachi, K.; Honda, S.; Hayashi, S.; Tezuka, Y., *Macromolecules*, **2008**, *41*, 7898.
- ¹²⁹ Kricheldorf, H.R.; Langanke, D., *Macromol. Chem. Phys.*, **1999**, *200*, 1183.
- ¹³⁰ Minatti, E.; Viville, P.; Borsali, R.; Schappacher, M.; Deffieux, A.; Lazzaroni, R., *Macromolecules*, **2003**, 4125.
- ¹³¹ Qiu, X.-P.; Tanaka, F.; Winnik, F.M., *Macromolecules*, **2007**, *40*, 7069.

- ¹³² Schappacher, M.; Deffieux, A., *Science*, **2008**, 1512.
- ¹³³ Schappacher, M.; Deffieux, A., *Angew. Chem. Int. Ed.*, **2009**, 48, 5930.
- ¹³⁴ Yang, W.-Y.; Ahn, J.-H.; Yoo, Y.-S.; Oh, N.-K.; Lee, M., *Nat. Mater.*, **2005**, 4, 399.
- ¹³⁵ Nasongkla, N.; Chen, B.; Macareg, N.; Fox, M.E.; Frechet, J.M.; Szoka, F.; *J. Am. Chem. Soc.*, **2009**, 131, 3842.

Chapter 2: The one-pot synthesis of α,ω -chain end functional, stereoregular, poly(lactide)

2.1 Introduction

Poly(lactide) (PLA) is an aliphatic poly(ester) that is biocompatible, biodegradable and can be derived from renewable resources.^{1,2} PLAs of well-defined molecular dimensions are commonly synthesised by the controlled ring-opening polymerisation (ROP) of lactide.³⁻¹⁰ In this manner, the molecular characteristics of the polymer chains such as end groups, molecular weight and molecular weight distribution can be readily dictated. The combination of the ‘green’ credentials of PLA with its facile degradability, readily available stereocontrol and the high levels of control afforded by the ROP methodologies applied make it an appealing polymer for applications ranging from packaging, to biomedicine and microelectronics.^{1,2,4,11,12} Indeed, a great deal of research has focussed on controlling both the polymer structure and functionality, including telechelic, star-shaped and block copolymers, as well as the synthesis of stereoregular polymers from racemic feedstocks.

Functional poly(ester)-containing block copolymers are gaining interest as a consequence of their unique properties.¹³⁻¹⁵ Both the comparatively non aggressive degradability of PLA and the crystallinity arising from its stereoregular forms gives it unique and useful characteristics that can be particularly attractive as part of a block copolymer. For example, the self-assembly of PLA-containing block copolymers in bulk or thin films provides nanostructured materials that can be transformed into nanoporous materials using ‘soft-etch’ methodology that displays a decreased effect on other functional groups within the materials.^{13,16-18}

Stereoregular PLAs have been shown to vary in their physical properties with effects on crystallinity and T_m , which in turn affects the degradation rate of the polymer.^{3,9,19} Furthermore, the interaction of complimentary homochiral poly(*L*-lactide) and poly(*D*-lactide) leads to the formation of a stereocomplex and their application as components in block copolymers can have significant effects on the properties of micellar structures thereby derived.¹⁹⁻²³

The controlled ROP of cyclic esters can be mediated by a range of species including metal-based complexes and salts,^{3-5,9} small molecule organic catalysts^{6,7} and enzymes.¹⁰ Undoubtedly the most widely studied of these are metal-based catalysts with several being reported to exert high levels of control over the polymerisation process. One major advantage of metal-based catalysts is the access to stereoregular PLAs at room temperature and above.⁹ Of the range of metal complexes reported for the stereocontrolled ROP of lactide, aluminium complexes bearing various ancillary ligands have proven to be extremely versatile. The family of salen bearing aluminium complexes (where salen is *N,N'*-bis(salicylaldimine)-1,2-ethylenediamine) are particularly interesting with subtle changes in the ligand structure resulting in the ability to tune the tacticity of the polymers produced.²⁴⁻³⁸ Stereocontrolled ROP has been achieved in this manner with both chiral and achiral ligands and while the mechanism of stereocontrol for the latter complexes remains under debate,^{25,26,28} they provide a useful tool for the synthesis of stereoregular PLAs.

The active aluminium alkoxide species are often derived *in situ* by the addition of an initiating alcohol to a methyl aluminium complex, thus potentially providing facile manipulation of the α -chain end group of the polymer by the judicious choice

of initiating alcohol. While in simple linear polymers and block copolymers this approach provides sufficient versatility to prepare a wide range of materials, more complex copolymer structures such as telechelic, ABA/ABC and star-shaped copolymers require additional functionalisation at the ω -chain end of the polymer. Most commonly, quenching the polymerisation with a protic source results in a hydroxyl ω -chain end from which further post-polymerisation modification can be performed. Ideally, the manipulation of these chain ends would be performed *in situ* after completion of the polymerisation. Dubois, Jérôme and Tessy  reported that the isolation and reaction of the aluminium alkoxide species, generated from the triethyl aluminium catalysed ROP of ϵ -caprolactone, with methacryloyl chloride in the presence of pyridine provided a simple methodology for the preparation of ω -chain end functional macromonomers.^{39,40}

In this chapter, the development of a one-pot synthetic technique allowing for the production of stereoregular poly(lactide)s with controlled functionality at both the α - and ω -chain ends is reported. The availability of the chain ends for further functionalisation is demonstrated through the application of ‘Click’ chemistry. Finally, the syntheses of multi block copolymers with a central PLA block and functional multi-arm star polymers are demonstrated.

2.2 One pot α - and ω - chain end functionalisation

2.2.1 Aluminium salen/salan catalysts

As has been clearly shown in the literature, control over the microstructure of PLA can have a significant impact on the properties and behaviour of the material that it makes up. For this reason it was vital that during all the polymerisations used throughout this research it was possible to control and determine the stereoregularity of the PLA. To this end it was determined that metal-based catalysts would be used in preference to the more recent organic catalytic techniques. Through the application of the sterically hindered catalysts **1-3 (Figure 2.2.1.1)** it was possible to access heterotactic, atactic and isotactic stereoblock PLAs respectively.

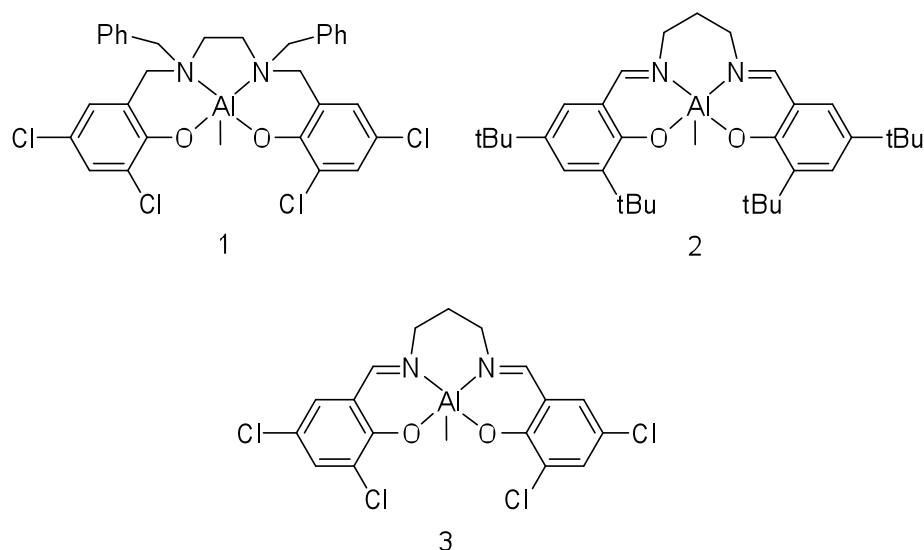


Figure 2.2.1.1 Aluminum complexes applied as catalysts in the stereoregular ROP of lactide.^{29,38}

These catalysts also have an advantage over other metal catalysts, namely that the initiating alkoxide species can be generated *in situ* through reaction between the aluminium methyl and an alcohol (**Figure 2.2.1.1**). Through the application of a range of initiating alcohols, the synthesis of PLAs displaying different α -chain end functionality can be derived from a single initiator. Although different alcohols have previously been employed for this purpose, a study has not been carried out to show the range of α -chain end functionality that is available.

Upon quenching with a protic source this alcohol initiated polymerisation procedure results in a ω -hydroxyl chain end, the target for which post-polymerisation modifications can be performed to furnish a range of functionality. In work reported by Dubois, Jérôme and Tessy  , an isolated Al-capped poly(ϵ -caprolactone) was reacted with methacryloyl chloride in the presence of pyridine.³⁹⁻

⁴⁰ In line with this report, a one-pot methodology to perform this transformation *in situ* was examined by quenching of the lactide polymerisation using an acid chloride. This procedure employs a much more hindered catalyst and would ideally proceed without the requirement to isolate the metal containing species or addition of extraneous base.

2.2.2 Polymerisation and functionalisation procedure

The stereocontrolled ROP of *rac*-lactide initiated by *iso*-propanol (IPA) was carried out using **1** at 70 °C in toluene solution. For a targeted DP = 20, the polymerisation was carried out for 4 h before the reaction mixture was crash cooled by plunging the reaction ampoule into an ice bath. Subsequent addition of 10 eq. of anthranoyl chloride and stirring the resultant solution at 70 °C for five days enabled the isolation of a heterotactic PLA with *iso*-propyl and anthracene end groups. Several precipitations in cold petroleum ether were required to remove excess anthranoyl chloride (**Figure 2.2.2.1**).

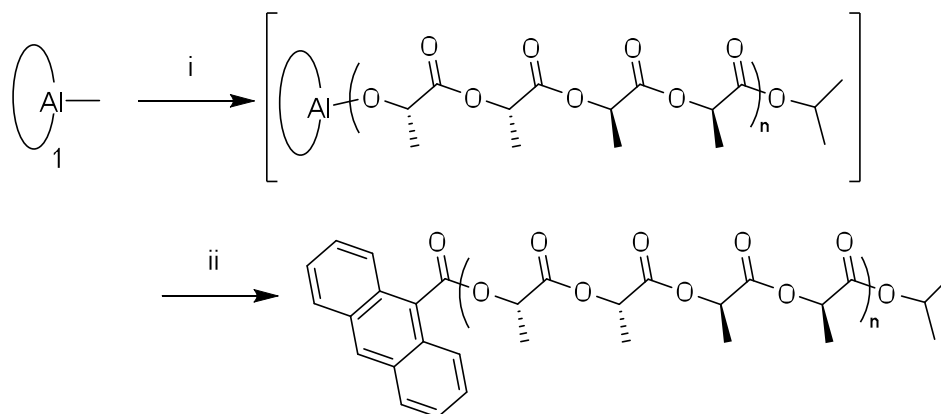


Figure 2.2.2.1 *In situ* functionalisation of the ω -chain end of heterotactic PLA. i) IPA, n eq. *rac*-lactide, toluene, 70°C , 4 h; ii) *in situ* addition of anthranoyl chloride, 70°C , 120 h.

Analysis of the resultant polymer by ^1H NMR (**Figure 2.2.2.2**) unambiguously demonstrates the presence of the anthracene functionality in a concentration comparable to that of the α -chain end *iso*-propyl functionality. Importantly stereocontrol of the polymer is maintained as shown by the quartet representing CHCH_3 ($\delta = 5.2$ ppm). Importantly, by comparison to a polymerisation quenched with methanol, GPC analysis confirms that no adverse effects are observed on the polymer with low polydispersity being maintained (MeOH quench: $M_n = 3970$ g.mol^{-1} , $\text{PDI} = 1.11$; anthranoyl chloride quench: $M_n = 3470$ g.mol^{-1} , $\text{PDI} = 1.08$). Furthermore, analysis of the polymer using both DRI and UV detection demonstrates the UV active anthracene group to be distributed throughout the polymer (DRI: $M_n = 3470$ g.mol^{-1} , $\text{PDI} = 1.08$; UV: $M_n = 3330$ g.mol^{-1} , $\text{PDI} = 1.11$).

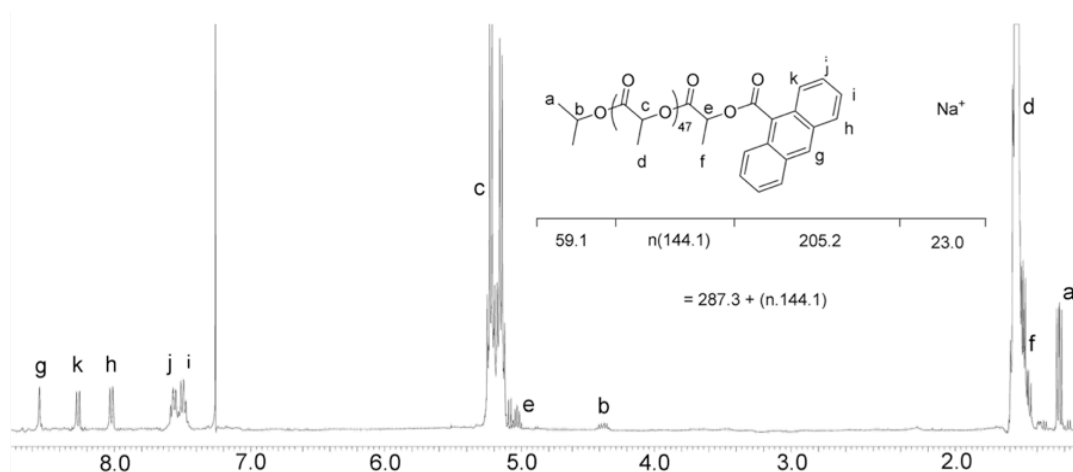


Figure 2.2.2.2 ^1H NMR spectrum of anthracene functionalised PLA (heterotactic stereochemistry not shown)

MALDI-ToF MS analysis (**Figure 2.2.2.3**) exclusively reveals peaks that correspond to the predicted molecular weight of the functional polymer. Additionally, the peaks in the MALDI-ToF MS spectrum are exclusively separated by 144 Da indicating that very little or no transesterification occurs even after the increased reaction times at high temperature that are necessary for the quenching procedure.

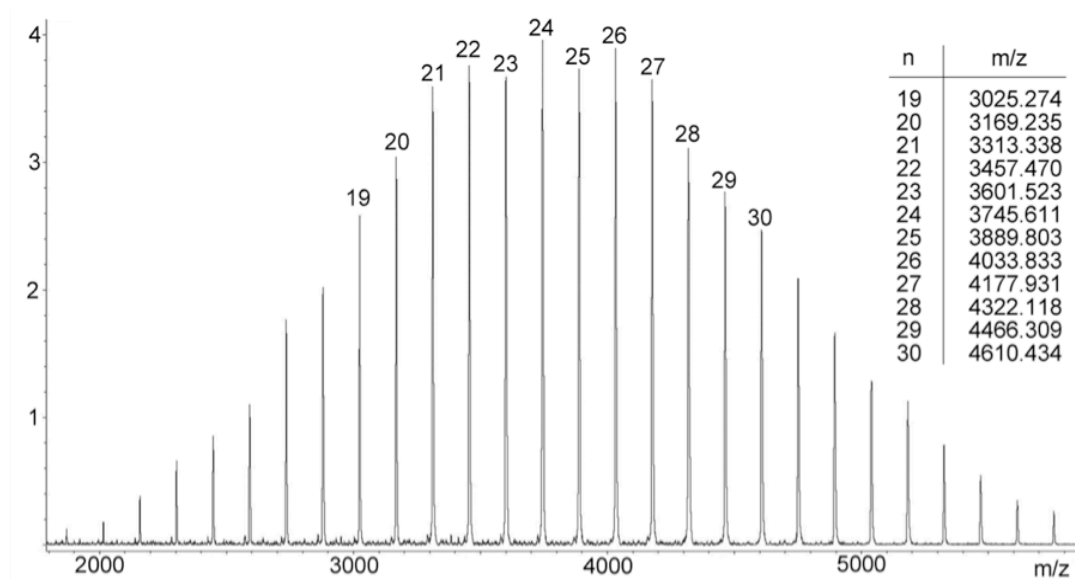


Figure 2.2.2.3 MALDI-ToF MS of anthracene functionalised PLA

2.2.3 Versatility of the Quench Procedure

The versatility of this reaction was investigated by applying different catalysts (with their resultant different steric and electronic demands), different PLA chain lengths and a range of functional acid chlorides, **Figure 2.2.4.1**. All of the catalysts used in this study were successfully applied in this one-pot process thus enabling the synthesis of a range of highly stereoregular PLAs to be realised. As illustrated in **Table 2.1**, the method also proceeds effectively using a range of acid chlorides including primary and secondary alkyl, aryl and pyridyl. In this final case the polymer forms a salt resulting in reduced solubility that requires an aqueous acidic

work up to yield the pure polymer. Notably, attempts to quench the polymerisation with pivaloyl chloride did not result in functionalisation of the ω -chain end of the polymer, most likely reflecting the increased steric demands of the tertiary α -carbon in combination with the bulky ancillary ligand of the ROP catalyst. The extended reaction times that are required for complete conversion of the chain end are also likely to be a result of this same steric hindrance.

In all cases, analysis of the polymers by ^1H NMR, GPC and MALDI-ToF MS revealed that the narrow PDI of the polymers was maintained and complete end-group conversion was observed with molecular weights measured matching closely to those calculated (**Table 2.1**).

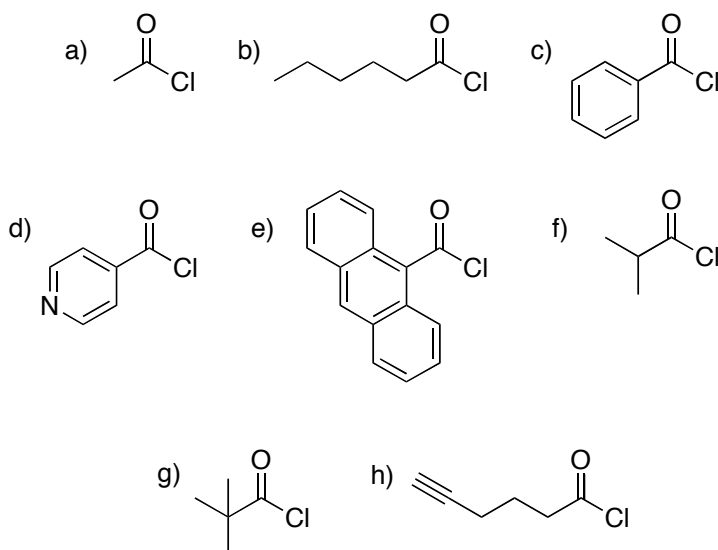


Figure 2.2.4.1 Acid chlorides that were applied for ω -chain end functionalisation.

a) acetyl chloride; b) hexanoyl chloride; c) benzoyl chloride; d) isonicotinoyl chloride; e) anthranoyl chloride; f) isobutyryl chloride; g) pivaloyl chloride; h) hexynoyl chloride.

Table 2.1. Preparation of ω -chain end functionalised poly(lactide)s

Entry	Target DP ^a	Quenching agent ^b	Catalyst	M_n (GPC) g.mol ^{-1 c}	PDI ^c	Mass (Calc) ^d	M_{ass} (MALDI) ^e
1	20	Methanol	1	3970	1.11	2965.1	2965.4
2	20	acetyl chloride ^e	1	3810	1.09	3223.5	3224.0
3	20	hexanoyl chloride	1	3760	1.07	3063.2	3063.8
4	20	benzoyl chloride	1	3890	1.09	3069.2	3069.4
5	20	Isonicotinoyl chloride	1	4040	1.07	3070.2	3070.7
6	20	anthranoyl chloride	1	3470	1.08	3169.3	3169.2
7	20	isobutyryl chloride	1	3890	1.08	3035.2	3035.4
8	20	pivaloyl chloride	1	-	-	3047.9	2965.3
9	10	hexynoyl chloride	1	2530	1.07	1618.2	1617.9
10	20	benzoyl chloride	2	3870	1.10	3069.2	3069.4
11	20	benzoyl chloride	3	3730	1.22	3069.2	3069.6
12	10	benzoyl chloride	1	1760	1.13	1628.2	1628.9
13	50	benzoyl chloride	1	9000	1.06	-	-
14	100	benzoyl chloride	1	17440	1.06	-	-

Polymerisation reactions carried out using catalysts as previously described in the literature using *iso*-propanol initiator.

^a Targeted degree of polymerisation. ^b Reactions were stirred at 70 °C for 120 h in each case. ^c Determined by GPC analysis. ^d Calculated and determined by MALDI-ToF MS for a single DP20 polymer chain. ^e Pyrene butanol applied as initiating alcohol.

2.2.4 Telechelic and star shaped polymers

Application of the simple methodology that has been introduced here enables the facile synthesis of α - and ω -chain end functional, stereoregular PLAs. This procedure could also be useful in the synthesis of ω -chain end functional telechelic and star-shaped polymers as generation of the catalytic alkoxide species *in situ* enables facile initiation from multifunctional alcohols. In this manner, initiation from 1,3-propanediol, 1,1,1-tris(hydroxymethyl)ethane and dipentaerythritol in the presence of **1** at 70 °C resulted in the synthesis of telechelic, 3-arm and 6-arm star-shaped polymers respectively, **Figure 2.2.4.2**.

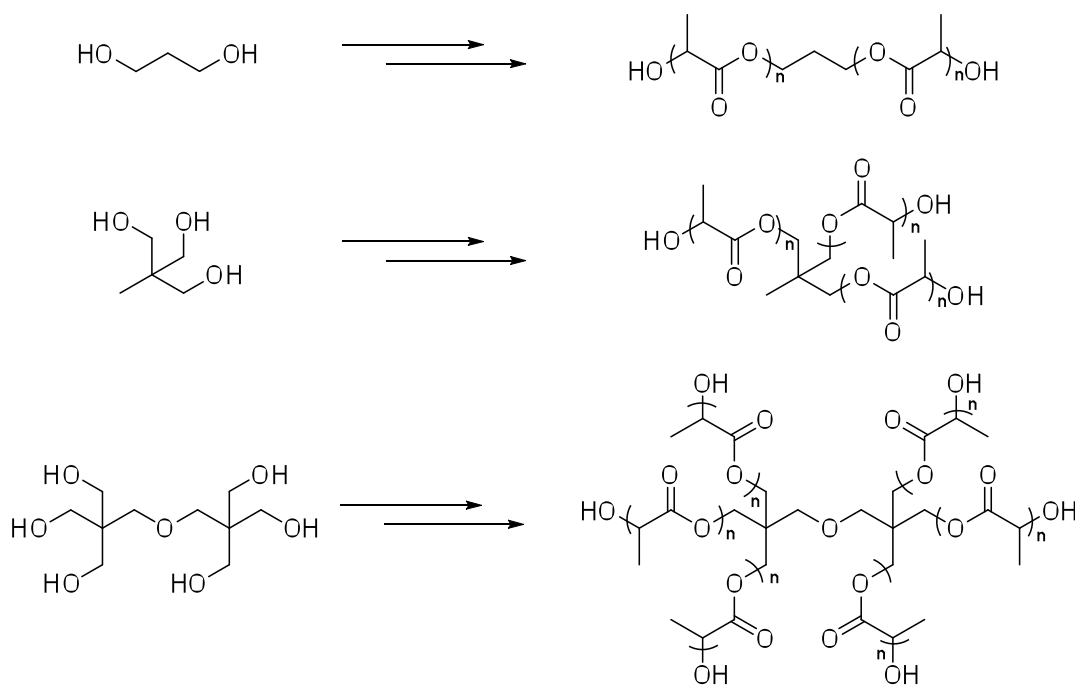


Figure 2.2.4.2 Synthesis of telechelic and star shaped PLA

In the case of dipentaerythritol, the aluminum alkoxide complex was prepared *in situ* before addition of *rac*-lactide to overcome the poor solubility of the alcohol in toluene. This was achieved by simply stirring the alcohol with the aluminium complex for 16 hours at 70 °C prior to addition of lactide. Quenching these reactions by addition of benzoyl chloride resulted in the appropriate ω -chain end multifunctional heterotactic PLAs ([LA]/[OH] = 10: initiator = 1,3-propanediol, M_n = 3590 g.mol⁻¹, PDI = 1.12; initiator = 1,1,1-tris(hydroxymethyl)ethane M_n = 7100 g.mol⁻¹, PDI = 1.05; initiator = dipentaerythritol, M_n = 9130 g.mol⁻¹, PDI = 1.16). MALDI-ToF analysis reveals molecular weights exclusively related to the expected product in each case, shown for 1,1,1-tris(hydroxymethyl)ethane in **Figure 2.2.4.3**.

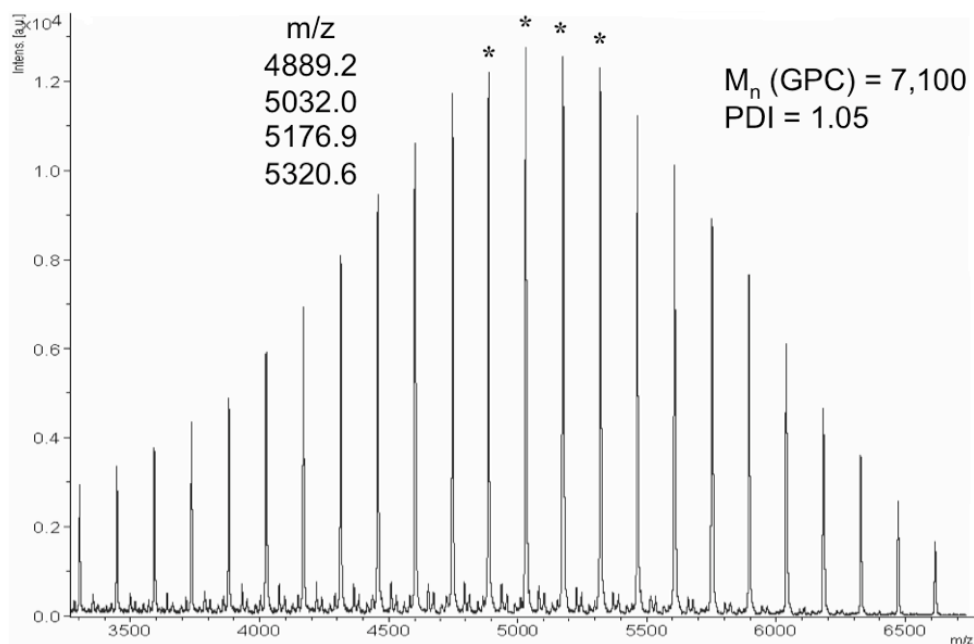


Figure 2.2.4.3 MALDI-ToF MS analysis of 1,1,1-tris(hydroxymethyl)ethane initiated star polymer.

2.2.5 Synthesis of block copolymers

Extension of this methodology also enables the ready synthesis of block copolymers with a stereoregular PLA block, either by initiating or quenching the ROP with an acid chloride functional polymer or initiator for further polymerisation. A polyethylene glycol (PEG) mono methyl ether, with an average M_w of 550 daltons (Aldrich), was converted to the acid chloride by treatment with a large excess of succinyl chloride (**Figure 2.2.5.1**).⁴¹ Quenching the polymerisation using 10 eq. of this macromolecular acid chloride and heating at 70 °C for five days, resulted in a PLA-PEG block copolymer ($[M]/[I] = 10$; MeOH quench: $M_n = 1640 \text{ g.mol}^{-1}$, $\text{PDI} = 1.18$; after Me-PEG-COCl quench: $M_n = 3100 \text{ g.mol}^{-1}$, $\text{PDI} = 1.06$).

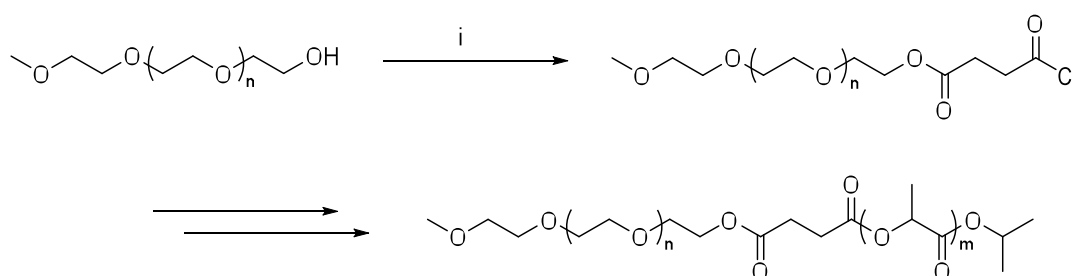


Figure 2.2.5.1 Synthesis of acid chloride functional polyethylene glycol. i) 50 eq. succinyl chloride, CH_2Cl_2 , 16 h, and subsequent application in the quenching of PLA polymerisation.

Quenching the polymerisation with a macromolecular acid chloride in this fashion limits the range of block copolymers that could be synthesised. For this reason it is necessary to introduce functionalities that would enable sequential polymerisation procedures to be examined. The combination of ROP with controlled radical polymerisation strategies such as reversible addition fragmentation chain transfer (RAFT) enables access to a wide range of highly functional, partially degradable block copolymers.⁴² The RAFT chain transfer agent, 4-(chlorocarbonyl)benzyl dodecyl carbonotrithioate, **4**, was synthesised *via* a previously reported one-pot procedure (**Figure 2.2.5.2**).⁴³

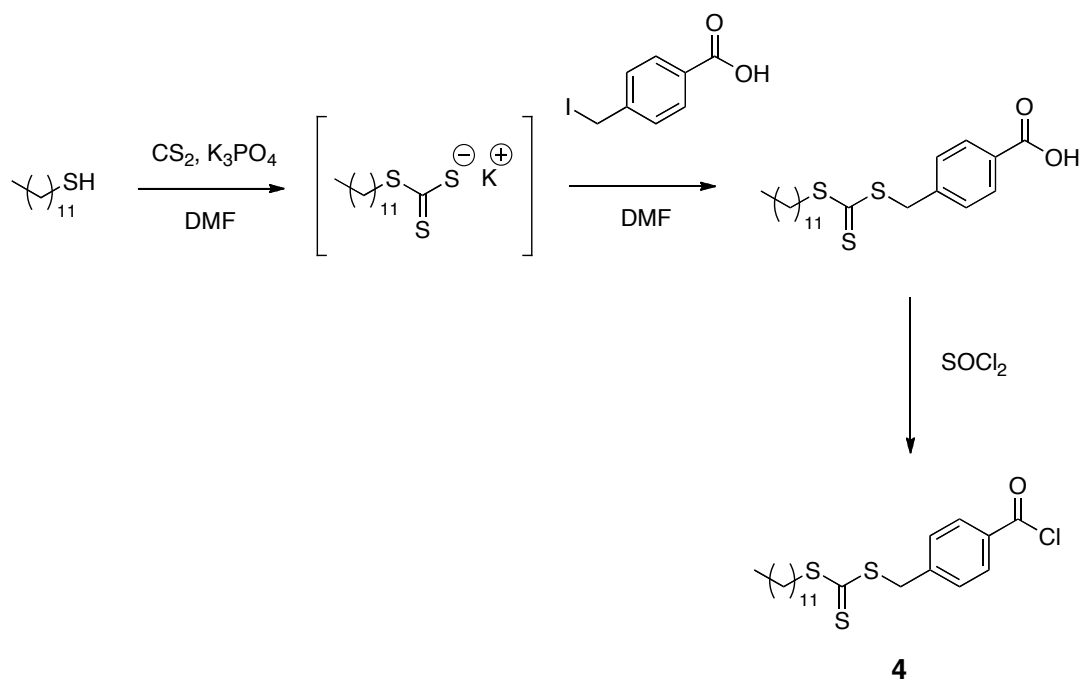


Figure 2.2.5.2 Synthesis of RAFT chain transfer agent acid chloride, **4**.

Chain end functionalisation of linear, telechelic and star-shaped polymers was successfully achieved using the one-pot quenching methodology reported here, with the presence of the RAFT chain transfer agent being demonstrated by both ^1H NMR and MALDI-ToF MS analysis of the resultant polymers, **Figure 2.2.5.3**. Chain extension of the PLAs, by the polymerisation of styrene, was undertaken in toluene solution (30 vol. % styrene) at 120 °C. In all cases, ^1H NMR and GPC analysis of the resultant copolymers confirmed the chain extension of the PLAs in line with the expected conversion of the styrene, producing linear, telechelic and star-shaped block copolymers (**Figure 2.2.5.4, Figure 2.2.5.5**).

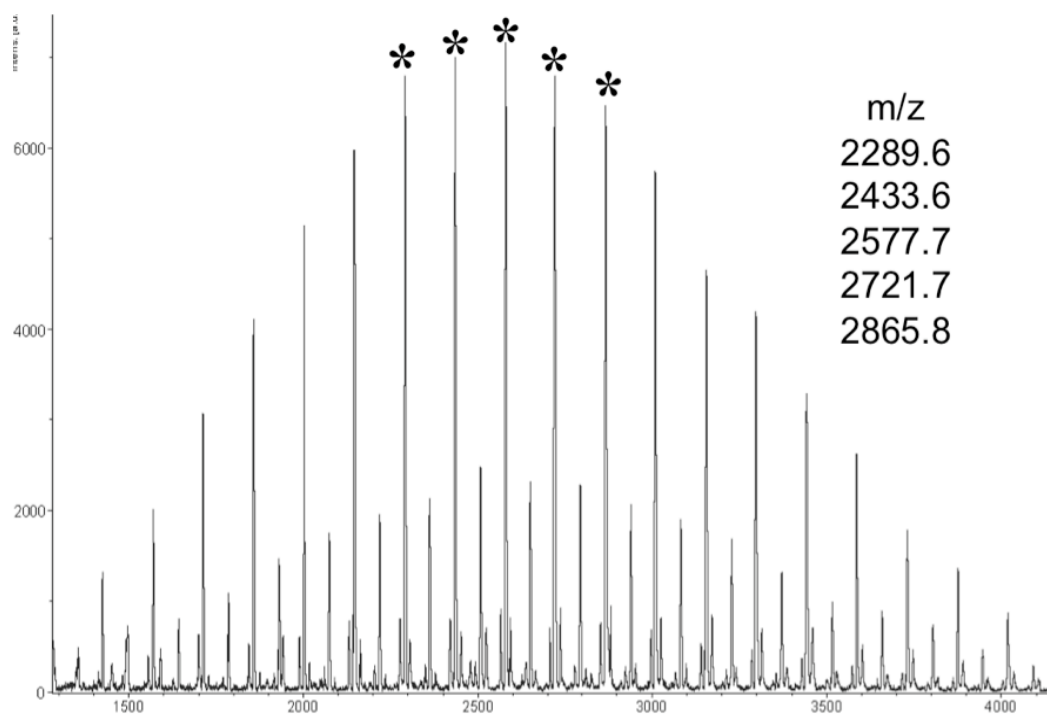


Figure 2.2.5.3 MALDI-ToF MS analysis of RAFT chain transfer agent bearing PLA.

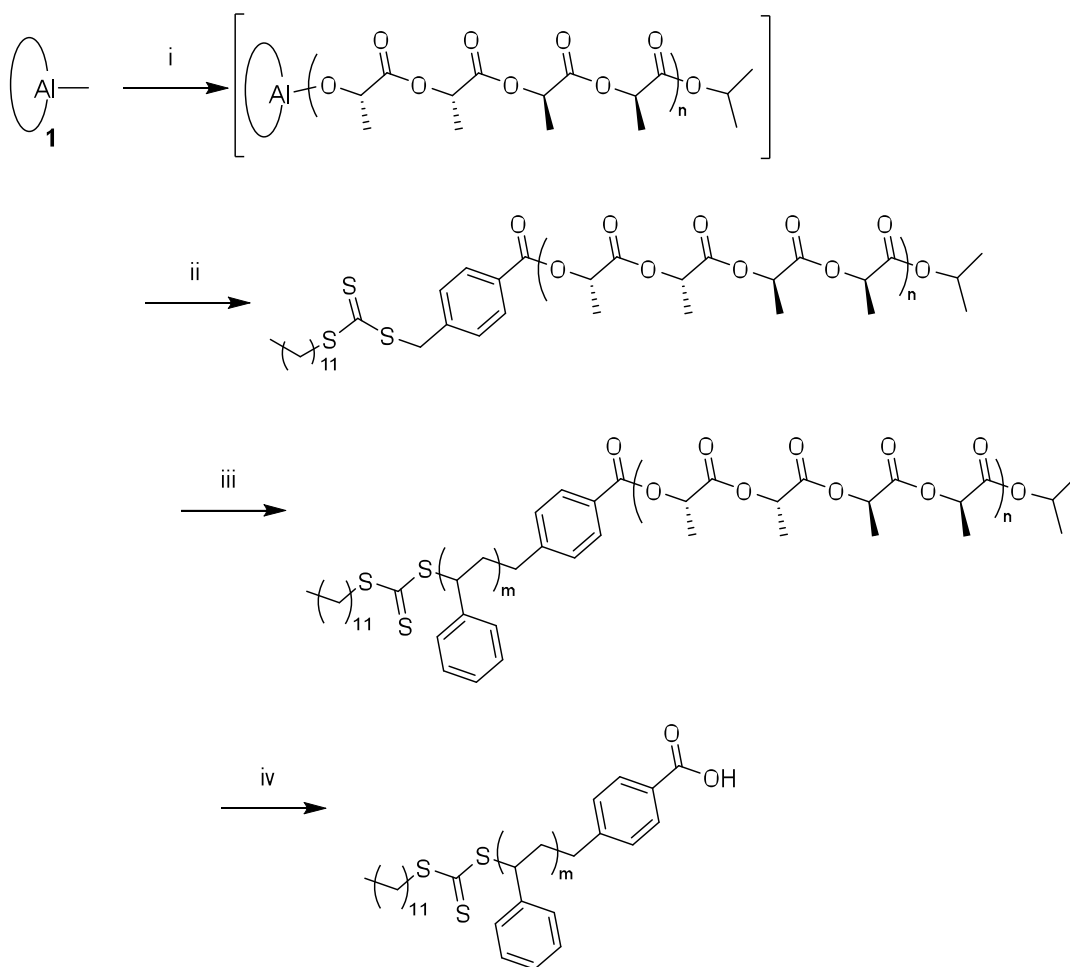


Figure 2.2.5.4 Synthesis and subsequent degradation of PLA-*b*-PS. i) IPA, *rac*-lactide, toluene, 70 °C, 2 h; ii) **4**, toluene, 70 °C, 120 h; iii) Styrene, toluene, 16 h, 120 °C; iv) TBD, MeOH, toluene, 16 h, 110 °C.

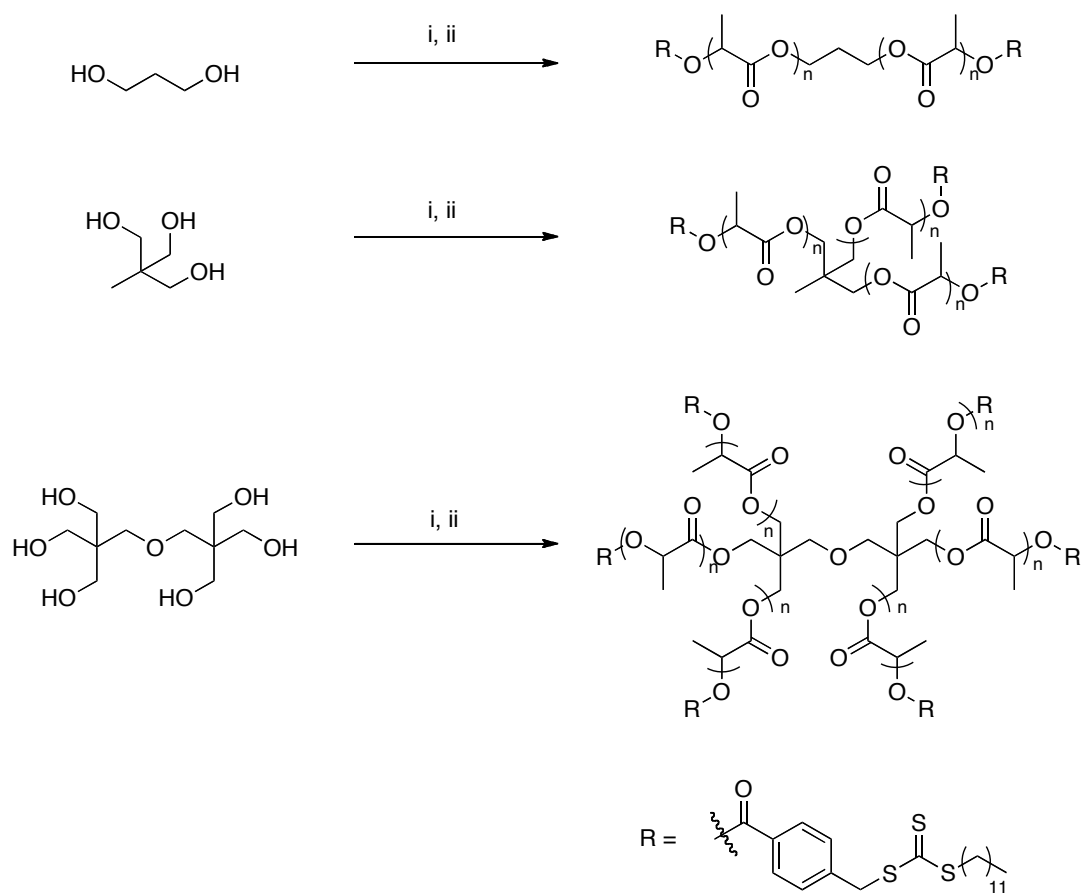


Figure 2.2.5.5 Synthesis of RAFT chain transfer agent bearing telechelic and star shaped PLA. i) **1**, *rac*-lactide, toluene, 70 °C, 2 h; ii) **4**, toluene, 70 °C, 120 h.

Table 2.2. GPC data for synthesis and degradation of multi-arm stars

Initiating alcohol	RAFT quenched PLA		PLA-b-PS ^[a]		PS after degradation ^[b]	
	M_n g.mol ⁻¹ [c]	PDi ^[c]	M_n g.mol ⁻¹ [c]	PDi ^[c]	M_n g.mol ⁻¹ [c]	PDi ^[c]
None	-	-	7600	1.28	7380	1.32
Propan-2-ol	2490	1.08	8950	1.26	8050	1.34
1,3-Propanediol	6190	1.09	17190	1.33	7890	1.35
1,1,1-Tris(hydroxymethyl)ethane	8790	1.11	23490	1.22	7450	1.39
Dipentaerythritol	9490	1.04	24030	1.18	7420	1.42

^[a]Styrene, toluene, 16 h, 120 °C; ^[b]TBD, MeOH, toluene, 16 h, 110 °C; ^[c]Determined by GPC analysis.

In order to confirm that PS was successfully grown from the PLA telechelic and star-shaped polymers, degradation by transesterification of the PLA was performed using MeOH in the presence of 1,5,7-triazabicyclo[4.4.0]dec-5-ene, TBD, at 110 °C. The GPC data for the degraded polymer was representative of the polystyrene produced from a non-macro initiator; in each case only linear poly(styrene) chains of roughly the same molecular weight remained (**Figure 2.2.5.5** and **Table 2.2**).

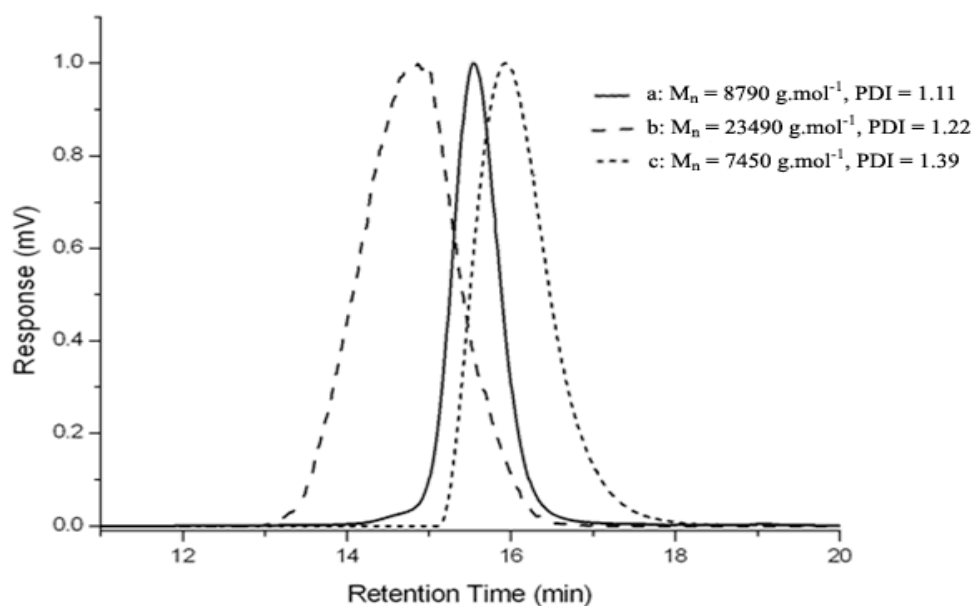


Figure 2.2.5.6 GPC traces for a) 3-arm heterotactic PLA star-shaped polymer b) 3-arm (heterotactic PLA)-*b*-PS star-shaped polymer c) PS after degradation of poly(ester).

Notably, under milder conditions degradation of the PLA from the block copolymers was ineffective. Further investigations of this effect were undertaken by monitoring the degradation of linear and 6-arm star PLAs with -OH, -Ph (from benzoyl chloride quench), and -poly(styrene) end groups using *in situ* ^1H NMR spectroscopy (**Table 2.3**). In order to clearly observe the resonances attributable to the PLA, reduced molar concentrations of TBD were applied such that 1 mol equiv (to polymer) of TBD was applied in a 20:80 d_4 -MeOD: d_8 -toluene solution (10

mg/mL). After 24 h at 100 °C the resonances attributed to the methine resonances in the -OH end-capped polymers ($\delta = 5.10\text{-}5.25$ ppm) had largely been reduced to baseline noise and subsequent analysis by GPC revealed no polymer chains were present. However, under the same conditions, the -Ph and -poly(styrene) end-capped PLAs displayed no significant degradation (only a slight broadening of the PDI for the -Ph end-capped PLA). Under more forcing conditions (48 h at 110 °C) the -Ph end-capped PLAs displayed significant degradation such that only very low oligomers remained in the case of both linear and star polymers with $M_n = ca. 1000$ g mol⁻¹ (initial M_n s: linear = 3890 g.mol⁻¹, 6-arm star = 9130 g.mol⁻¹). Again however, the PLA-*b*-PS block copolymers displayed no significant degradation; only a slight broadening in PDI was observable by GPC. Under the higher TBD loadings required to degrade the PLA component in these block copolymers (5 mol equiv of TBD (to copolymer), 110 °C in 20:80 MeOH:toluene, 5 mg/mL) it was notable that the molecular architecture also affected the degradation behaviour of the polymers such that the star-shaped polymers resisted degradation for a significantly longer time period in comparison to the linear chains. It is postulated that these effects are a combination of the inhibition of autocatalysed degradation by the alcohol bearing polymer chain end⁴⁴ and a consequence of the inaccessibility of the modified polymer cores arising from poor solubility and greater protection offered by the larger polymeric groups.

Table 2.3 Degradation conditions for ω - functional PLA

Initiator ^(a)	ω -end group	M_n g.mol ^{-1(b)}	After degradation at 100 °C for 24 h, 1 eq TBD				After degradation at 110 °C for 48 h, 1 eq TBD				After degradation at 110 °C for 72 h, 5 eq TBD			
			M_n g.mol ^{-1(b)}	PD _i ^(b)	M_n g.mol ^{-1(b)}	PD _i ^(b)	M_n g.mol ^{-1(b)}	PD _i ^(b)	M_n g.mol ^{-1(b)}	PD _i ^(b)	M_n g.mol ^{-1(a)}	PD _i ^(b)	M_n g.mol ^{-1(a)}	PD _i ^(b)
iso-propanol	-OH	3,970	1.11	- [c]	- [c]	- [c]	nr ^(d)	nr ^(d)	nr ^(d)	nr ^(d)	nr ^(d)	nr ^(d)	nr ^(d)	nr ^(d)
dipentaerythritol	-OH	5,650	1.10	- [c]	- [c]	- [c]	nr ^(d)	nr ^(d)	nr ^(d)	nr ^(d)	nr ^(d)	nr ^(d)	nr ^(d)	nr ^(d)
iso-propanol	-Ph	3,890	1.09	3,650	1.17	1,090	1.20	nr ^(d)	nr ^(d)	nr ^(d)	nr ^(d)	nr ^(d)	nr ^(d)	nr ^(d)
dipentaerythritol	-Ph	9,130	1.16	8,800	1.23	1,400	1.50	nr ^(d)	nr ^(d)	nr ^(d)	nr ^(d)	nr ^(d)	nr ^(d)	nr ^(d)
iso-propanol	-PS	8,950	1.26	9,030	1.31	9,350	1.46	8,050	1.34	nr ^(d)	nr ^(d)	nr ^(d)	nr ^(d)	nr ^(d)
dipentaerythritol	-PS	24,030	1.18	24,240	1.19	22,370	1.63	7,420	1.42	nr ^(d)	nr ^(d)	nr ^(d)	nr ^(d)	nr ^(d)

^(a) Polymerisations carried out as previously reported to form linear and star shaped structures; ^(b) Determined by GPC analysis;^(c) No polymer was observed by GPC analysis; ^(d) Degradation not carried out where previous conditions had already been effective.

2.3 ‘Click’ chemistry

The techniques demonstrated here allow for the facile functionalisation of stereoregular poly(lactide), however an area that has received a great deal of interest lately is ‘click’ chemistry. This branch of chemistry has recently become of particular interest in polymer chemistry and has proven to be a particularly versatile and useful range of techniques.⁴⁵⁻⁴⁷

2.3.1 Copper catalysed azide alkyne cycloaddition

Although previous work has demonstrated the application of CuAAC chemistry for the functionalisation of poly(lactide),⁴⁸⁻⁵¹ this technique has proven to be difficult without seeing significant degradation of the polymer chain. This may be due to this procedure involving only the chain end of the polymer in comparison to that of various reports where the backbone of the polymer is targeted. Also, it is possible that to indentify complete conversion is more difficult on such a large number of click reactions, in comparison to one per polymer chain.

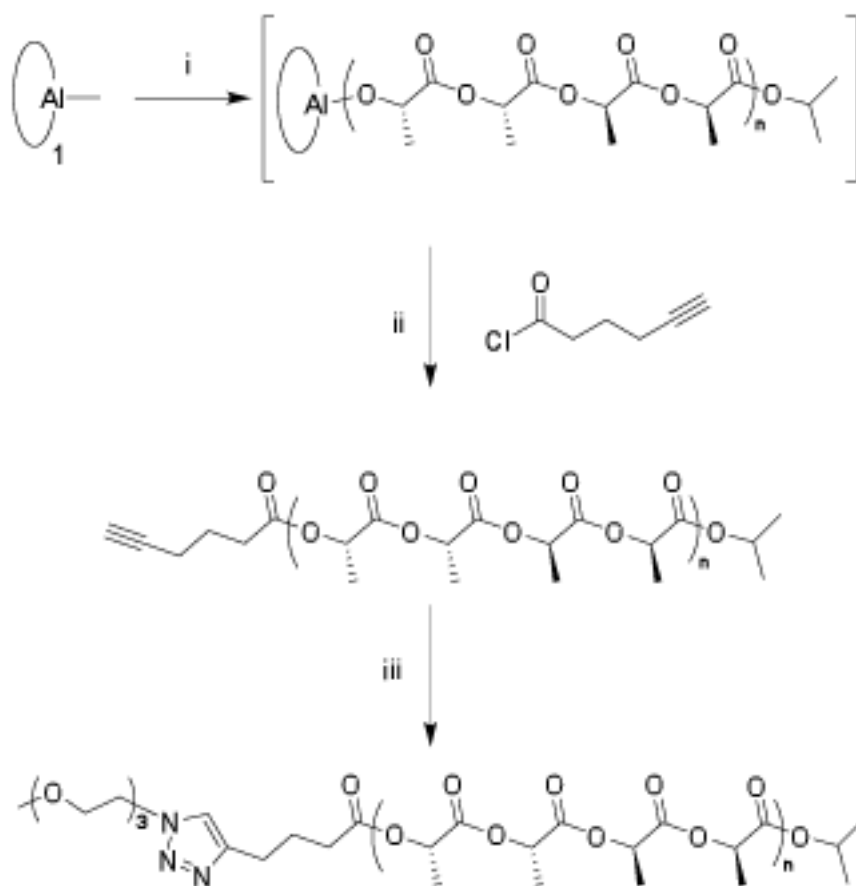


Figure 2.3.1.1 The application of CuAAC chemistry for chain end functionalisation. i) IPA, *rac*-lactide, toluene, 70°C , 2 h; ii) hexynoyl chloride, toluene, 70°C iii) azido triethylene glycol, CuI, NEt_3 , THF, 25°C , 7 days.

It was possible to synthesise and apply both alkyne and azide functional acid chlorides and alcohols, e.g. **Figure 2.3.1.1**, thus furnishing the multifunctional polymers with groups that would undergo the copper catalysed Huisgen 1,3-dipolar cycloaddition reaction. Through the application of azido triethylene glycol, CuI, and NEt_3 in a solution of THF for 7 days at ambient temperature, as previously

2.3.2 Thiol-ene ‘click’ reaction

As a consequence of the problems highlighted previously it was necessary to pursue a different ‘click’ reaction that would be tolerant towards polyesters. The application of a Diels Alder type of ‘click’ functionalisation would certainly be an attractive possibility, however, the reversible nature of these reactions, and the elevated temperature at which they must be applied suggests they may be an undesirable candidate for this research. Recent reports have shown the use of thiol-ene chemistry as being a robust and tolerant ‘click’ type reaction that can be carried out at ambient temperature. Of these various reactions the reaction between a thiol and a maleimide is particularly attractive as the catalyst is simply TEA, a reagent has previously shown to cause no degradation of the polymer.

To incorporate a maleimide functionality on to the α -chain end of the polymer was simple through the application of the alcohol **5**, **Figure 2.3.2.1**.⁵² It is important to note that the maleimide functionality must be protected for both metal and organic catalysis of the polymerisation to proceed. Refluxing in toluene for 24 h can be used to carry out deprotection of the maleimide functionality, although recent work on the deprotection of a small molecule analogue has shown that a small amount of dimerisation can occur during this process. For that reason a much more desirable technique is to carry out the deprotection by placing the polymer in a vacuum oven at 100 °C for 16 h. This technique for deprotecting the maleimide only proceeds to completion on the polymer chain and it is postulated that this is because the temperatures involved are above the T_g of the polymer.

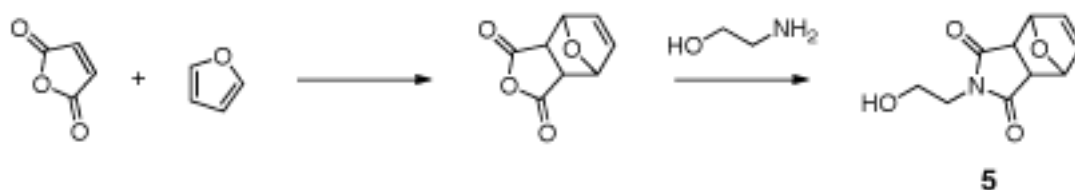


Figure 2.3.2.1 Synthesis of alcohol bearing protected maleimide functionality, **5**.

Once the polymer had been synthesised it was possible to carry out ‘click’ reactions using a range of thiols that are all commercially available. The results of this study are demonstrated in **Table 2.4**, and, although more hindered thiols are relatively slow to complete functionalisation compared to the smaller molecules, it was possible to incorporate a wide range of functionality in this way.

Table 2.4 ‘Click’ conjugation of thiols to maleimide-functional PLAs^[a]

Entry	DP ^[b]	RSH	Time ^[c]	M_n g.mol ⁻¹ ^[d]	PDI ^[d]
1	20	-	-	5240	1.09
2	20	PhSH	40 min	5410	1.08
3 ^[e]	20	PhSH	<5 min	5450	1.10
4 ^{[f][g]}	20	Me(CH ₂) ₁₁ SH	6 h	5580	1.07
5 ^[h]	20	Me(CH ₂) ₁₁ SH	120 h	4790	1.16
6 ^[i]	20	Me(CH ₂) ₁₁ SH	6 h	3880	1.19
7 ^{[f][g][j]}	20	ⁱ PrSH	6 h	5290	1.09
8 ^{[f][g][j]}	20	^t BuSH	1 week	5060	1.16
9	20	PhCH ₂ SH	2 h	5290	1.08
10	20	Thioglycerol	1.5 h	5830	1.10
11	20	HOOC(CH ₂) ₂ SH	1.5 h	5280	1.07
12	20	Cysteamine	1.5 h	4860	1.07
13	20	Cysteine ethyl ester	1.5 h	5470	1.06
14	50	-	-	13600	1.05
15	50	PhSH	1 h	13600	1.05
16 ^[k]	50	Glutathione	48 h	14000	1.04
17	100	-	-	24200	1.04
18	100	PhSH	1 h	23000	1.05
19 ^[k]	100	Glutathione	48 h	22500	1.07

^[a]Reactions carried out in 7 mM THF solution of polymer, 1.05 eq. thiol and 1 eq. NEt₃. ^[b]Degree of polymerisation of maleimide functional PLA, measured by ¹H NMR spectroscopy. ^[c]Time to reach >99.5% maleimide conversion as determined by ¹H NMR spectroscopy. ^[d]Determined by GPC analysis. ^[e]2 eq. RSH. ^[f]5 eq. RSH. ^[g]2 eq. NEt₃. ^[h]5 eq. NEt₃. ^[i]10 eq. NEt₃. ^[j]Conjugations performed in CH₂Cl₂. ^[k]Conjugations performed in DMF at 40 °C.

Identification that the reaction is completed quantitatively is largely gained from ^1H NMR and MALDI-ToF MS analysis. The conversion of the maleimide functionality to that of a succinimide provides the obvious disappearance of the resonance at 6.8 ppm, **Figure 2.3.2.2**. It is also possible to see the appearance of a range of resonances between 3.5 - 4.5 ppm, with complicated, but assignable, coupling due to the unsymmetrical nature of the succinimide functionality. Importantly there is no degradation of the polymer chain, and no racemisation of the stereoregularity is observed.

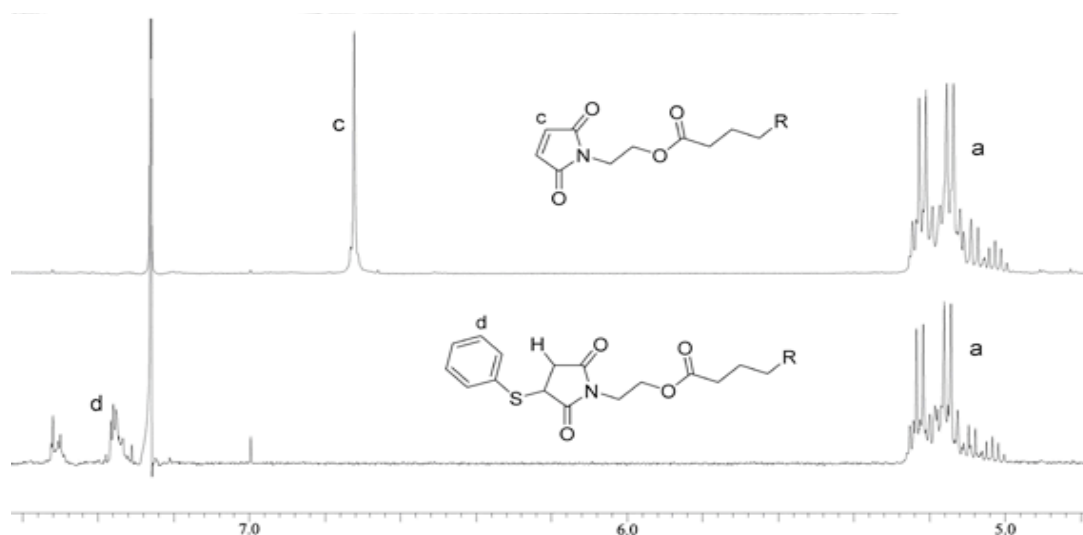


Figure 2.3.2.2 ^1H NMR analysis demonstrating quantitative ‘click’ conjugation with thiophenol (Integrals: resonance a = 20; c = 2.4; d = 6.0).

For a similar conjugation, MALDI-ToF MS analysis, **Figure 2.3.2.3**, demonstrates incorporation of thiophenol through an increase in the molecular weight of the

2.3.3 Thiol-ene ‘click’ chemistry on the ω - chain end

The application of the reaction between a thiol and maleimide provides an excellent route to functionalisation of the α -chain end of the polymer, however, it was important to employ the same chemistry at the ω -chain end as well. This was achieved through the synthesis of the maleimide acid chloride **6**, **Figure 2.3.3.1**. This synthetic route allowed for the conversion of the maleimide alcohol, that was already available, through the application of the ring opening of glutaric anhydride followed by conversion to the acid chloride using oxalyl chloride. This technique should prove useful for increasing the range of acid chlorides that are available for this technique.

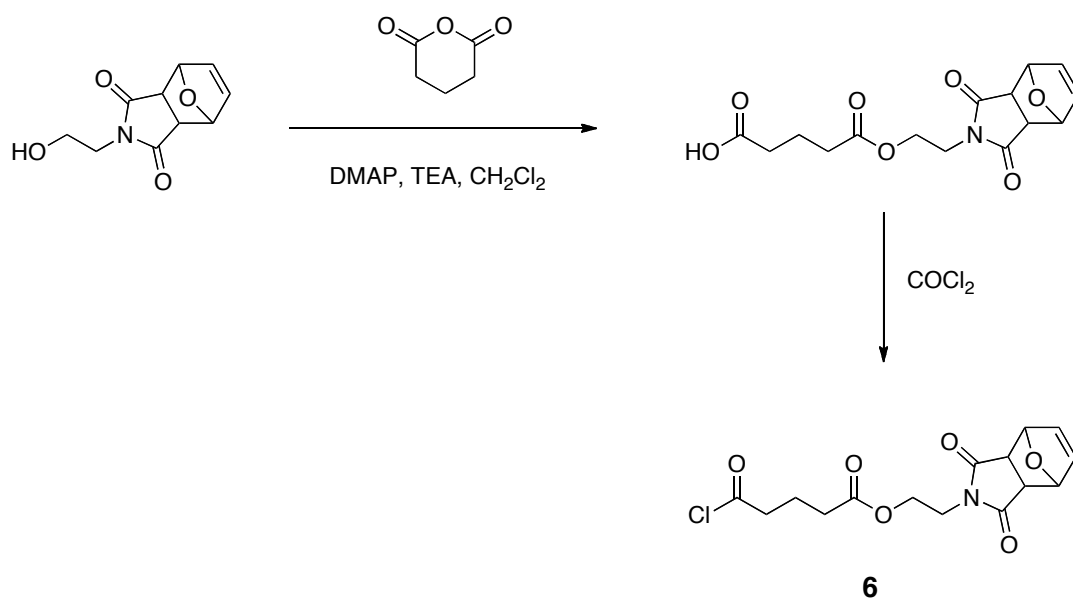


Figure 2.3.3.1 Synthesis of maleimide functional acid chloride, **6**.

Incorporation of the maleimide acid chloride, **6**, was carried out in exactly the same way as for previous functional polymers, **Figure 2.3.3.2**, with evidence of its presence provided by ¹H NMR and MALDI-ToF MS analysis. It is important to note at this stage that the furan protecting group is never seen during MALDI-ToF MS analysis as the reverse Diels-Alder reaction appears to occur quantitatively during the ionisation process. Incidences of this occurring will be discussed in further detail in Chapter 3. The availability of the ω-chain end maleimide was demonstrated by the conjugation of thiophenol using identical methods to those described previously, **Figure 2.3.3.2**.

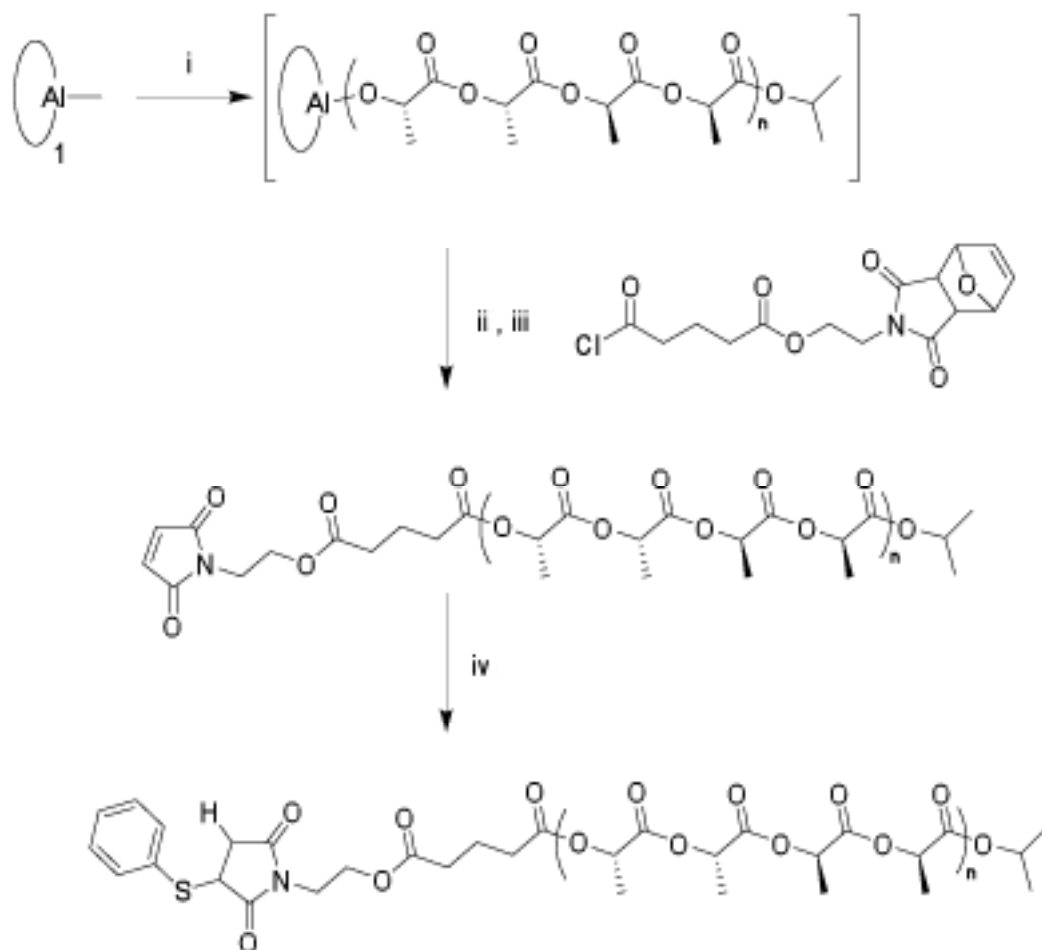


Figure 2.3.3.2 Synthesis of poly(lactide) bearing ω - chain end maleimide functionalisation. i) IPA, *rac*-lactide, toluene, 70 °C, 2 h; ii) toluene, 70 °C, 120 h; iii) heat; iv) thiophenol, TEA, RT, 2 h.

2.3.4 Telechelic and star shaped polymers

Using the techniques described earlier it was also possible to synthesise both telechelic and star shaped polymers bearing the maleimide functionality, **table 2.5**. These polymers are of particular interest as they provide an opportunity to access a range of more complex architectures. The possibilities of this are investigated further in the subsequent chapters. MALDI-ToF MS analysis in each case demonstrates the presence exclusively of the multifunctional polymer and that complete conjugation is possible to all chain ends, again using thiophenol as a model.

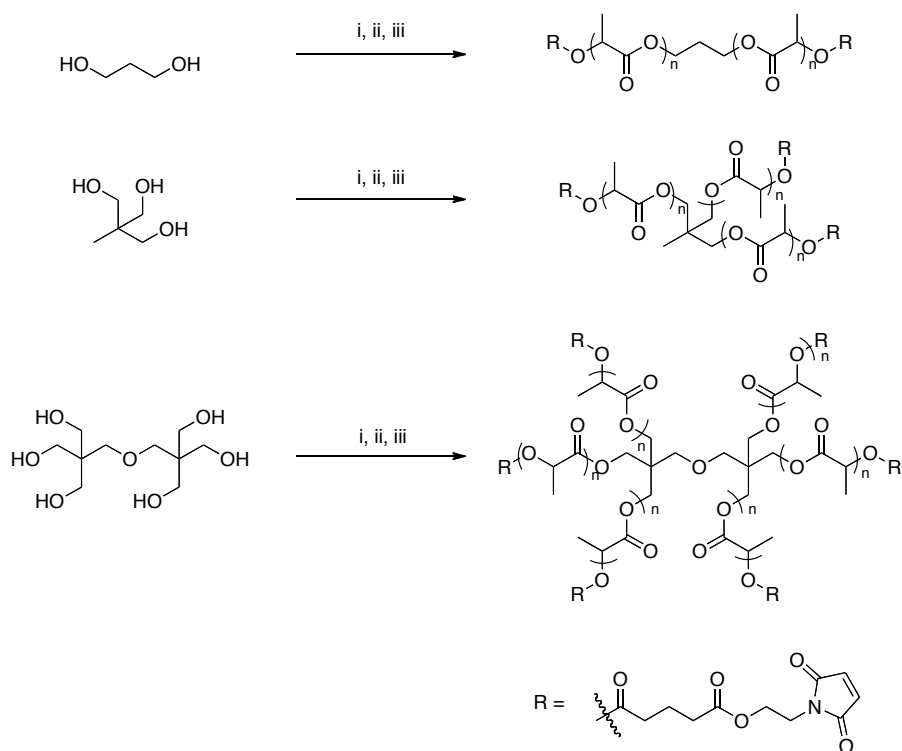


Figure 2.3.4.1 Synthesis of maleimide bearing telechelic and star shaped PLA. i)

1, *rac*-lactide, toluene, 70 °C, 2 h; ii) **6**, toluene, 70 °C, 120 h; iii) heat.

Table 2.5 Click functionalisation of the PLA ω -chain end.

Initiating alcohol	Before thiophenol conjugation		After thiophenol conjugation	
	M_n g.mol ⁻¹ [c]	PDI ^[c]	M_n g.mol ⁻¹ [c]	PDI ^[c]
Propan-2-ol ^[a]	3730	1.12	3870	1.10
propanediol ^[b]	4080	1.08	4140	1.08
1,1,1-Tris(hydroxymethyl)ethane ^[b]	7740	1.05	7340	1.15
dipentaerthritol ^[b]	10250	1.12	9440	1.09

^[a][LA]/[OH] = 20 ; ^[b][LA]/[OH] = 10 ; Conjugations carried out under an atmosphere of nitrogen, using 1.05 eq. thiophenol, 2eq. TEA as catalyst in CH₂Cl₂.

^[c]Obtained from GPC.

2.4 Conclusion

In conclusion, a one-pot synthetic route for the synthesis of a range of α - and ω -chain end functionalised poly(lactide)s has been demonstrated. This technique is tolerant to functionality such that handles for ‘click’ chemistry and molecules suitable for the mediation of mechanistically distinct polymerisations can be incorporated. This methodology has been further extended to allow for the synthesis of functionalised telechelic and star-shaped polymers, as well as showing the synthesis of block copolymers *via* two different approaches.

2.5 References

- ¹ Drumright, R. E.; Gruber, P. R.; Henton, D. E., *Adv. Mater.*, **2000**, *12*, 1841.
- ² Auras, R.; Harte, B.; Selke, S., *Macromol. Biosci.*, **2004**, *4*, 835.
- ³ Jerome, C.; Lecomte, P., *Adv. Drug Deliv. Rev.*, **2008**, *60*, 1056.
- ⁴ Albertsson, A. C.; Varma, I. K., *Biomacromolecules*, **2003**, *4*, 1466.
- ⁵ Dechy-Cabaret, O.; Martin-Vaca, B.; Bourissou, D., *Chem. Rev.*, **2004**, *104*, 6147.
- ⁶ Kamber, N. E.; Jeong, W.; Waymouth, R. M.; Pratt, R. C.; Lohmeijer, B. G. G.; Hedrick, J. L., *Chem. Rev.*, **2007**, *107*, 5813.
- ⁷ Bourissou, D.; Moebs-Sanchez, S.; Martin-Vaca, B., *C. R. Chim.*, **2007**, *10*, 775.
- ⁸ Wu, J. C.; Yu, T. L.; Chen, C. T.; Lin, C. C., *Coord. Chem. Rev.*, **2006**, *250*, 602.
- ⁹ Nakano, K.; Kosaka, N.; Hiyama, T.; Nozaki, K., *J. Chem. Soc., Dalton Trans.*, **2003**, 4039.
- ¹⁰ Varma, I. K.; Albertsson, A. C.; Rajkhowa, R.; Srivastava, R. K., *Prog. Polym. Sci.*, **2005**, *30*, 949.
- ¹¹ Albertsson, A. C.; Varma, I. K., *Adv. Polym. Sci.*, **2002**, *157*, 1.
- ¹² Urich, K. E.; Cannizzaro, S. M.; Langer, R. S.; Shakesheff, K. M., *Chem. Rev.*, **1999**, *99*, 3181.
- ¹³ Hillmyer, M. A., *Adv. Polym. Sci.*, **2005**, *190*, 137.
- ¹⁴ Duncan, R., *Nat. Rev. Drug. Discovery*, **2003**, *2*, 347.
- ¹⁵ Martina, M.; Hutmacher, D. W., *Polym. Int.*, **2007**, *56*, 145.
- ¹⁶ Chen, L.; Phillip, W. A.; Cussler, E. L.; Hillmyer, M. A., *J. Am. Chem. Soc.*, **2007**, *129*, 13786.

- ¹⁷ Zalusky, A. S.; Olayo-Valles, R.; Wolf, J. H.; Hillmyer, M. A., *J. Am. Chem. Soc.*, **2002**, *124*, 12761.
- ¹⁸ Cavicchi, K. A.; Russell, T. P., *Macromolecules*, **2007**, *40*, 1181.
- ¹⁹ Tsuji, H., *Macromol. Biosci.*, **2005**, *5*, 569.
- ²⁰ Bishara, A.; Kricheldorf, H. R.; Domb, A. J., *Macromol. Symp.*, **2005**, *225*, 17.
- ²¹ Kang, N.; Perron, M. E.; Prud'homme, R. E.; Zhang, Y. B.; Gaucher, G.; Leroux, J. C., *Nano Lett.*, **2005**, *5*, 315.
- ²² Kim, S. H.; Nederberg, F.; Zhang, L.; Wade, C. G.; Waymouth, R. M.; Hedrick, J. L., *Nano Lett.*, **2008**, *8*, 294.
- ²³ Hu, J. L.; Han, Y. D.; Zhuang, X. L.; Chen, X. S.; Li, Y. S.; Jing, X. B., *Nanotechnology*, **2007**, *18*, 18.
- ²⁴ Zhong, Z. Y.; Dijkstra, P. J.; Feijen, J., *Angew. Chem. Int. Ed. Engl.*, **2002**, *41*, 4510.
- ²⁵ Chisholm, M. H.; Patmore, N. J.; Zhou, Z. P., *Chem. Commun.*, **2005**, 127.
- ²⁶ Nomura, N.; Ishii, R.; Yamamoto, Y.; Kondo, T., *Chem. Eur. J.*, **2007**, *13*, 4433.
- ²⁷ Pang, X.; Du, H. Z.; Chen, X. S.; Wang, X. H.; Jing, X. B., *Chem. Eur. J.*, **2008**, *14*, 3126.
- ²⁸ Chisholm, M. H.; Gallucci, J. C.; Quisenberry, K. T.; Zhou, Z. P., *Inorg. Chem.*, **2008**, *47*, 2613.
- ²⁹ Hormnirun, P.; Marshall, E. L.; Gibson, V. C.; White, A. J. P.; Williams, D. J., *J. Am. Chem. Soc.*, **2004**, *126*, 2688.
- ³⁰ Majerska, K.; Duda, A., *J. Am. Chem. Soc.*, **2004**, *126*, 1026.
- ³¹ Nomura, N.; Ishii, R.; Akakura, M.; Aoi, K., *J. Am. Chem. Soc.*, **2002**, *124*, 5938.
- ³² Ovitt, T. M.; Coates, G. W., *J. Am. Chem. Soc.*, **1999**, *121*, 4072.

- ³³ Ovitt, T. M.; Coates, G. W., *J. Am. Chem. Soc.*, **2002**, *124*, 1316.
- ³⁴ Radano, C. P.; Baker, G. L.; Smith, M. R., *J. Am. Chem. Soc.*, **2000**, *122*, 1552.
- ³⁵ Zhong, Z. Y.; Dijkstra, P. J.; Feijen, J., *J. Am. Chem. Soc.*, **2003**, *125*, 11291.
- ³⁶ Spassky, N.; Wisniewski, M.; Pluta, C.; LeBorgne, A., *Macromol. Chem. Phys.*, **1996**, *197*, 2627.
- ³⁷ Du, H. Z.; Pang, X.; Yu, H. Y.; Zhuang, X. L.; Chen, X. S.; Cui, D. M.; Wang, X. H.; Jing, X. B., *Macromolecules*, **2007**, *40*, 1904.
- ³⁸ Hormnirun, P.; Marshall, E. L.; Gibson, V. C.; Pugh, R. I.; White, A. J. P., *Proc. Nat. Acad. Sci.*, **2006**, *103*, 15343.
- ³⁹ Dubois, P.; Jerome, R.; Teyssie, P., *Makromol. Chem. Macromol. Symp.*, **1991**, *42*, 103.
- ⁴⁰ Dubois, P.; Jerome, R.; Teyssie, P., *Macromolecules*, **1991**, *24*, 977.
- ⁴¹ Crisci, L.; Della Volpe, C.; Maglio, G.; Nese, G.; Palumbo, R.; Rachiero, G. P.; Vignola, M. C., *Macromol. Biosci.*, **2003**, *3*, 749.
- ⁴² Perrier, S.; Takolpuckdee, P., *J. Poly. Sci. Part A. Polym. Chem.*, **2005**, *43*, 5347.
- ⁴³ Skey, J.; O'Reilly, R. K., *Chem. Commun.*, **2008**, 4183.
- ⁴⁴ Kurokawa, K.; Yamashita, K.; Doi, Y.; Abe, H., *Biomacromolecules*, **2008**, *9*, 1071.
- ⁴⁵ Hawker, C. J.; Fokin, V. V.; Finn, M. G.; Sharpless, K. B., *Aust. J. Chem.*, **2007**, *60*, 381.
- ⁴⁶ Lutz, J. F., *Angew. Chem. Int. Ed. Engl.*, **2007**, *46*, 1018.
- ⁴⁷ Binder, W.H.; Sachsenhofer, R., *Macromol. Rapid Commun.*, **2007**, *28*, 15.
- ⁴⁸ Jiang, X.; Vogel, E. B.; Smith, M. R.; Baker, G. L., *Macromolecules*, **2008**, *41*, 1937.

- ⁴⁹ Li, H. Y.; Riva, R.; Jerome, R.; Lecomte, P., *Macromolecules*, **2007**, *40*, 824.
- ⁵⁰ Parrish, B.; Breitenkamp, R. B.; Emrick, T., *J. Am. Chem. Soc.*, **2005**, *127*, 7404.
- ⁵¹ Riva, R.; Schmeits, S.; Jerome, C.; Jerome, R.; Lecomte, P., *Macromolecules*, **2007**, *40*, 796.
- ⁵² Mantovani, G.; Lecolley, F.; Tao, L.; Haddleton, D. M.; Clerx, J.; Cornelissen, J.; Velonia, K., *J. Am. Chem. Soc.*, **2005**, *127*, 2966.

Chapter 3: The application of ‘Click’ chemistry for the synthesis of cyclic poly(lactide)

3.1 Introduction

The control over polymer architecture has been an area of fundamental research for decades.¹ Star-shaped, dendritic and brush polymeric architectures display greatly altered physical properties to their linear counterparts leading to novel behavior of the material. While conceptually the constraint of polymer chain ends to produce a cyclic polymer is simple, in practice the synthetic inaccessibility of cyclic polymers has led to a limited ability to study the physical and self-assembly properties of pure cyclic polymers.^{2,3} Architectural effects, such as the constraint of cyclic polymers, are especially highlighted with degradable polymers where a single degradation would lead to significant alterations in the linear polymers properties.⁴ Poly(lactide) (PLA) and its copolymers are biocompatible and biodegradable polymers that have found many uses in biomedicine. By judicious choice of catalyst, access to these polymers *via* the ring opening polymerisation (ROP) of lactide enables a high level of control over a variety of molecular and hence physical characteristics to be achieved. The living nature of many of these polymerisations enable facile control over the chain end functionality and a narrow molecular weight distribution to be achieved.^{5,6,7}

The increased recent interest in the synthesis of pure cyclic polymers has led to many improved synthetic methodologies. These have primarily been focused around two routes: restriction of chain ends during polymer growth and post-polymerisation connection of polymer chain ends. In the field of biodegradable polymers, following comparable work by the group of Hodge,⁸ Chisholm and coworkers reported the application of surface initiated techniques, taking advantage

of trans-esterification reactions to selectively cleave and expand macrocycles of oligo(esters).⁹ This technique, while effective leads to a loss of stereopurity of the polymers. Following an initial report by Kricheldorf and coworkers,¹⁰ Jerome *et al.* have utilised the ring-opening polymerisation of lactide and caprolactone by cyclic tin(IV) complexes to synthesise a range of cyclic polymer architectures.¹¹ Hedrick, Waymouth and coworkers have also demonstrated the application of N-heterocyclic carbenes to mediate a zwitterionic polymerisation of lactide, which, in the absence of protic initiating species results in the synthesis of cyclic PLAs.^{12,13} While these latter methods are excellent for the synthesis of cyclic polymers,^{14,15} the application of sensitive reagents in the polymerisation and cyclisation steps, lack of reported stereoregular polymerisations and/or access to block copolymers led us to examine alternative synthetic approaches.

The alternate route involving the cyclisation of linear pre-polymer offers much greater versatility in polymer design, although the efficiency of the cyclisation step is critical to the purity of the resultant macrocycles. This approach is exemplified by the report of Laurent and Grayson in which α -alkyne- ω -azido-poly(styrene)s were cyclised using the Huisgen-1,3-dipolar cycloaddition under pseudo-high dilution conditions.^{16,17} This approach has been adopted in several other studies using both the α -alkyne- ω -azido polymer cyclisation^{18,19} and a comparable approach in which an alkyne-functional polymer is cyclised by addition of a bis-azido functional molecule.^{20,21} Having shown that Michael addition ‘thiol-ene’ click chemistry provides a mild and highly effective tool to effect poly(lactide) functionalisation with a complete absence of degradation,^{22,23} further investigation

into its efficiency for the synthesis of cyclic stereoregular poly(lactide) was carried out.

3.2 Cyclic poly(lactide)

3.2.1 Synthesis

The synthesis of a telechelic, stereoregular PLA with maleimide functionality on both α - and ω - chain-ends has been reported here, and the availability of these groups has been demonstrated. It was postulated that this symmetrical polymer could be used in the synthesis of cyclic polymers through the application of 1,2-ethanedithiol reacting with the chain ends, **Figure 3.2.1.1**.

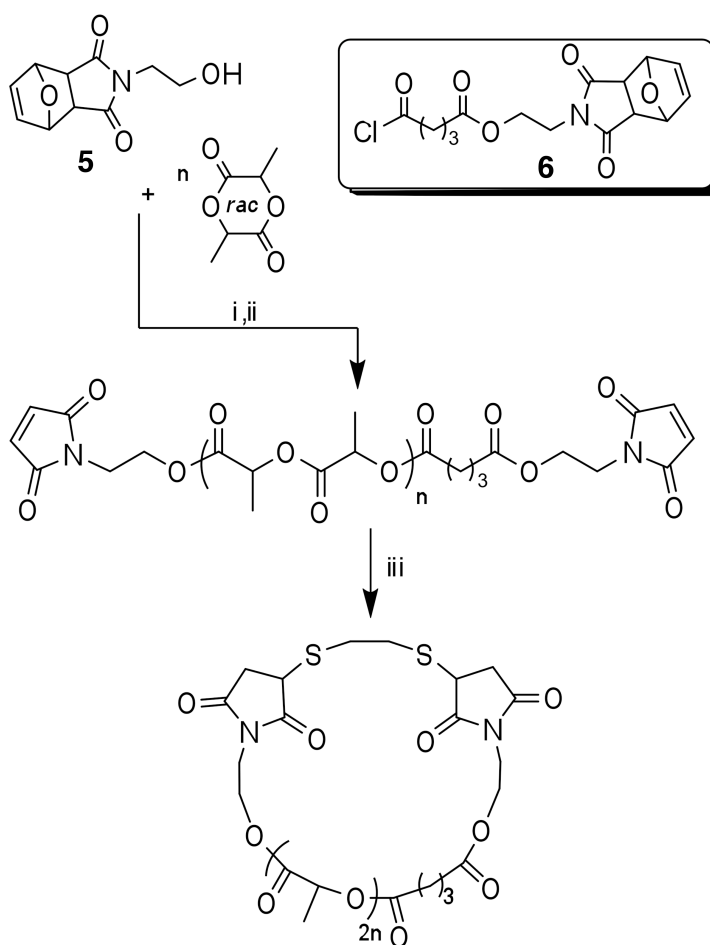


Figure 3.2.1.1 Cyclisation of the stereoregular PLA. i) **5**, Al salen, toluene. 70 °C, 4 h; then in situ addition of **6**, 70 °C, 120 h; ii) Vacuum, 100 °C, 24 h; iii) 1 eq. 1,2-ethanedithiol, CH₂Cl₂, NEt₃, Na₂S₂O₅.

Using a *pseudo* high dilution technique, adapted from those previously reported in the literature, it was possible to quantitatively cyclise the PLA with ethane dithiol. The procedure for the high dilution involved the use of two syringe pumps, one containing each of the polymer and the dithiol (~7 mM CH₂Cl₂ solution of each).

Slow injection of these solutions ($\sim 0.4 \text{ mL.h}^{-1}$) into the reaction vessel containing NEt_3 and a small amount of Na_2SO_4 in CH_2Cl_2 was carried out for between 10-24 hours depending on required yield. This is followed by filtration, removal of the solvent and finally precipitating the resulting solid in cold petroleum ether (b.p. 40-60 °C). In this way it is possible to synthesise around 100 mg of cyclic polymer in 12 hours.

Attempts to allow for the use of one syringe pump, through the pre mixing of the polymer and dithiol resulted in a small amount of the ‘thiol-ene’ reaction occurring under the undesirably concentrated conditions of the syringe. It was postulated that through the application of a small amount of trifluoroacetic acid (TFA) in the syringe solution, this could be retarded; but the TFA appears to catalyse the reaction. This mechanism of an acid catalysed alternative of the ‘thiol-ene’ click reaction was not the subject of further investigation.

3.2.2 Characterisation

Analysis of the cyclic polymer by MALDI-ToF MS, ^1H NMR and GPC, shows unambiguously that complete cyclisation has occurred. MALDI-ToF MS analysis demonstrates an increase in the molecular weight of the polymer by 94 Da, the weight of a single ethane dithiol unit, **Figure 3.2.2.1**. Importantly, there is only a single distribution observed in any region of the spectra, demonstrating that there are no impurities of larger linear or cyclic products.

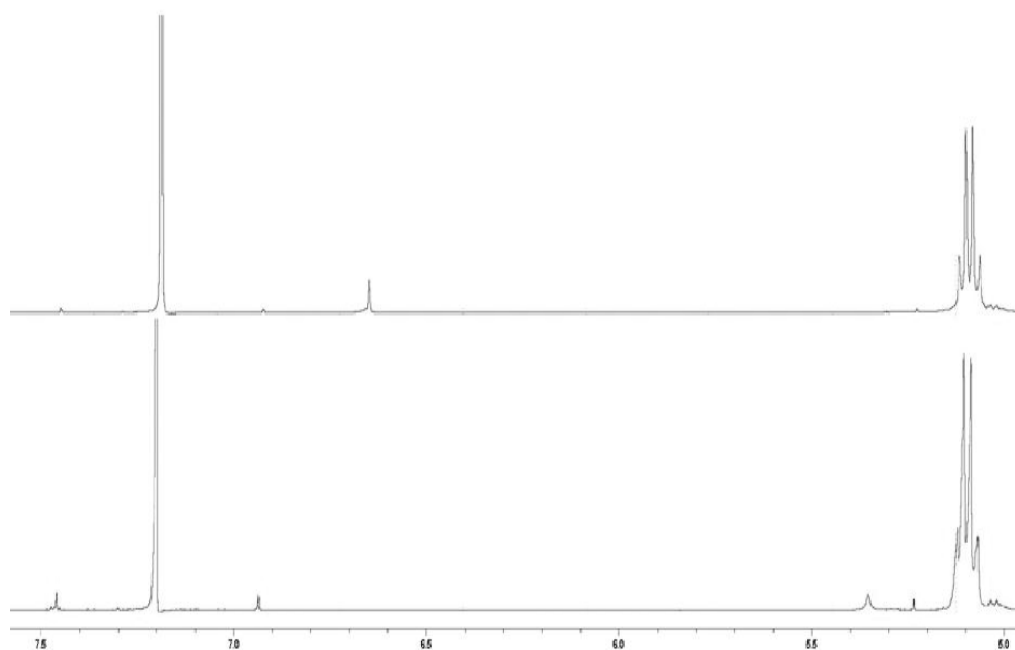


Figure 3.2.2.2 ^1H NMR of linear (top) and cyclic polymers (bottom) (Isotactic polymer used for simplicity).

The final piece of evidence is the reduction in molecular weight by GPC (Linear polymer $M_n = 5770 \text{ g.mol}^{-1}$, $\text{PDI} = 1.08$; Cyclic polymer $M_n = 3990 \text{ g.mol}^{-1}$, $\text{PDI} = 1.07$) as has been reported for cyclic polymers in the literature, **Figure 3.2.2.3**. This phenomenon is caused by the reduction in hydrodynamic volume that occurs when the chain ends become tethered. This reduction can be quantified through the value P , calculated by $M_n(\text{Cyclic}) / M_n(\text{Linear})$. Various literature sources quote this value to be between 0.6 and 0.9 dependent on the polymer type and chain length. The cyclisation that I carried out gives a value of 0.69, a figure that is therefore consistent with cyclic product. Importantly, the GPC trace also shows no signs of

high molecular weight impurities that would usually be associated with either linear polymers or larger cycles.

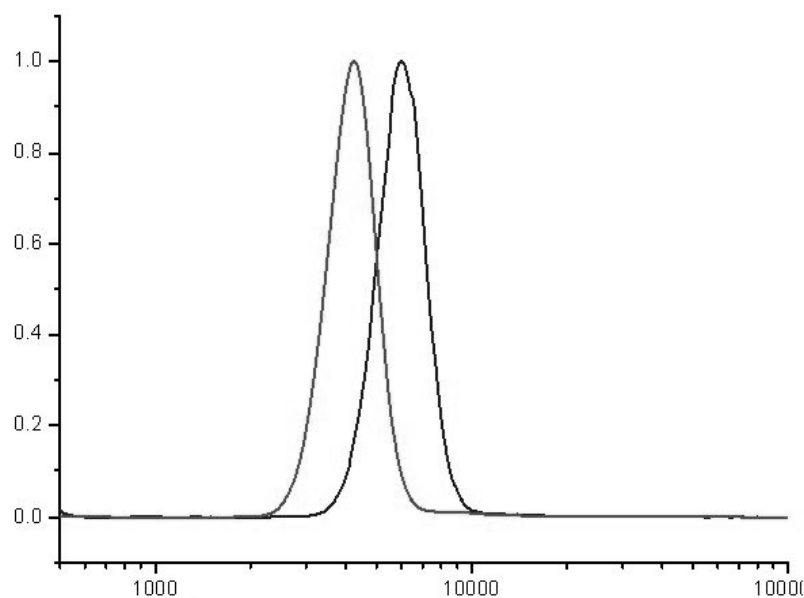


Figure 3.2.2.3 GPC traces of polymer chain before, grey (left) and after, black (right) cyclisation.

3.2.3 Versatility of cyclisation

As with the previous ‘click’ conjugations that have carried out here, no adverse effects on the polymer chain, i.e. transesterification, were observed during the reaction. The lack of transesterification is further evidenced by the fact that a single

degradation of the polymer chain would result in a linear by-product, an occurrence that is certainly not being observed. This simple reaction can be extended to quantitatively complete cyclisations of polymers with various tacticities as well as a range of different chain lengths; this data are shown in **Table 3.1**.

Table 3.1 Preparation of a range of cyclic poly(lactides)

Tacticity ^[a]	Target DP ^[b]	Linear Polymer		Cyclic Polymer		P ^[d]
		M_n g.mol ⁻¹ [c]	PDI ^[c]	M_n g.mol ⁻¹ [c]	PDI ^[c]	
Heterotactic	10	2,370	1.14	1,710	1.16	0.72
Heterotactic	20	5,280	1.14	3,740	1.11	0.71
Isotactic	20	5,770	1.08	3,990	1.06	0.69
Stereoblock	20	3,060	1.11	2,230	1.13	0.73
Atactic	20	3,930	1.15	3,110	1.12	0.79
Isotactic	50	11,080	1.08	8,120	1.09	0.73

^[a] Determined by ¹H NMR spectroscopy, conversion >95 %, catalysts as reported in Chapter 1; ^[b] Targeted degree of polymerisation based on [LA]/[initiator]; ^[c] Determined by GPC analysis; ^[d] Determined by $M_n(\text{Cyclic}) / M_n(\text{Linear})$.

3.2.4 Organic catalysis of cyclic poly(lactide)

The use of organocatalytic techniques in the polymerisation of lactide has briefly been discussed in Chapter 1. It would be ideal if this method could be transferred to this area despite the current difficulties of introducing stereocontrol during the polymerisation. Despite numerous efforts, it was not possible to incorporate the one pot ω -chain end functionalisation method to an organic catalyst. However, it is possible through the application of an acid chloride to allow end group conversion from the hydroxy functionality that is routinely present after the ROP of lactide **Figure 3.2.4.1**. The application of either 1,3-propanediol or **5** as the initiator, a thiourea and sparteine catalyst system and subsequent reaction with the maleimide bearing acid chloride seen earlier it was possible to, in two steps, simply synthesise the required telechelic polymer for cyclisation. Cyclic polymers synthesised from 1,3-propanediol in this way gave results identical to those synthesised from metal catalysts (Linear polymer $M_n = 4,970 \text{ g.mol}^{-1}$, PDI = 1.07; Linear polymer substituted $M_n = 5,210 \text{ g.mol}^{-1}$, PDI = 1.06; Cyclic polymer $M_n = 3,110 \text{ g.mol}^{-1}$, PDI = 1.09). As a consequence of the lack of stereocontrol during polymerisation this method was not examined further, but cyclic polymer synthesised in this way is notable due to the advantages that organocatalytic techniques can provide.

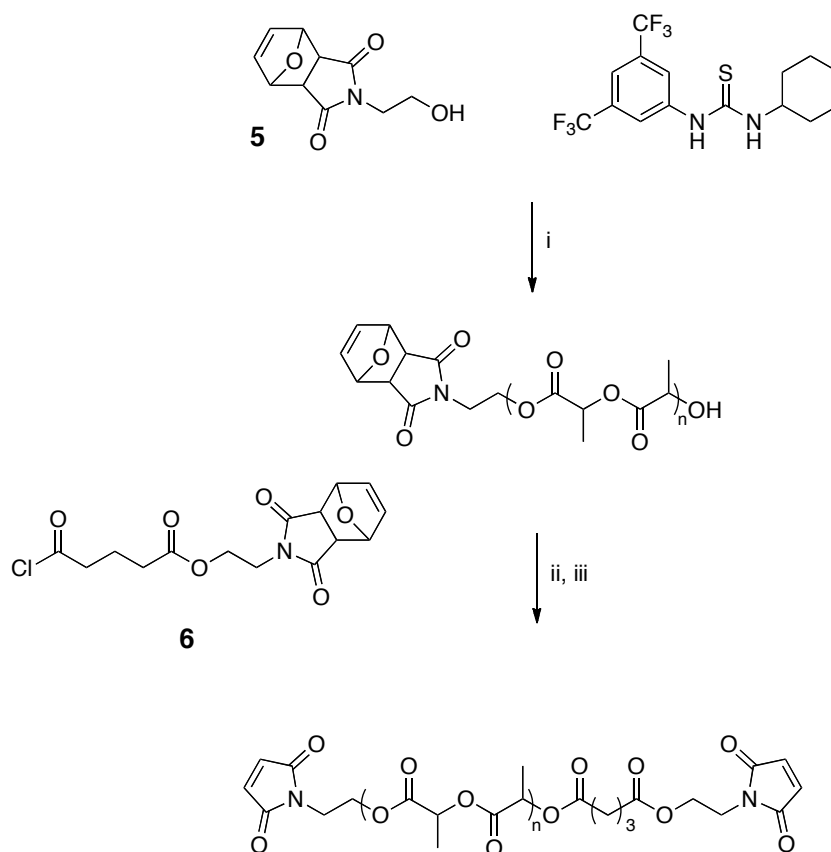


Figure 3.2.4.1 Synthesis of maleimide functional telechelic polymer *via* organic catalysis. i) **5**, thiourea, (-)-sparteine, CH_2Cl_2 , 30 mins; ii) **6**, NEt_3 , CH_2Cl_2 , 24 h; iii) heat, 24 h.

3.3 Cleavable cyclic poly(lactide)

3.3.1 Dithiol bridge cleavage

The synthetic route into cyclic polymers described gives us a simple opportunity to include a single point of functionality into the polymer chain through the application of a range of diols as initiators for the polymerisation. A degradable junction was of interest for two reasons, firstly it can provide further evidence for the cyclisation, and secondly it provides interesting opportunities in the future application of the cyclic polymers due to the differences in physical properties that the cleavage can initiate.

To achieve this 2-hydroxyethyl disulphide was incorporated into a cyclic polymer through initiation (Linear polymer $M_n = 5260 \text{ g.mol}^{-1}$, $\text{PDI} = 1.13$; Cyclic polymer $M_n = 3030 \text{ g.mol}^{-1}$, $\text{PDI} = 1.08$). The ability to selectively cleave the disulphide linker after the cyclisation enables us to reopen the polymer to a linear form. However, cleavage through the application of tBu_3P was found to be problematic and accurate data could not be recorded. It is postulated that inter-chain interactions and reformation of dithiol bridges occur upon exposure to air during the workup procedure. To overcome this problem it was postulated that it would be possible to cleave the dithiol and then functionalise with a maleimide in a single step. Thus, though the application of *N*-methylmaleimide (10 eq.), NEt_3 (10eq.),

and $^n\text{Bu}_3\text{P}$ it was possible to successfully cleave and cap both the linear and cyclic polymers, producing the expected polymer in both cases (Linear polymer $M_n = 5740 \text{ g.mol}^{-1}$, PDI = 1.11; Linear cleaved polymer $M_n = 2430 \text{ g.mol}^{-1}$, PDI = 1.14; Cyclic polymer $M_n = 3030 \text{ g.mol}^{-1}$, PDI = 1.08; Cyclic cleaved polymer $M_n = 3750 \text{ g.mol}^{-1}$, PDI = 1.11). The difference in retention time through the GPC column after cleavage for both polymers is significant, but the MALDI-ToF MS analysis unequivocally demonstrates the difference between the polymers. The difference between structures b) and d), **Figure 3.2.3.1** and **Figure 3.2.3.2**, is clear, with the cyclic polymer maintaining a nearly constant molecular weight after cleavage. The M_w demonstrates the inclusion of the two *N*-methylmaleimide functionalities. The cleavage of the polymers is useful evidence for the presence of cyclic polymers because, in the case of the cyclic polymer, cleavage causes an increase in molecular weight by GPC. Interestingly, the increase is $\sim 30 \%$, very close to the amount that we observed for the decrease upon cyclisation, as would be expected from the linear polymer. It is important to note here that there can be significant differences in GPC value upon changing only the chain end of the polymer; therefore seeing a result identical to the polymer before cyclisation would not be expected.

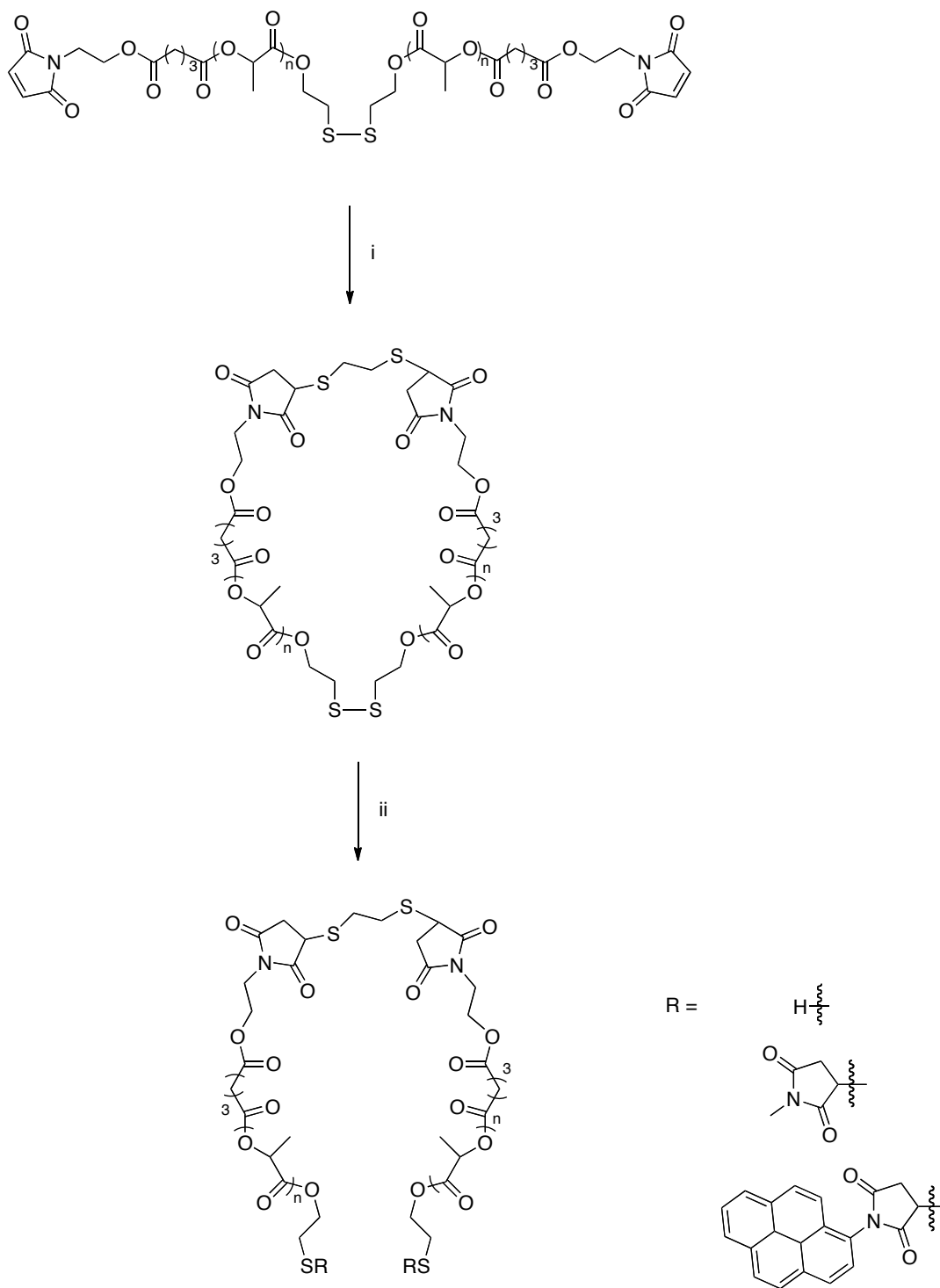


Figure 3.3.1.1 Synthesis and cleaving of dithiol bridged cyclic PLA. i) 1eq. 1,2-ethanedithiol, CH_2Cl_2 , NEt_3 , $\text{Na}_2\text{S}_2\text{O}_5$; ii) $^n\text{Bu}_3\text{P}$, CH_2Cl_2 or $^n\text{Bu}_3\text{P}$, NEt_3 , *N*-methylmaleimide, CH_2Cl_2 or $^n\text{Bu}_3\text{P}$, NEt_3 , *N*-(1-pyrenyl)maleimide, CH_2Cl_2 .

Both GPC and MALDI ToF MS results for the cyclic polymer shows completely the opposite behaviour to that demonstrated by the linear analogue. This occurrence is only possible if the polymer was cyclic in nature, suggesting that the architecture is that which was expected. This also draws interesting analogues to the degradation of the cyclic poly(lactide)s, where a single nucleophilic attack on the chain would result in an increase in the hydrodynamic volume, and a significant change in the physical properties of the polymer. Due to the time constraints of the project the degradation of the cyclic polymers was not examined, but would certainly provide an interesting area for study.

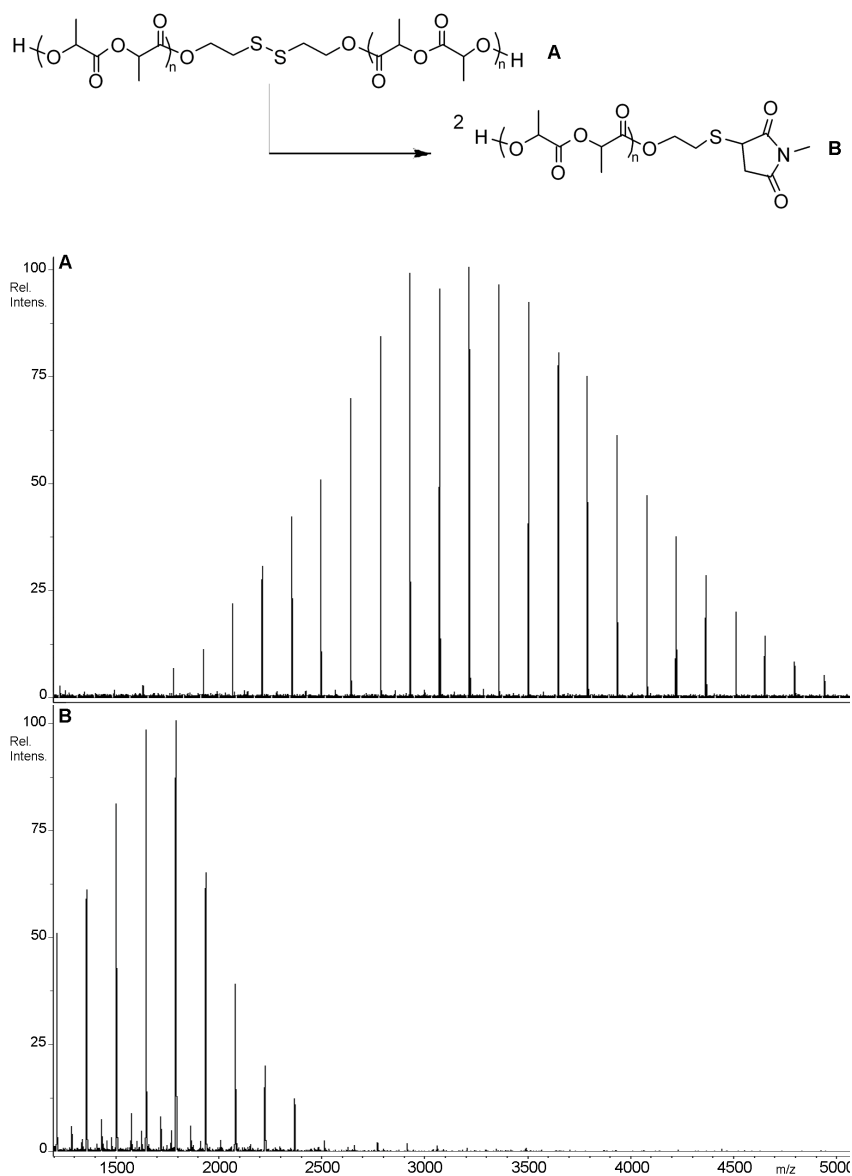


Figure 3.3.1.2 MALDI-ToF MS of linear polymers before and after cleavage of dithiol bridge with $^n\text{Bu}_3\text{P}$, NEt_3 and *N*-methylmaleimide.

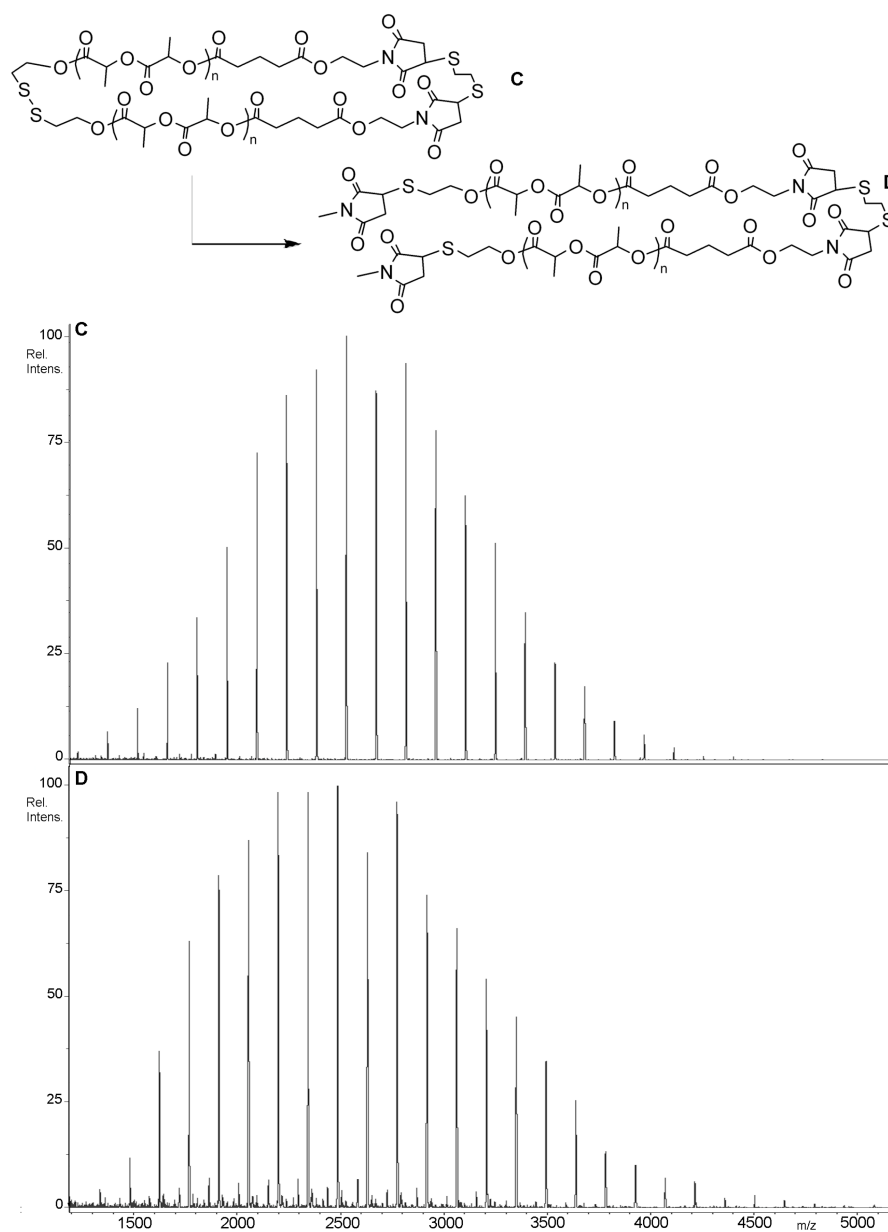


Figure 3.3.1.3 MALDI-ToF MS of cyclic polymers before and after cleavage of dithiol bridge with $n\text{Bu}_3\text{P}$, NEt_3 and *N*-methylmaleimide.

It was also possible to carry out the trapping procedure using *N*-(1-pyrenyl)maleimide. This had the advantage of enabling UV detecting GPC analysis to be carried out to identify the presence of the pyrene functionality in the cleaved linear and cyclic polymers. The results, **Table 3.2**, show that the pyrene is distributed evenly throughout the cleaved polymers as would be expected for the new chain end. Interestingly, the cyclic cleavage gives a much more significant intensity by GPC caused by the presence of two pyrene functionalities per chain.

Table 3.2 Linear and cyclic polymer cleavage with *N*-(1-pyrenyl)maleimide trapping.

		Linear polymer		Cyclic polymer	
		M_n g.mol ⁻¹ [a]	PDI ^[a]	M_n g.mol ⁻¹ [a]	PDI ^[a]
Before cleavage [b]	DRI	5,740	1.11	3,030	1.08
	UV	— ^[c]	— ^[c]	— ^[c]	— ^[c]
After cleavage [b]	DRI	2,390	1.14	3,850	1.36
	UV	2,470	1.21	5,970	1.26

[a] Determined by GPC analysis; [b] ⁿBu₃P, NEt₃ and *N*-(1-pyrenyl)maleimide; [c] No polymer detected by UV analysis.

3.3.2 Diels Alder bridge cleavage

As well as being able to carry out the cleavage of the polymer using a dithiol bridge, alternative cleavable junctions were worth investigating, opening up the possibility of cleavage using a range of stimuli. A temperature cleavable linker was proposed using a reverse Diels-Alder reaction similar to that of the furan protection of the maleimide. Due to this similarity of the reverse reactions, it was vital that the cleavage didn't occur during the deprotection of the maleimide.²⁴ Certainly this was the case when the deprotection is carried out in refluxing toluene, but appears to provide far less of a problem when it is carried out in the vacuum oven, see Chapter 2.3.2. However, to avoid this problem anthracene was applied as the diene, knowing that the reverse reaction occurs at a significantly higher temperature than with the furan. Synthesis of the initiator, **7**, was carried out as shown in **Figure 3.3.2.1**.

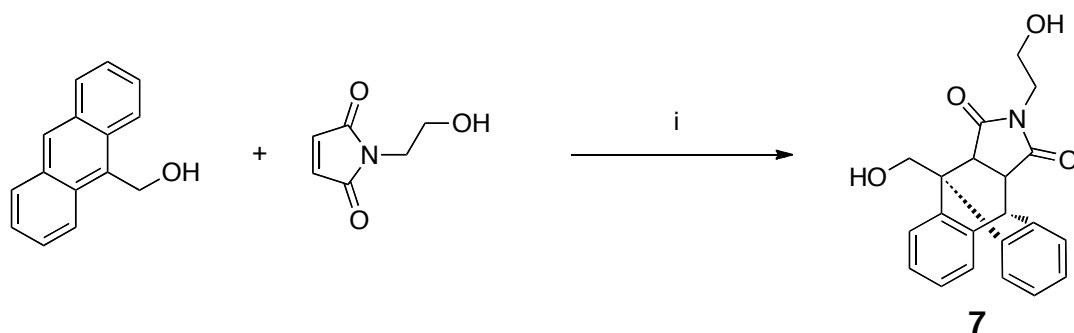


Figure 3.3.2.1 Synthesis of heat cleavable diol initiator, **7**. i) toluene, reflux, 16 h.

The diol was applied as the initiator for a polymerisation and subsequent cyclisation was confirmed by ^1H NMR and GPC analysis (Linear polymer $M_n = 5170 \text{ g.mol}^{-1}$, $\text{PDI} = 1.14$; Cyclic polymer $M_n = 2980 \text{ g.mol}^{-1}$, $\text{PDI} = 1.12$). MALDI-ToF MS analysis of the linear and cyclic polymers was particularly revealing for this reaction. It has already been observed that the furan maleimide reverse Diels-Alder reaction occurs in the laser of the MALDI-ToF MS instrument, and indeed the reverse Diels-Alder reaction occurs in this case also. However, due to the increased stability of the adduct, at low laser power the complete linear polymer is observed. In comparison, at high laser power a significant proportion has undergone the cleavage reaction, i.e. it has halved in molecular weight, **Figure 3.3.2.2**.

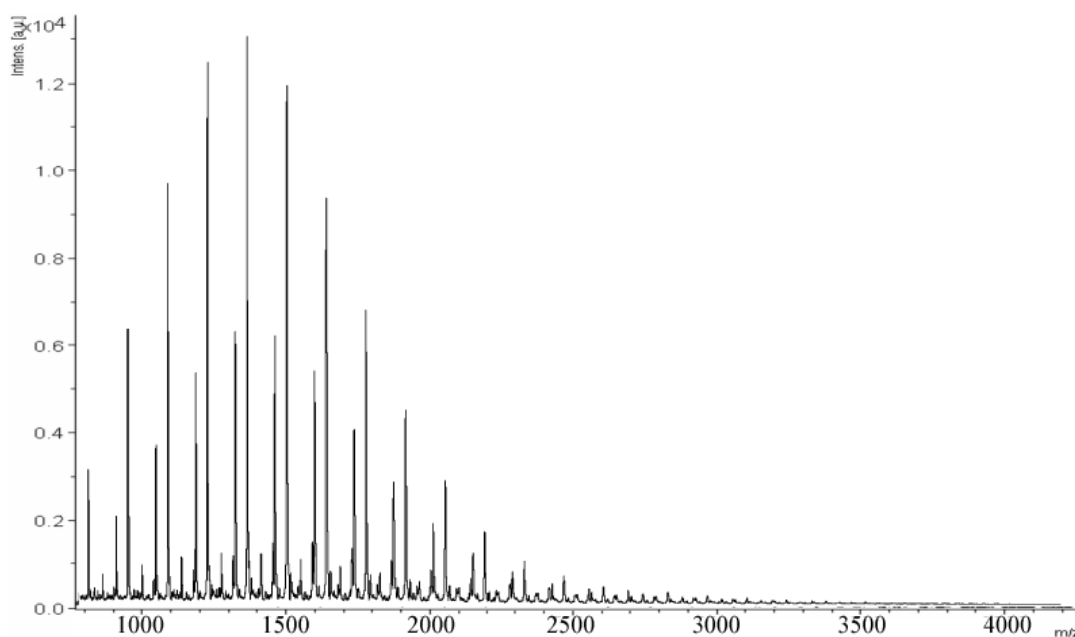


Figure 3.3.2.2 MALDI-ToF MS of linear Diels-Alder bridged polymer recorded under high laser power (small distribution at $M_w = \sim 3000$ corresponds to complete polymer).

During analysis of the cyclic product, despite the high laser power required to observe the polymer, no change in M_n occurs suggesting that no cleavage is occurring, **Figure 3.3.2.3**. Importantly, the reverse reaction affects no difference in the molecular weight and it would be impossible to see anything but the full molecular weight polymer. It is therefore reasonable to assume that the reverse Diels-Alder reaction would be occurring equally in both cases, and that the cyclisation and cleavage is occurring in the same way as observed for the dithiol example.

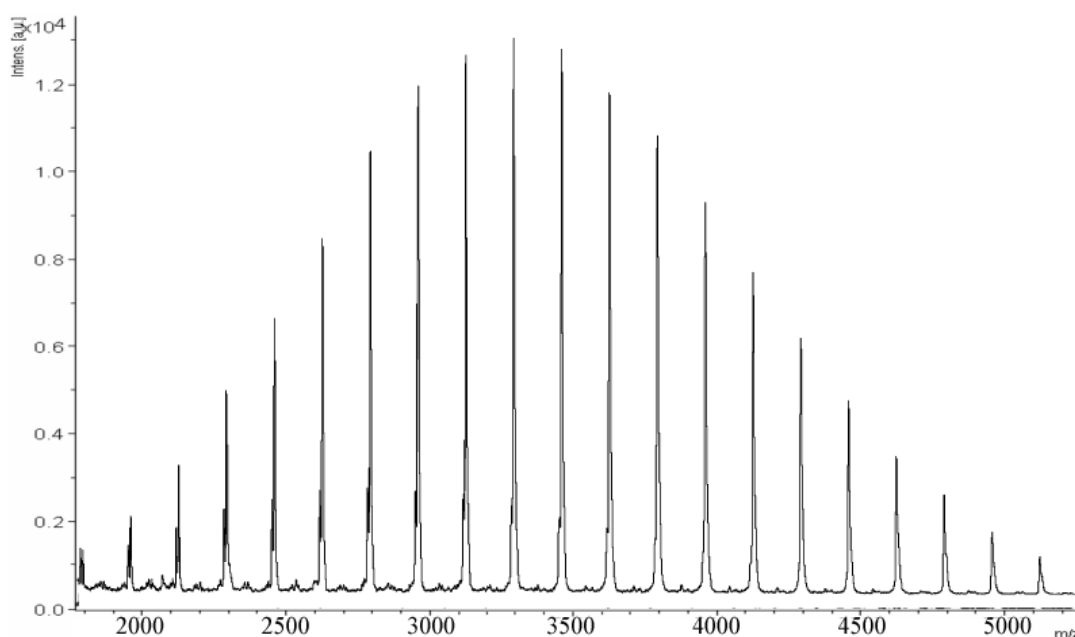


Figure 3.3.2.3 MALDI-ToF MS of cyclic diels alder bridged polymer under high laser power.

Unfortunately, due to the nature of the anthracene maleimide Diels-Alder reaction, it proved impossible to perform the reverse reaction without observing degradation of the polymer chain. Indeed, attempts to perform the reaction in refluxing toluene proved completely inefficient, requiring reaction times in excess of a week to cleave around 5 % of the polymer chains. It was necessary to carry out the reaction at 200 °C in a microwave to observe any significant reverse reaction occurring and the degradation of the polymer chain under these conditions results in a broadening of the PDi. This increase may also be due to incomplete cleavage of the polymer chains, and will no doubt cause issues with both the cyclic and stereoregular integrity of the poly(lactide). (Linear polymer $M_n = 5170 \text{ g.mol}^{-1}$, PDi = 1.14; Linear polymer cleaved $M_n = 3292 \text{ g.mol}^{-1}$, PDi = 1.28; Cyclic polymer $M_n = 2980 \text{ g.mol}^{-1}$, PDi = 1.12; Cyclic polymer cleaved $M_n = 3808 \text{ g.mol}^{-1}$, PDi = 1.26). MALDI-ToF MS analysis confirms that degradation of the polymer chain occurs, as well as transesterification, when carried out at a low laser power, **Figure 3.3.2.4**.

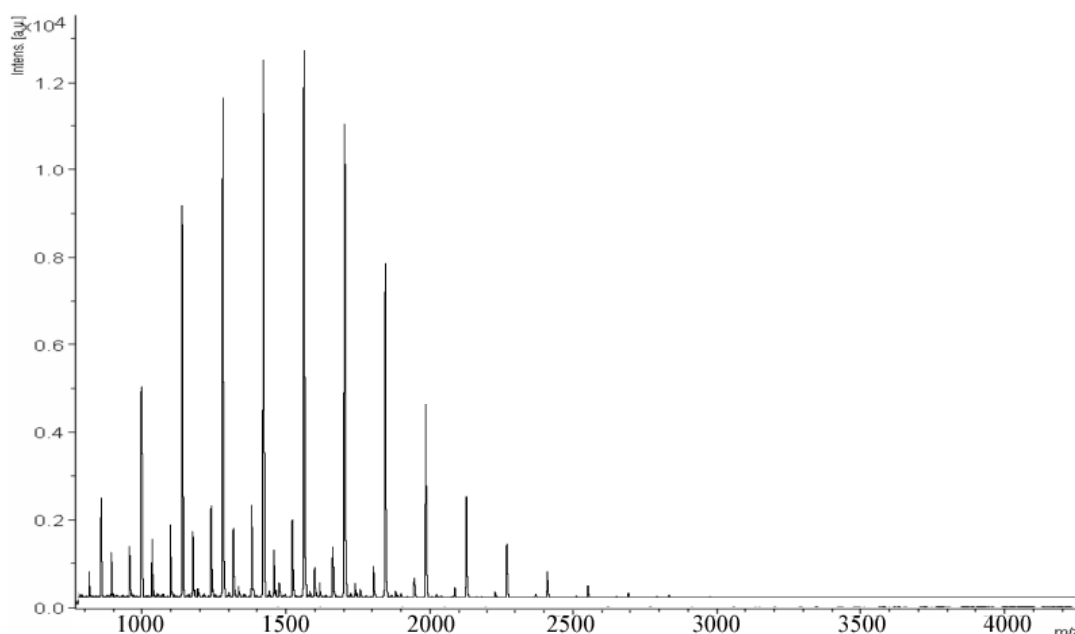


Figure 3.3.2.4 MALDI-ToF MS of linear diels alder bridged polymer cleaved at 200 °C in microwave.

In an effort to overcome this problem an alternative Diels-Alder reaction was sought, that between a cyclopentadiene functionality and maleimide. In principle there is no reason why this should not work, literature precedence suggest that the temperature should be different enough from our furan protection to proceed. However, in my hands I was unable to perform one reverse Diels-Alder in the absence of another, so this route was abandoned.

3.4 Single point functionality

3.4.1 Benzyl functionality

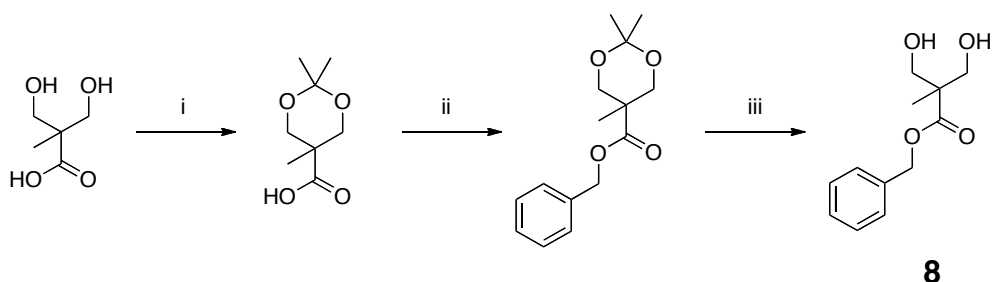


Figure 3.4.1.1 Benzyl functional diol initiator, **8**. i) 2,2-dimethoxypropane, PTSA, Acetone, 16 h; ii) DCC, CH₂Cl₂, 4h; then benzyl alcohol, DCC, DMAP, CH₂Cl₂, 16 h; iii) DOWEX H⁺ resin, CH₂Cl₂, 16 h.

In the same way that it was possible to incorporate a cleavable juncture in the polymer chain there was the potential to include a single point of functionality. To demonstrate this ability, the synthesis of the benzyl bearing diol, **8**, **Figure 3.4.1.1**, was undertaken from 2,2-bis(hydroxymethyl)propionic acid (MTC). This synthesis can be extended to allow for the synthesis of a range of functional groups, allowing their incorporation into the cyclic polymer. Incorporation was indeed observed with the synthesis of the expected polymer when the diol was used as an initiator, **Figure 3.4.1.2**.

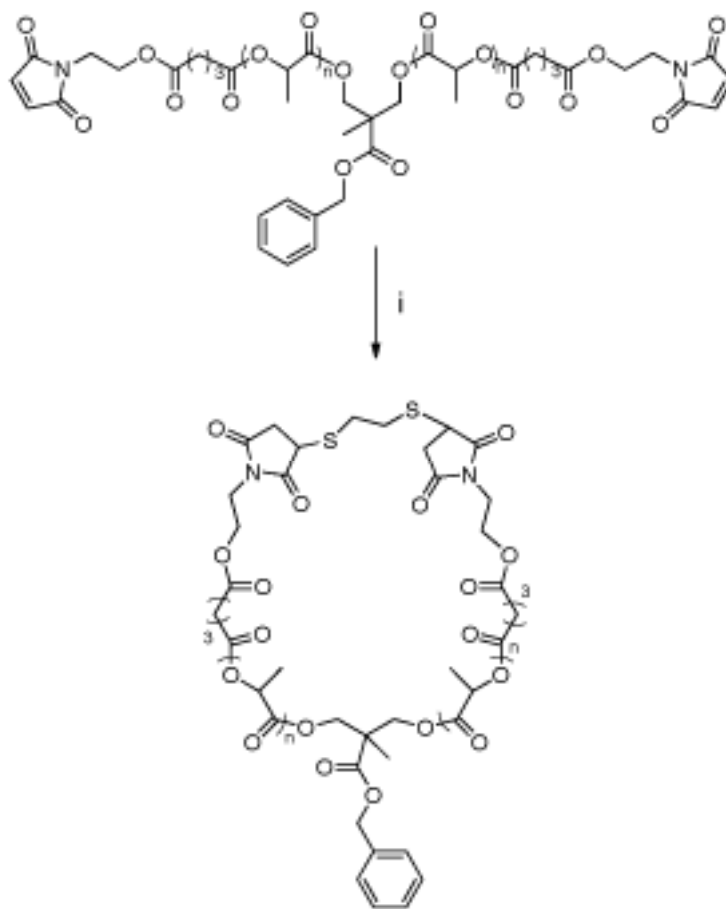


Figure 3.4.1.2 Benzyl functional cyclic polymer synthesis i) 1eq ethane dithiol, CH_2Cl_2 , NEt_3 , $\text{Na}_2\text{S}_2\text{O}_5$.

MALDI-ToF MS, ^1H NMR and GPC analysis (Linear Polymer $M_n = 7700 \text{ g}\cdot\text{mol}^{-1}$, $\text{PDI} = 1.10$; Cyclic polymer $M_n = 5290 \text{ g}\cdot\text{mol}^{-1}$, $\text{PDI} = 1.08$) all confirmed the synthesis of the expected cyclic polymer.

3.4.2 ‘Click’ functionality

This opportunity to incorporate a single point of functionality also, and more usefully, enables the inclusion of a ‘click’ functional handle onto the cyclic PLA. However, due to the nature of the cyclisation process a reaction that is compatible with the thiol-maleimide reaction must be used. Due to the problems that have previously been encountered through using both CuAAC reaction and selective Diels Alder deprotection, further investigation of the application of thiol-ene chemistry was required. Recently, it has been demonstrated that the nucleophilic attack of thiols can be carried out in the presence of either an alkene or an alkyne.^{25,26} Subsequently, through the use of a radical initiator it is possible to react another thiol with the alkene or alkyne functionality. It was postulated that it might be possible to extend this methodology to allow for the reaction of the thiol and maleimide in the presence of either an alkene or an alkyne.

3.4.2.1 Sequential ‘click’ reactions

To demonstrate the viability of this route, a linear polymer with an α -maleimide functionality and either an ω -alkene or alkyne functionality was prepared. Initially this polymer was reacted with dodecanethiol in the presence of NEt₃ for 2 hours,

allowing complete consumption of the maleimide to occur as previously demonstrated, **Figure 3.4.2.1**. ^1H NMR and MALDI-ToF MS confirmed that conversion of the maleimide had occurred. Importantly analysis also showed that no reaction had occurred to the alkene/alkyne chain end, **Figure 3.4.2.2**. Subsequent reaction with benzyl thiol in the presence of dimethyl phenyl phosphine (DMPP) for 2 - 24 h allows complete substitution of the alkene or alkyne functionality *via* a Michael addition. Confirmation was obtained from ^1H NMR and MALDI-ToF MS, **Figure 3.4.2.3**. GPC data shows no degradation of the polymer chain at any stage of the synthesis, **Table 3.3**.

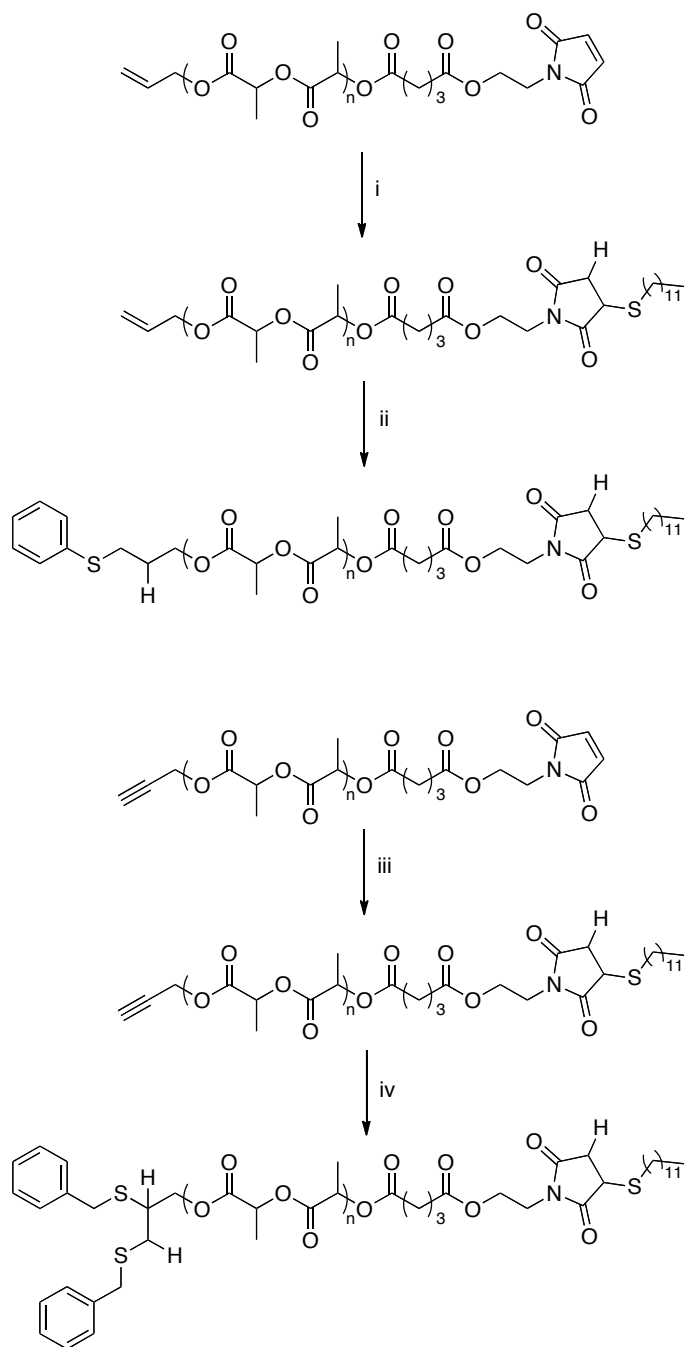


Figure 3.4.2.1 Sequential ‘click’ reactions with alkene and alkyne functionalities. i) 10 eq. NEt_3 , 10 eq. DDT, CH_2Cl_2 , 0.5 h; ii) 10 eq. benzyl thiol, DMPP, CH_2Cl_2 , 2 h; iii) 10 eq. NEt_3 , 10 eq. DDT, CH_2Cl_2 , 0.5 h; iv) 20 eq. benzyl thiol, DMPP, CH_2Cl_2 , 24 h.

Table 3.3 Sequential α - and ω -chain end conjugation.

	Alkene polymer		Alkyne polymer	
	M_n g.mol ⁻¹ [a]	PDI ^[a]	M_n g.mol ⁻¹ [a]	PDI ^[a]
Linear Polymer	5,980	1.21	6,140	1.09
Maleimide substituted^[b]	6,200	1.14	6,380	1.13
Thiophenol substituted^[c]	6,420	1.11	6,990	1.08

[a] Determined by GPC analysis; [b] Conjugation carried out with dodecanethiol; [c] Conjugation carried out with thiophenol.

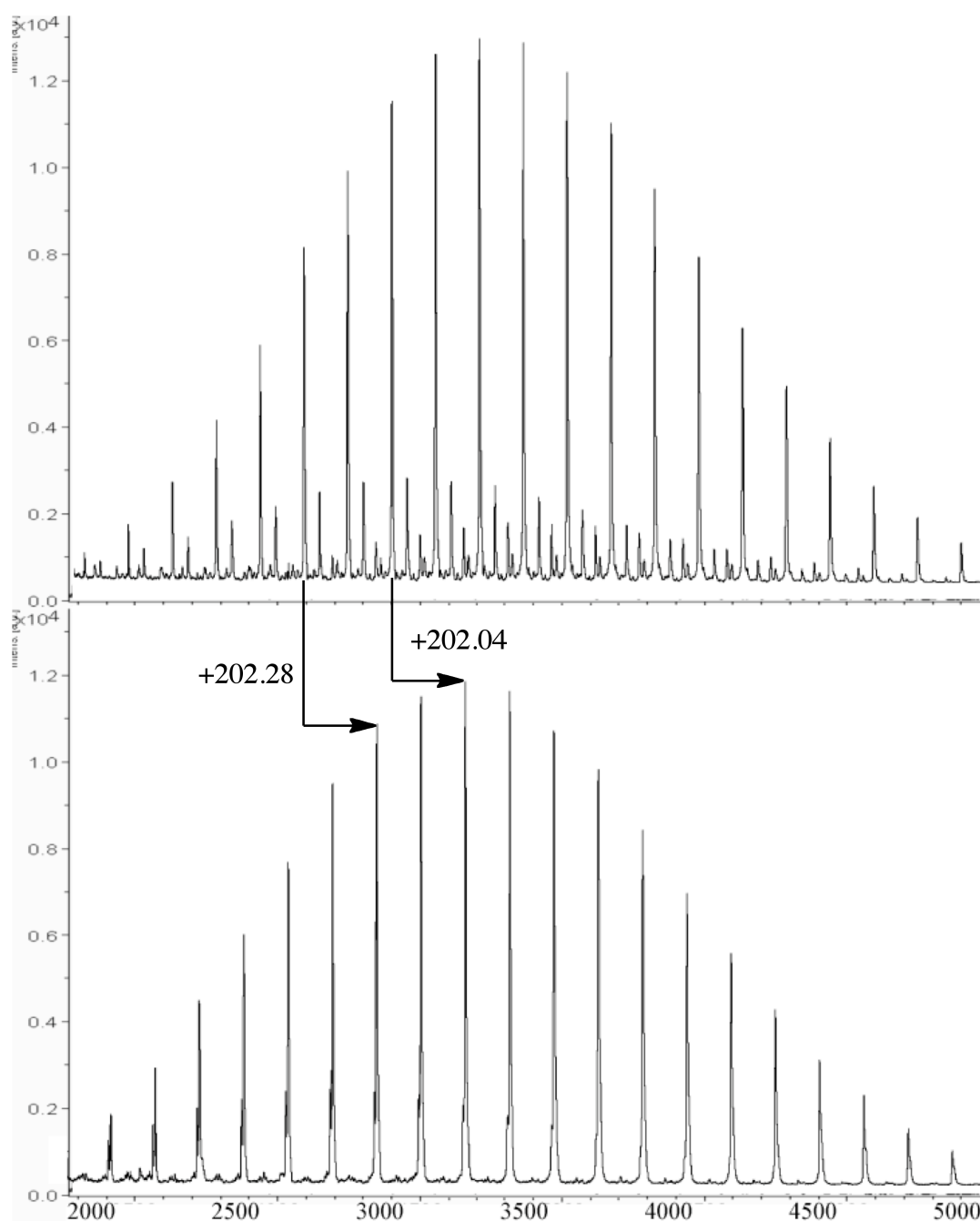


Figure 3.4.2.2 MALDI-ToF MS analysis of dodecanethiol conjugation, showing only single addition to maleimide chain end.

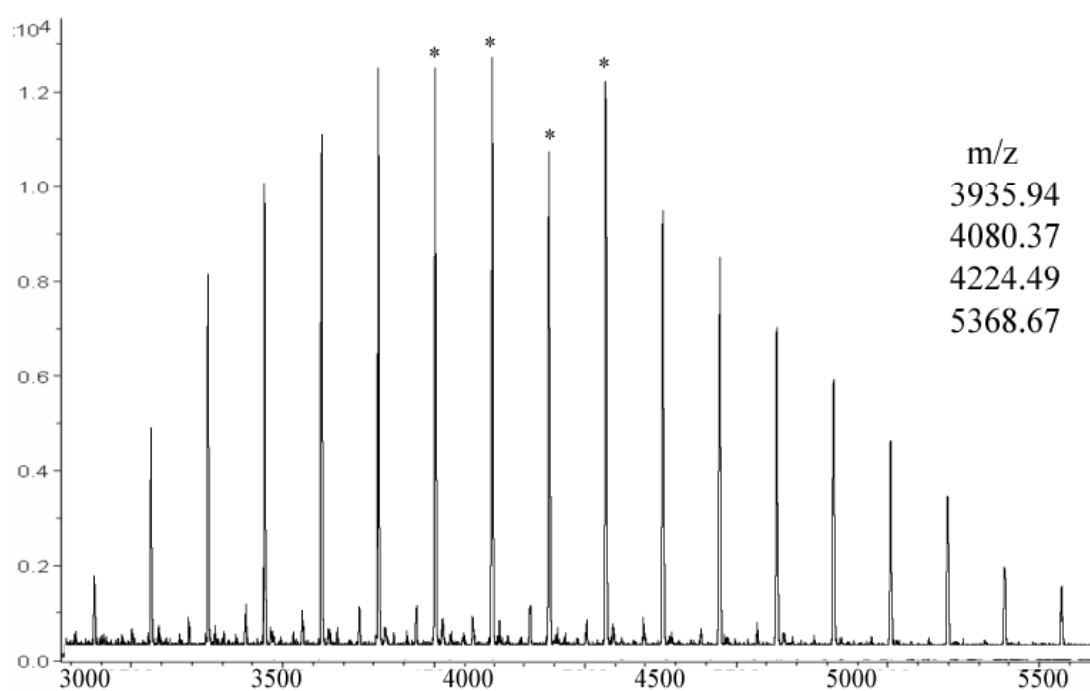


Figure 3.4.2.3 MALDI-ToF MS analysis of thiophenol conjugation to alkyne functional linear polymer, showing exactly two additions.

3.4.2.2 Cyclic polymer with 'click' functionality

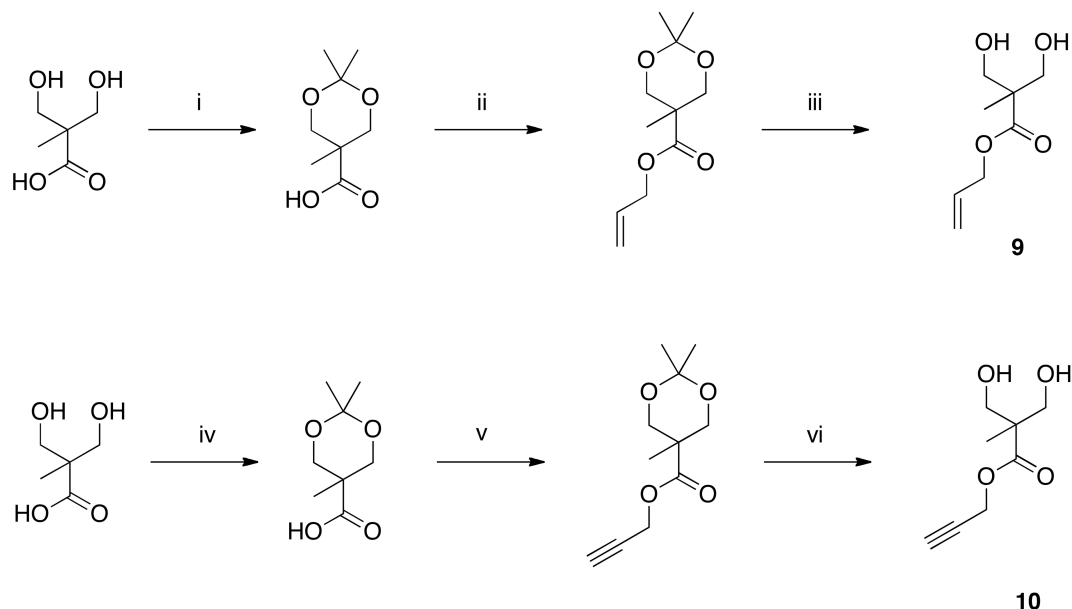


Figure 3.4.2.4 Diol initiator synthesis bearing 'click' functional handles, **9** & **10**. i)

2,2-dimethoxypropane, PTSA, Acetone, 16 h; ii) DCC, CH_2Cl_2 , 4h; then allyl alcohol, DCC, DMAP, CH_2Cl_2 , 16 h; iii) DOWEX H^+ resin, CH_2Cl_2 , 16 h; iv) 2,2-dimethoxypropane, PTSA, Acetone, 16 h; v) DCC, CH_2Cl_2 , 4h; then propargyl alcohol, DCC, DMAP, CH_2Cl_2 , 16 h; iii) DOWEX H^+ resin, CH_2Cl_2 , 16 h.

The simple synthesis of alkene, **9**, and alkyne, **10**, bearing initiators was carried out from 2,2-bis(hydroxymethyl)propionic acid (MTC) as previously described, a route allowing for the incorporation of a large range of possible functional handles as previously seen with the synthesis of the phenyl bearing diol, **Figure 3.4.2.4**. The polymerisation and subsequent cyclisation was then carried out in exactly the same

way as previously described and in both cases no reaction between the dithiol and alkene/alkyne was observed, **Table 3.4**. Indeed, after the cyclisation had been carried out it was also possible to perform further reactions at the alkene/alkyne site, **Figure 3.4.2.5**. To demonstrate this, benzyl thiol was applied with DMPP and resulted in the mono- and disubstituted products, exactly as has been previously reported for the linear polymer. MALDI-ToF MS, **Figure 3.4.2.6**, ^1H NMR and GPC all confirm the presence of the benzyl functionality, **Table 3.4**.

Table 3.4 Single point Michael addition to cyclic PLA.

	Alkene polymer		Alkyne polymer	
	$M_n \text{ g.mol}^{-1}$ [a]	PDI ^[a]	$M_n \text{ g.mol}^{-1}$ [a]	PDI ^[a]
Linear Polymer	7,350	1.11	7,290	1.05
Cyclic Polymer	5,820	1.18	5,900	1.11
Thiophenol substituted	6,650	1.13	8,600	1.04

[a] Determined by GPC analysis.

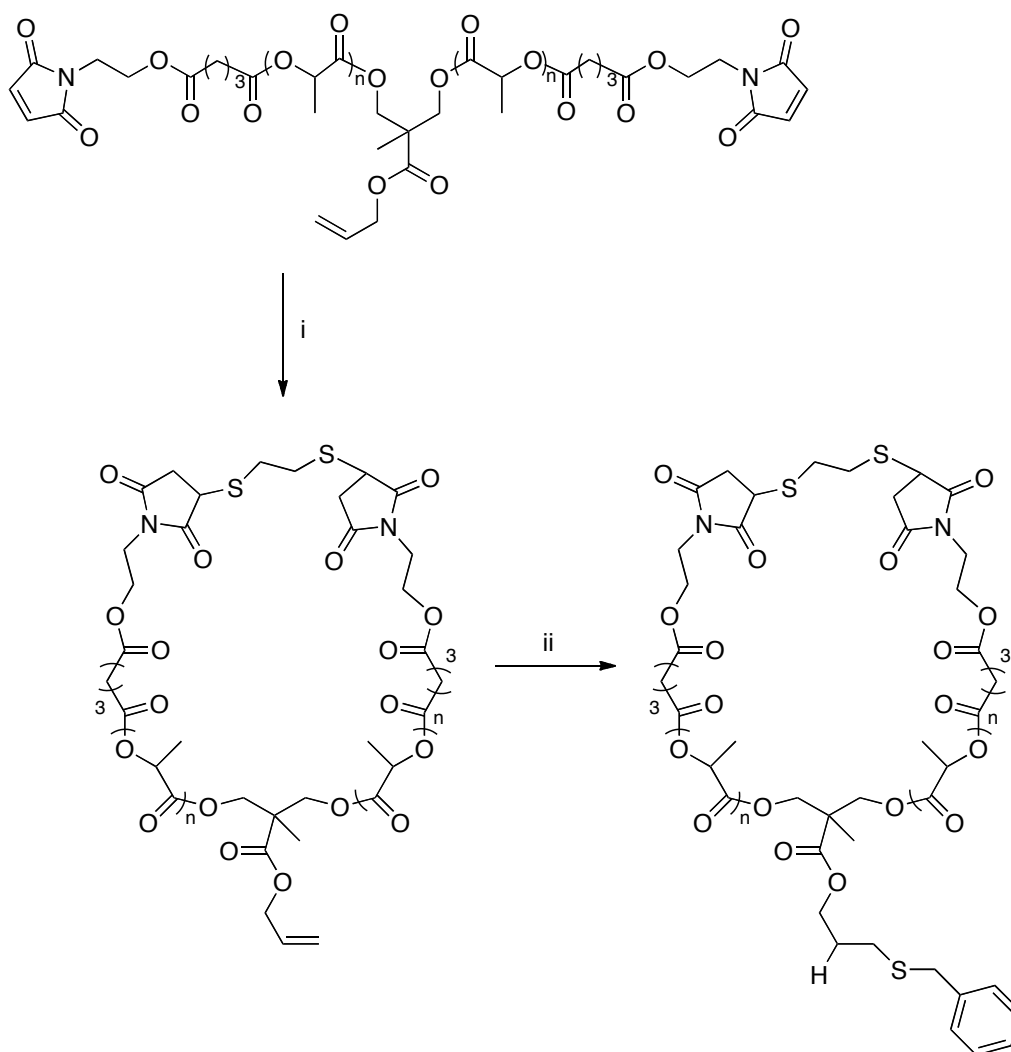


Figure 3.4.2.5 Incorporation and ‘click’ chemistry of a single point functionality onto cyclic PLA. i) 1eq ethane dithiol, CH_2Cl_2 , NEt_3 , $\text{Na}_2\text{S}_2\text{O}_5$; ii) 10 eq. benzyl thiol, DMPP, CH_2Cl_2 , 4 h.

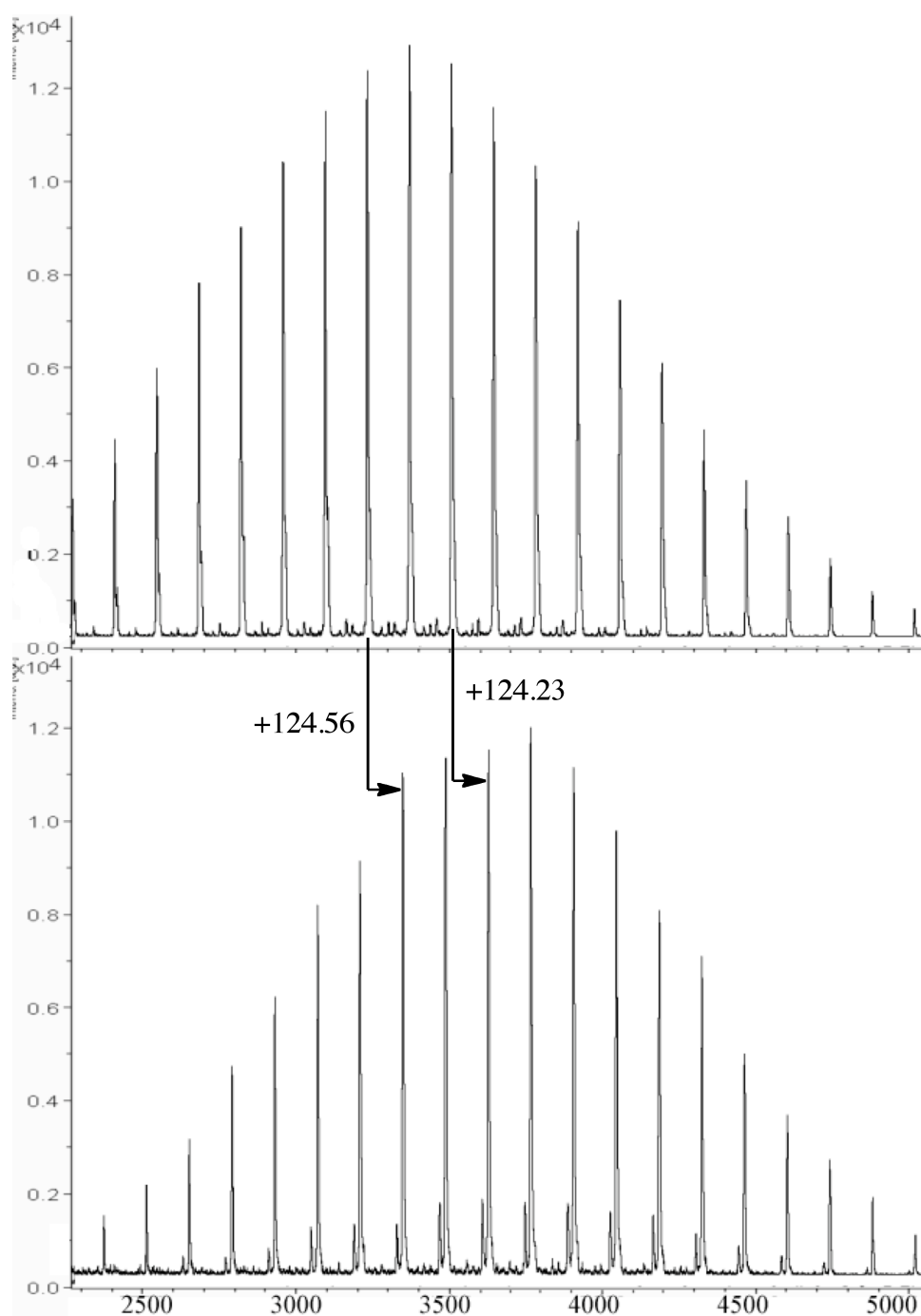


Figure 3.4.2.6 MALDI-ToF MS of benzyl thiol conjugation to alkene functional, cyclic poly(lactide).

3.5 Conclusion

In conclusion, a one-pot synthetic route for the synthesis of a range of α - and ω -chain end functionalised poly(lactide)s that is tolerant to a range of functional groups has been demonstrated. Importantly the mild nature of the Michael addition of thiols to maleimides, alkenes and alkynes, enables the stereoregularity of the polymer to be maintained. This can be extended to the application of a further, radically initiated, Michael addition at a single designed point on the cycle. The synthesis of cleavable cycles for the purposes of both further evidence for cyclisation and the further development and control of complex architectures has also been explored.

3.6 References

- ¹ Hawker, C. J.; Wooley, K. L. *Science* **2005**, *309*, 1200-1205.
- ² Kricheldorf, H. R. *J. Poly. Sci. Part A. Polym. Chem.* **2010**, *48*, 251-284.
- ³ Laurent, B. A.; Grayson, S. M. *Chem. Soc. Rev.* **2009**, *38*, 2202-2213.
- ⁴ Hoskins, J. N.; Grayson, S. M. *Macromolecules* **2009**, *42*, 6406-6413.
- ⁵ Dechy-Cabaret, O.; Martin-Vaca, B.; Bourissou, D. *Chem. Rev.* **2004**, *104*, 6147-6176.
- ⁶ Dove, A. P. *Chem. Commun.* **2008**, 6446-6470.
- ⁷ Jerome, C.; Lecomte, P. *Adv. Drug Deliv. Rev.* **2008**, *60*, 1056-1076.
- ⁸ Ruddick, C. L.; Hodge, P.; Cook, A.; McRiner, A. J. *J. Chem. Soc. Perkin Trans. I* **2002**, 629-637.
- ⁹ Chisholm, M. H.; Gallucci, J. C.; Yin, H. F. *Proc. Nat. Acad. Sci.* **2006**, *103*, 15315-15320.
- ¹⁰ Kricheldorf, H. R.; Langanke, D.; Stricker, A.; Rader, H. J. *Macromol. Chem. Phys.* **2002**, *203*, 405-412.
- ¹¹ Li, H. Y.; Jerome, R.; Lecomte, P. *Polymer* **2006**, *47*, 8406-8413.
- ¹² Culkin, D. A.; Jeong, W. H.; Csihony, S.; Gomez, E. D.; Balsara, N. R.; Hedrick, J. L.; Waymouth, R. M. *Angew. Chem. Int. Ed. Engl.* **2007**, *46*, 2627-2630.
- ¹³ Jeong, W.; Shin, E. J.; Culkin, D. A.; Hedrick, J. L.; Waymouth, R. M. *J. Am. Chem. Soc.* **2009**, *131*, 4884-4891.
- ¹⁴ Coulembier, O.; Moins, S.; De Winter, J.; Gerbaux, P.; Leclere, P.; Lazzaroni, R.; Dubois, P. *Macromolecules* **2010**, *43*, 575-579.

- ¹⁵ Guo, L.; Zhang, D. H. *J. Am. Chem. Soc.* **2009**, *131*, 18072-18073.
- ¹⁶ Laurent, B. A.; Grayson, S. M. *J. Am. Chem. Soc.* **2006**, *128*, 4238-4239.
- ¹⁷ Eugene, D. M.; Grayson, S. M. *Macromolecules* **2008**, *41*, 5082-5084.
- ¹⁸ Goldmann, A. S.; Quemener, D.; Millard, P. E.; Davis, T. P.; Stenzel, M. H.; Barner-Kowollik, C.; Wuller, A. H. E. *Polymer* **2008**, *49*, 2274-2281.
- ¹⁹ Lonsdale, D. E.; Bell, C. A.; Monteiro, M. J. *Macromolecules* **2010**, *43*, 3331-3339.
- ²⁰ Clark, P. G.; Guidry, E. N.; Chan, W. Y.; Steinmetz, W. E.; Grubbs, R. H. *J. Am. Chem. Soc.* **2010**, *132*, 3405-3412.
- ²¹ Schulz, M.; Tanner, S.; Barqawi, H.; Binder, W. H. *J. Poly. Sci. Part A. Polym. Chem.* **2010**, *48*, 671-680.
- ²² Stanford, M. J.; Dove, A. P. *Macromolecules* **2009**, *42*, 141-147.
- ²³ Pounder, R. J.; Stanford, M. J.; Brooks, P.; Richards, S. P.; Dove, A. P. *Chem. Commun.* **2008**, 5158-5160.
- ²⁴ Rickborn, B., *Org. React.*, **1998**, *52*, 1.
- ²⁵ Kade, M.J.; Burke, D.J.; Hawker, C.J., *J. Polym. Sci. Part A: Polym. Chem.*, **2010**, *48*, 743.
- ²⁶ Lowe, A.B.; Hoyle, C.E.; Bowmon, C.N., *J. Mater. Chem.*, **2010**, *20*, 4745.

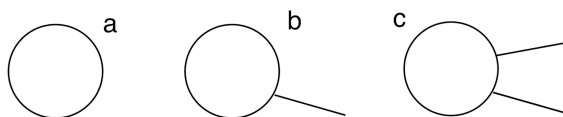
Chapter 4: Complex architectures of cyclic poly(lactide)s

4.1 Introduction

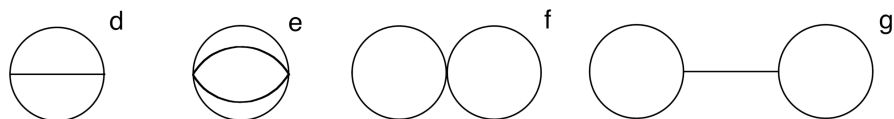
As has been previously discussed, control over the architecture of the polymer allows for control of the physical properties of the resultant material. Complex polymer architectures in particular are of interest due to the novel ways in which the polymer chains interact during self-assembly. Access to these structures has recently been an area of interest due to the increased use of ‘click’ type chemistries in the field of polymeric materials. Incorporation of cyclic polymer provides an even greater range of possible architectures, an area that was introduced in Chapter 1.

Previous reports in the literature demonstrate a range of possible polymer architectures that have previously been synthesised.¹ Architectures of particular interest in this area include the doubly fused tricyclic loop of Tezuka and coworkers^{2,3} and multi armed brushes of Huang *et al.*^{4,5} A range of possible architectures that include cyclic polymers is shown in **Figure 4.1.1**.

Mono-cyclic



Bi-cyclic



Multi-cyclic

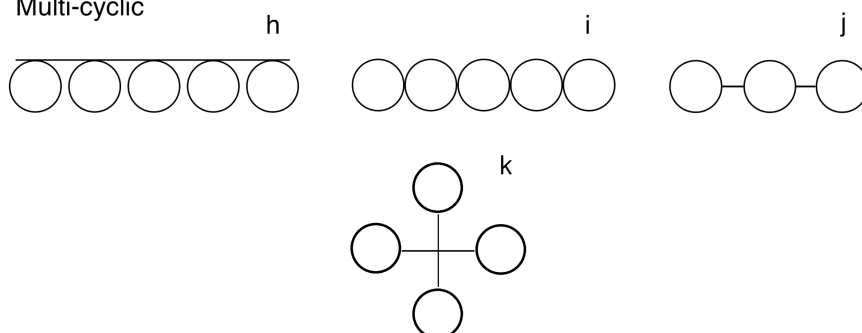


Figure 4.1.1 Cyclic polymer architectures, a) cyclic;⁶ b) ‘tadpole’ shaped;⁷ c) tadpole;⁸ d) ‘theta’ shaped;⁹ e) ‘Doubly fused bicyclic’ structure;¹⁰ f) spirocyclic;¹¹ g) ‘handcuff’ shaped;¹² h) backbone linked;¹³ i) enchained;¹⁴ j) enchained with linkers;¹⁵ k) ‘quatrefoil’ shaped.¹⁶

Block copolymers are also of particular interest due the possibility of their self-assembly and the differences that they offer in physical properties. As has already been shown in Chapter 2, the methodology that is employed here can be easily applied to the synthesis of block copolymers, but the introduction of the cyclic poly(lactide) would be of particular interest. Using a tin catalyst as previously

discussed, Kricheldorf *et al.* were able to synthesise cyclic poly(lactide)-*b*-poly(caprolactone) structures, and also to obtain ‘tadpole’ shaped polymer architectures.¹⁷ Other, non-poly(lactide), examples are a lot more common and several have already been outlined in Chapter 1. Self-assembly of cyclic polymers has previously been shown to produce interesting and alternative structures to identical linear polymers, which makes it an area of particular interest. In the field of biodegradable polymers access to an increased range of architectures through self-assembly could prove particularly useful. Applications in industry, such as biomedicine, will benefit greatly from the range of physical properties that will be available from these architectural changes.

4.2 One pot synthesis of multi-cyclic polymers

The ideal situation in any synthesis is to be able to complete the method in a single step. The robust methodology that has been developed here for the synthesis of cyclic polymers allows for some interesting variations in a single pot. The use of a dithiol to complete cyclisation in this way sparked interest in what would happen if a multi-armed thiol were applied instead. The ready availability of these compounds meant that this could provide a simple technique for the synthesis of complex architectures.

4.2.1 Cyclisations using trimethylolpropane tris-(3-mercaptopropionate)

Figure 4.2.1.1 shows the intended formation of the ‘handcuff’ shaped polymer that would occur during this synthesis. The one-pot synthesis of this architecture would be particularly novel. Exact molar quantities of the polymer to thiol are vital and dilute stock solutions were made to facilitate this. Characterisation of this polymer would be challenging, with various literature examples suggesting that this polymer will have a molecular weight somewhere between one and two times the molecular weight of the linear chain. GPC evidence alone would therefore be quite hard to rely on, MALDI-ToF MS analysis should give us much more idea as to what has occurred during the cyclisation step.

The reaction of linear polymer with trimethylolpropane tris-(3-mercaptopropionate) was carried out using exactly the same procedure as earlier cyclisations, no additional time was given in initial reactions and results suggest that this would not be required. Indeed, only the cyclisation would even require high dilution, the linking of the chains could be carried out in concentrated conditions, as it is intermolecular. The GPC analysis showed that the molecular weight had increased from the linear polymer, suggesting the presence of a more complex architecture than simply a cycle, and importantly within the limits suggested by the literature: the cyclic structure having an M_n almost exactly $1.5 \times$ that of the linear polymer

(Linear polymer, $M_n = 2490 \text{ g.mol}^{-1}$, PDI = 1.24; ‘Handcuff’ shaped polymer, $M_n = 3720 \text{ g.mol}^{-1}$, PDI = 1.07).

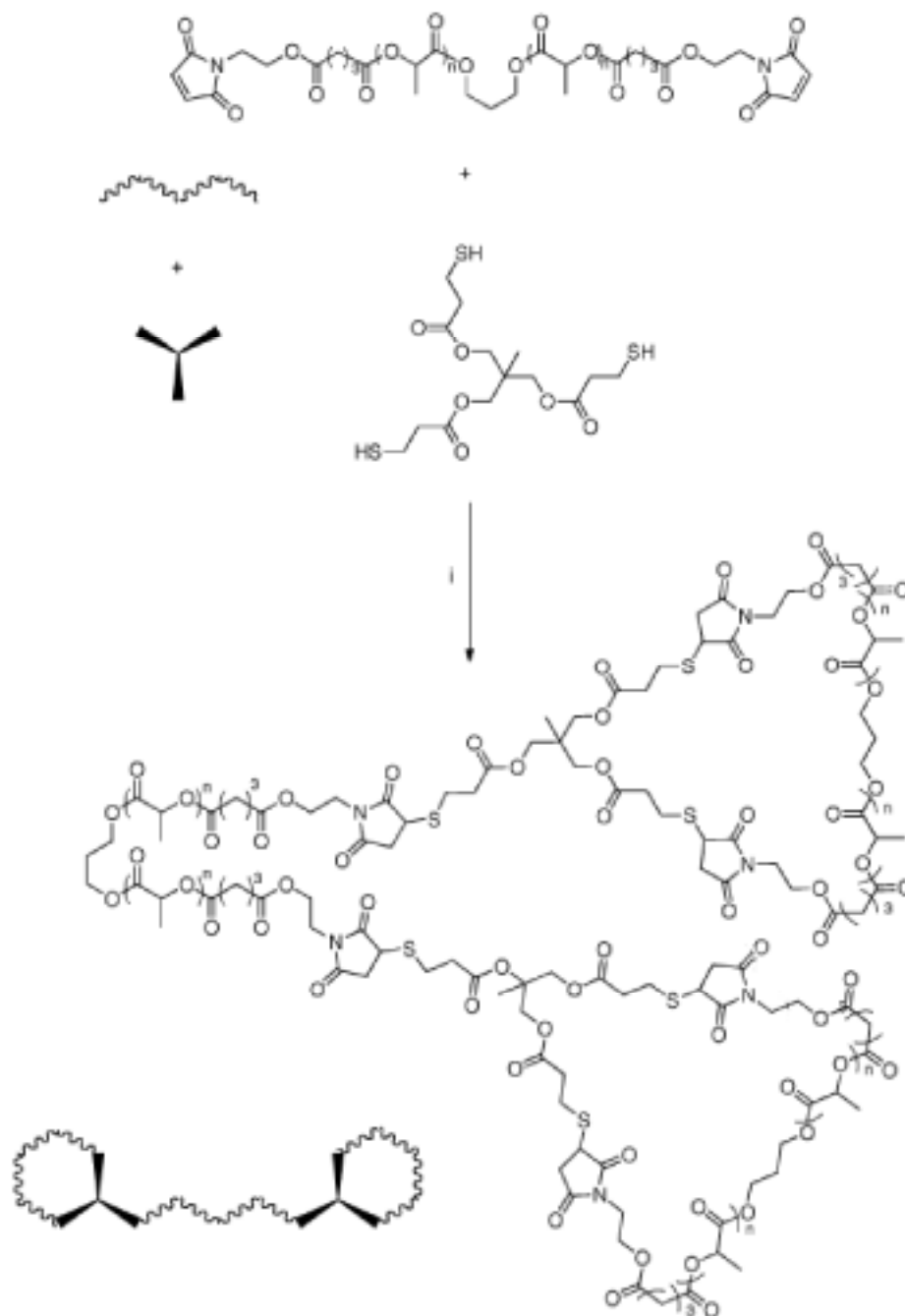


Figure 4.2.1.1 One pot synthesis of ‘handcuff’ shaped poly(lactide); i) 0.67 eq trimethylolpropane tris-(3-mercaptopropionate), CH_2Cl_2 , NEt_3 , $\text{Na}_2\text{S}_2\text{O}_5$.

MALDI-ToF MS analysis shows the inclusion of two thiol bridging species and reveals the molecular weight to be that expected, **Figure 4.2.1.2**. However, due to the complexity of the polymer and the comparative size of the two bridging species, the spectra obtained did not provide ideal levels of response and suggests the degree of polymerisation to be smaller than expected (this is not unprecedented; when the sample does not provide strong responses by MALDI-ToF MS only low M_w species are observed). ^1H NMR analysis confirms complete conversion of the maleimide functionalities.

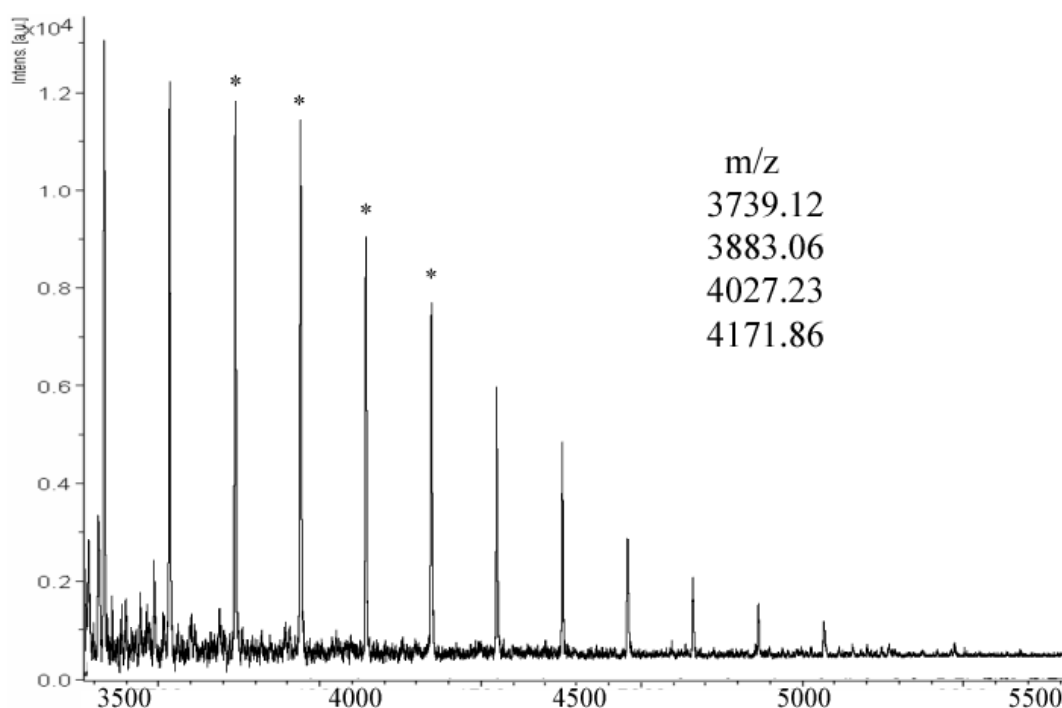


Figure 4.2.1.2 MALDI-ToF MS of the ‘handcuff’ shaped poly(lactide).

There is a possibility that the polymer formed in this synthesis may also be ‘theta’ shaped. Theoretically, this should be unfavourable as the cyclisation process has

been shown to proceed at the same dilution. Thus, the initial reaction should preferentially form the cyclic product with one thiol remaining rather than joining two separate trimethylolpropane tris-(3-mercaptopropionate) molecules. If any of this product were present, a broadening of the PDI may be expected to occur.

4.2.2 Cyclisations using pentaerythritol tetrakis-(3-mercaptopropionate)

In exactly the same way demonstrated with trimethylolpropane tris-(3-mercaptopropionate), a three-armed thiol, it is possible to complete cyclisation using pentaerythritol tetrakis-(3-mercaptopropionate), a four-armed thiol. Counter intuitively this actually forms a smaller polymer structure than that of the trimethylolpropane tris-(3-mercaptopropionate) example; as there is now no polymer bridging the two cycles, **Figure 4.2.2.1**. GPC analysis of the spirocyclic polymer reveals a lower M_n than observed for the ‘handcuff’ shaped polymer, as would be expected without the bridging polymer chain, and also shows an increase over the linear chain (Linear polymer, $M_n = 2,490 \text{ g.mol}^{-1}$, PDI = 1.24; Spirocyclic polymer, $M_n = 3,500 \text{ g.mol}^{-1}$, PDI = 1.12). Notably, in both this and the ‘handcuff’ shaped polymer, a low PDI is maintained and no other species are visible by GPC, ^1H NMR or MALDI-ToF MS analysis. Again, ^1H NMR analysis confirms

complete conversion of the maleimide functionality, and solubility in CH_2Cl_2 and CHCl_3 suggests the presence of a pure simple polymer.

MALDI-ToF analysis again confirms the inclusion of the thiol containing bridge, although this time the polymer gives a much more substantial response, giving a better signal to noise ratio, **Figure 4.2.2.2**.

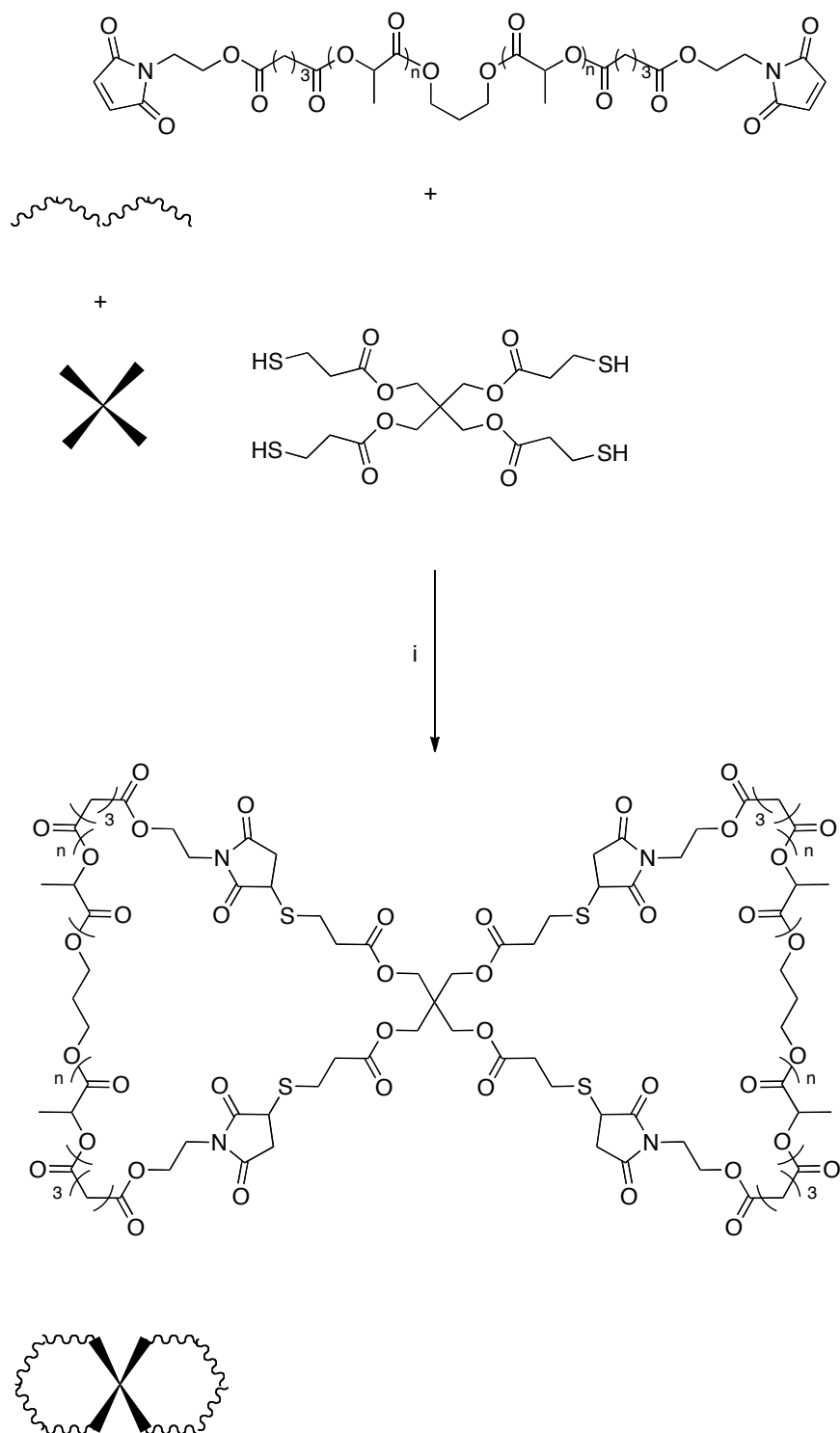


Figure 4.2.2.1 One pot synthesis of spirocyclic poly(lactide); *i*) 0.5 eq. Pentaerythritol tetrakis-(3-mercaptopropionate), CH_2Cl_2 , NEt_3 , $\text{Na}_2\text{S}_2\text{O}_5$.

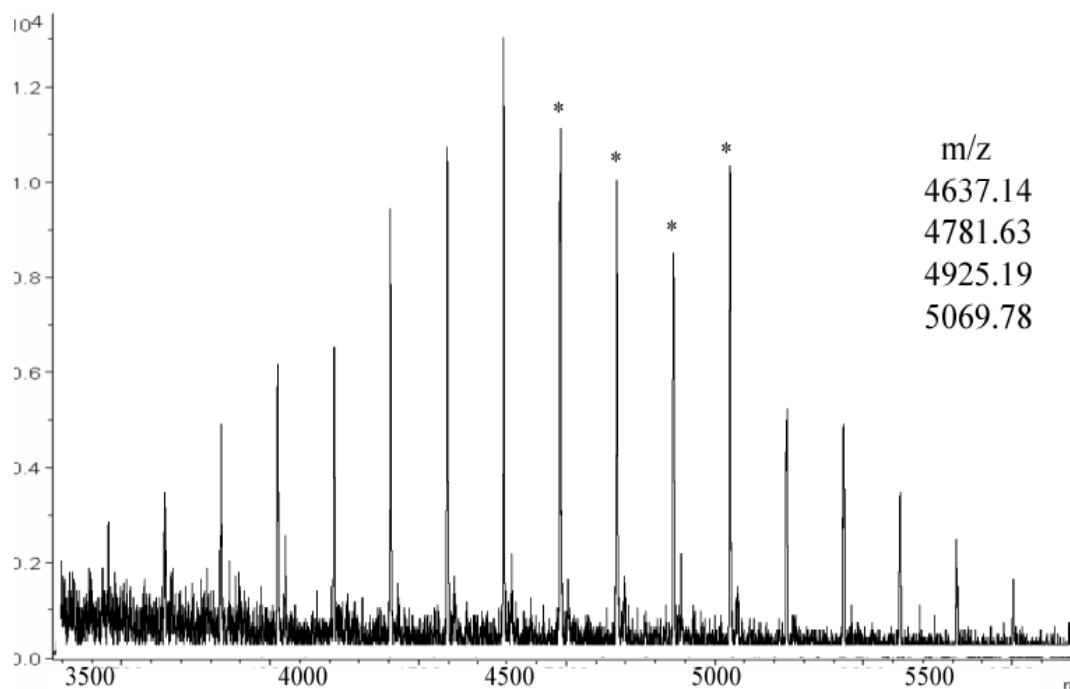


Figure 4.2.2.2 MALDI-ToF MS of the spirocyclic poly(lactide).

Theoretically it would be possible to form more complex and structurally different polymers, for example a ‘doubly fused bicyclic’ structure, using this technique. The dilutions used suggest the formation of the simplest possible structure in each case as previously discussed for trimethylolpropane tris-(3-mercaptopropionate). It is also interesting to note that complex cross-linked structures can also be formed if the reaction is carried out under concentrated conditions, but these form a gel that is insoluble in conventional solvents.

4.3 Cyclic PLA with a ‘click’ functional handle

‘Click’ chemistry has already played an important role in this thesis, and its robust nature in mild conditions in the presence of stereocontrolled poly(lactide) makes it an ideal method for the development of further architectures. In Chapter 3, a method for the synthesis of cyclic and linear poly(lactide) chains bearing a single alkene functionality was demonstrated and it was with these polymers, **Figure 4.3.1**, that all further conjugations were carried out. An alkene bearing polymer was chosen to simplify the procedure; the methods should work with the alkyne bearing polymer chains, but with each polymer possibly reacting with two thiols it was deemed to be overcomplicating the methodology. A linear polymer was chosen with an M_n of approximately half that of the cyclic polymer to more accurately represent the cyclic polymer in terms of hydrodynamic volume. This will enable a better comparison of results when the steric hindrance of the polymer chains becomes evident.

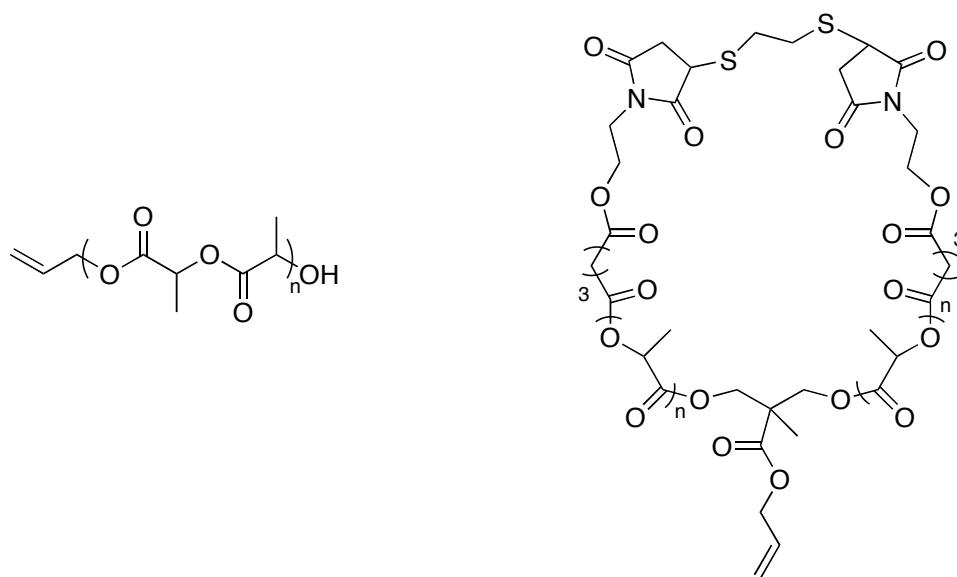


Figure 4.3.1 Alkene bearing linear and cyclic poly(lactide) for thiol-ene conjugations.

Conjugation of these polymer chains with multi-thiol species, **Figure 4.3.2**, should result in a selection of multi cyclic polymers. Conjugations were carried out as previously described in Chapter 3, with dimethyl phenyl phosphine catalyst. Purification of the resultant polymers was carried out by sequential precipitations in petroleum ether (b.p. 40 – 60 °C). The results are shown in **Table 4.1**.

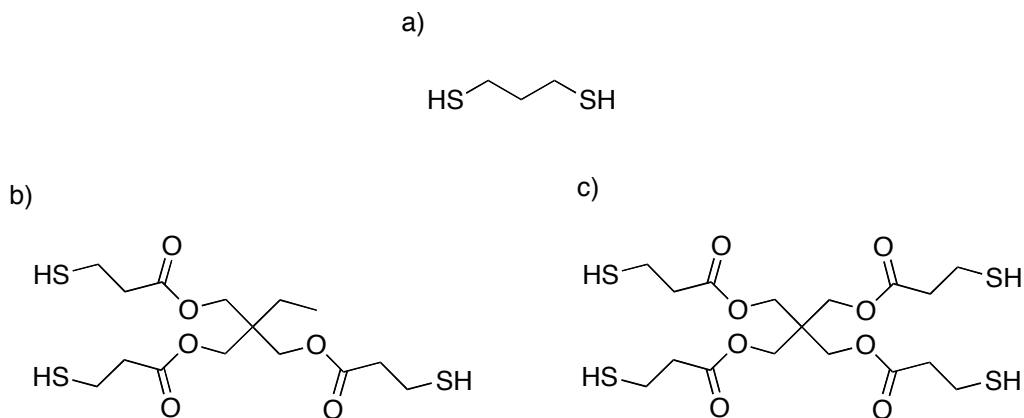


Figure 4.3.2 Conjugations were carried out with a) 1,3-propanedithiol, b) trimethylolpropane tris-(3-mercaptopropionate) c) pentaerythritol tetrakis-(3-mercaptopropionate).

Table 4.1 Preparation of a range of linear and cyclic poly(lactide) stars

Conjugating thiol	Linear poly(lactide)		Cyclic poly(lactide)	
	M_n g.mol ⁻¹ [a]	PDI ^[a]	M_n g.mol ⁻¹ [a]	PDI ^[a]
-	2,490	1.24	5,820	1.18
1,3-Propanedithiol	7,910	1.18	11,660	1.04
Trimethylolpropane tris-(3-mercaptopropionate)	9,100	1.18	15,320	1.07
Pentaerythritol tetrakis-(3-mercaptopropionate)	9,530	1.29	13,240	1.09

^[a] Determined by GPC analysis.

The results show that the conjugations proceed as expected, and the resultant polymers are, by molecular weight, the size that we would predict them to be based on the literature. However, pentaerythritol tetrakis-(3-mercaptopropionate) does not follow the expected trend in the data, and the broadening of the PDI is also a concern as it suggests that incomplete conjugation is occurring. It is postulated that this may be due to the inaccessibility of the core once three conjugations have occurred, this could possibly be overcome by increasing reaction times, but then the undesirable possibility of thiol-thiol coupling or degradation of the polymer chains by transesterification may occur. The idea that steric hindrance is causing incomplete conjugation is evidenced by the comparatively higher molecular weight of the linear polymer conjugation. Despite the similarity in hydrodynamic volume it is reasonable to assume the core of the cyclic conjugated polymer would be more crowded than the linear counterpart.

¹H NMR analysis of the polymers reveals that > 98 % of the maleimide functionality is consumed during the conjugation for all the polymers except pentaerythritol tetrakis-(3-mercaptopropionate) where this drops to ~90 %, confirming concerns that only a three armed star is formed.

4.4 Cyclic PLA as a macroinitiator

In Chapter 2 it was demonstrated that PLA is tolerant of further polymerisation techniques such as RAFT, and through the application of an initiator bearing a

RAFT mediator it would be possible to synthesise a block copolymer from the cyclic polymer in this way. However, the synthesis of more and more complex diols provides its own difficulties, mainly in purification to a level high enough to accurately synthesise linear pre-cycles. A much better method would be to use ‘click’ chemistry to add an initiator for a second polymerisation to the cyclic poly(lactide).

To this end it was possible to conjugate thioglycerol onto a cyclic polymer using an identical procedure to that detailed in Chapter 3, **Figure 4.4.1**. Conjugation was evidenced by both MALDI ToF MS and ^1H NMR. The polymer was then purified by precipitation and dried thoroughly before being applied as a macro-initiator in the stereocontrolled polymerisation of *rac*-lactide, **Figure 4.4.2**.

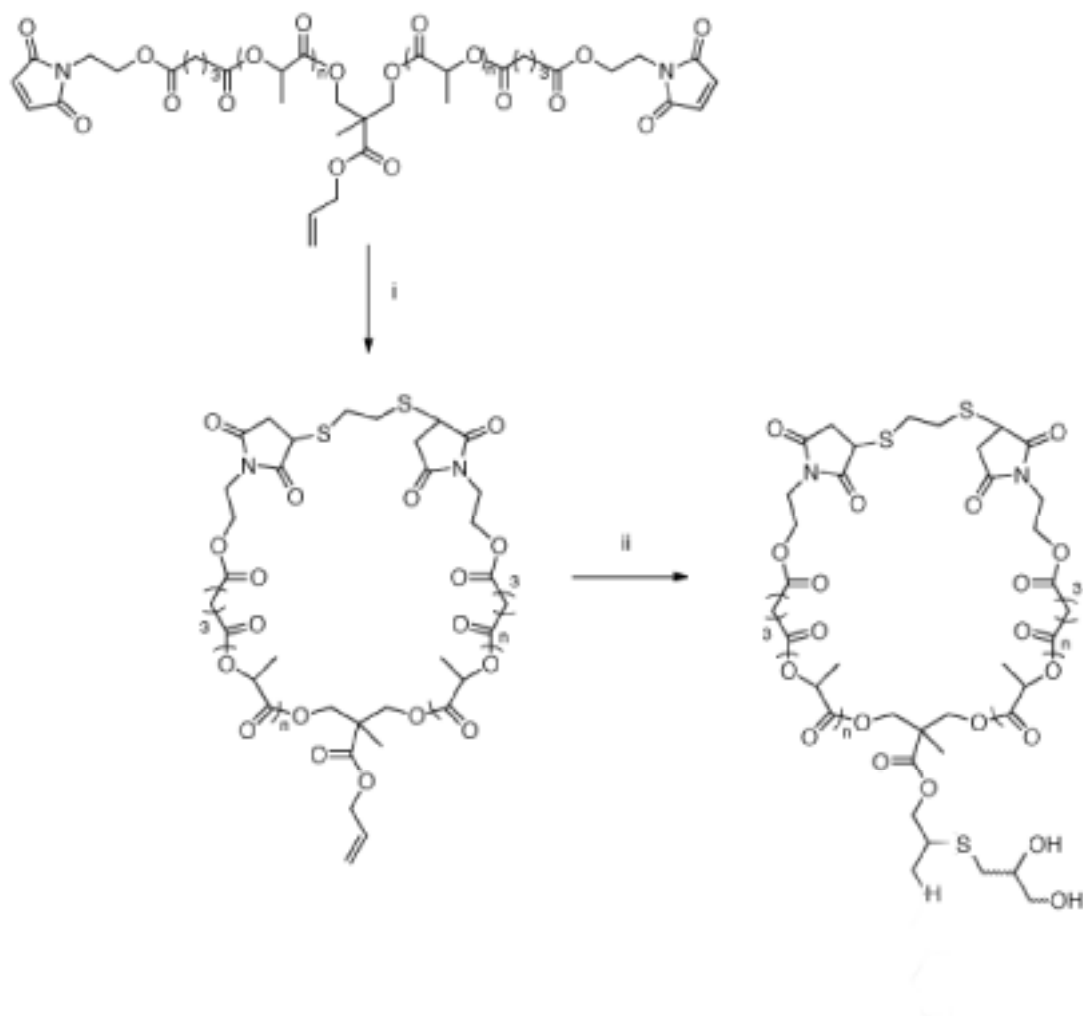


Figure 4.4.1 Thioglycerol conjugation to cyclic polymer. i) 1eq. ethane dithiol, CH_2Cl_2 , TEA, $\text{Na}_2\text{S}_2\text{O}_5$; ii) 10 eq. thioglycerol, DMPP, CH_2Cl_2 , 4 h.

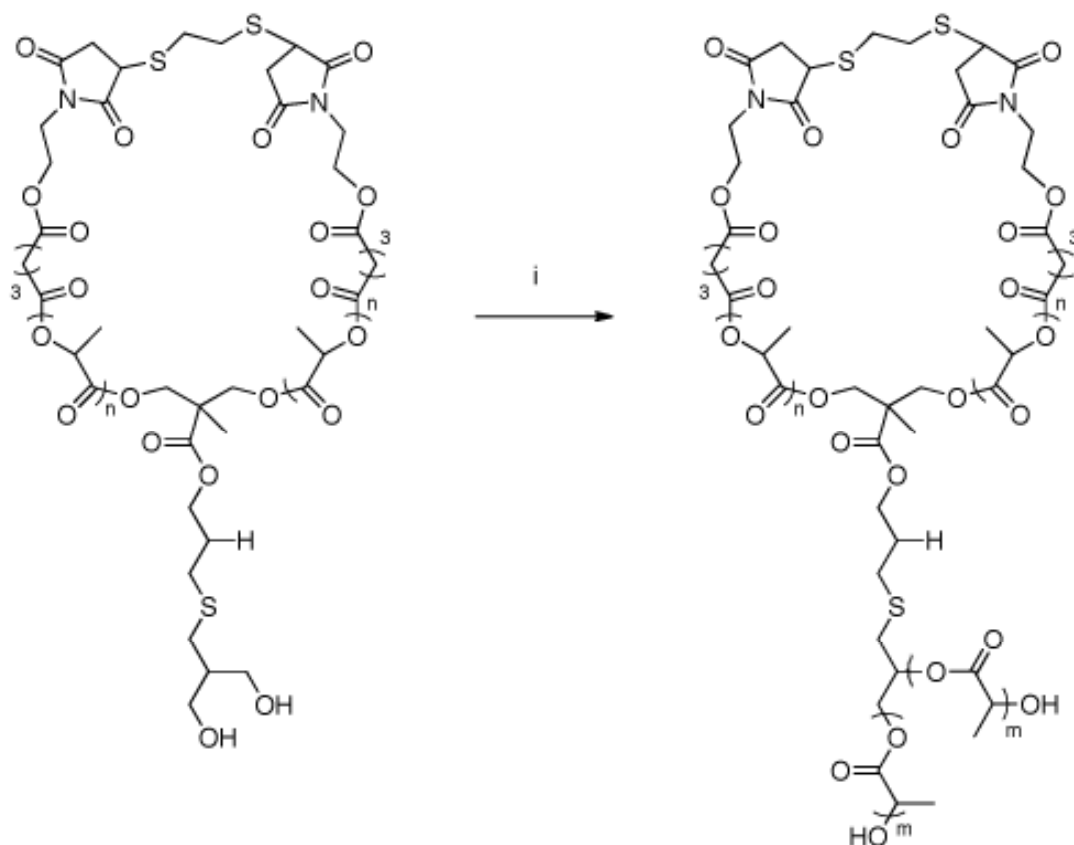


Figure 4.4.2 Thioglycerol chain extension. i) *rac*-lactide, Al salen, toluene, 70 °C, 4 h.

GPC and MALDI-ToF MS analysis show that the macro-initiator has undergone further polymerisation, and the low PDI of the polymerisation suggests that two chains have grown equally from each cycle (or one chain from each alcohol). (Cycle ‘clicked’ with thioglycerol $M_n = 7100 \text{ g.mol}^{-1}$, PDI = 1.11; Cycle after chain extension (target for each chain, DP = 20 $M_n \sim 5500 \text{ g.mol}^{-1}$) $M_n = 20,600 \text{ g.mol}^{-1}$, PDI = 1.06).

The possibility of applying a RAFT polymerisation in this manner is hampered by the synthesis of a thiol bearing RAFT initiator. This synthesis is not a trivial process, as thiols are already employed early in the synthesis. As this was only a one possible route to a cyclic poly(lactide) containing block copolymer it was abandoned in favour of the synthesis described in the next section.

4.5 PEG-*b*-PLA block copolymers

4.5.1 PEG bearing thiol synthesis

Several methods for converting PEG chain ends to thiols have previously been reported in the literature. However, despite this range the simplest and most high yielding procedure attempted was using the DCC coupling of 3-thiopropionic acid to the polymer chain end, **Figure 4.5.1.1**. GPC analysis of the resulting thiol bearing PEG polymers is shown in **Table 4.2**.

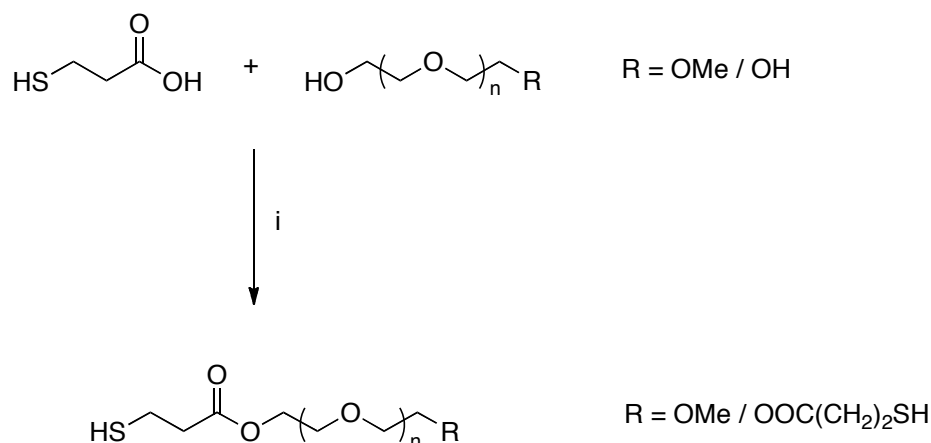


Figure 4.5.1.1 Synthesis of PEG bearing thiol chain ends. i) 20 eq. 3-thiopropionic acid, DCC, CH₂Cl₂, DMAP, 48 h.

Table 4.2 Preparation of a range of thiol bearing PEG chains

PEG polymer ^[a]	Hydroxy bearing PEG		Thiol bearing PEG ^[b]	
	<i>M_n</i> g.mol ⁻¹ [c]	PDI ^[c]	<i>M_n</i> g.mol ⁻¹ [c]	PDI ^[c]
TEG HS-SH ^[d]	-	-	-	-
600 HS-SH	670	1.11	780	1.16
2000 HS-SH	1,990	1.09	2,140	1.21
2000 HS-Me	2,040	1.06	2,110	1.14

^[a] Molecular weight as described by Sigma-Aldrich; ^[b] GPC taken after conjugation with *N*-methyl maleimide; ^[c] Determined by GPC analysis; ^[d] Tetraethylene glycol conversion confirmed by ¹H NMR analysis.

MALDI-ToF MS analysis for these polymers was particularly troublesome for me to obtain. The thiopropionic acid adds a molecular weight of 88 Da to the polymer chain; exactly the same weight as two ethylene glycol units. This meant that to establish if conjugation of the thiopropionic acid had occurred, and if not the level of conjugation that had occurred, it was first necessary to perform a ‘click’ reaction to the thiol. Through the application of *N*-methyl maleimide it was possible to be confident that this conjugation would reach 100 % completion in the time scale of the reaction, and therefore it would be possible to determine that any remaining unconjugated polymer must contain no thiol group. Indeed, this was the case and MALDI-ToF MS could be used to demonstrate complete conversion during the original DCC coupling reaction.

¹H NMR analysis also confirmed the complete conversion with the integrals showing that the 3-thiopropionic acid had been incorporated. The resonances from the thiopropionic acid were very close to that of the ethylene glycol, so the ‘click’ product with methyl maleimide was also helpful for the determination of these resonances.

4.5.2 PEG to cyclic PLA Grafting

All of the different thiol containing PEG polymers were conjugated to both the cyclic and linear PLA chains, **Figure 4.5.2.1**. An increased reaction time of 24 h was allowed for the conjugations to occur due to the nature of the PEG thiol and

PLA solubilities in CH_2Cl_2 , and the reduced conjugation rate that is observed when working with two polymer chain-ends. Excess of the PEG thiol species was used in the single conjugation example as this allowed for facile purification by washing with water, but in the case of the dithiol PEG an excess of PLA had to be used. The purification of this polymer was therefore particularly difficult and the altered solubility of the block copolymer made this an even greater challenge. Indeed, it was not possible to achieve pure polymer for analysis by NMR, so GPC data was relied upon to show that conjugation had occurred in these cases. The data obtained from GPC analysis is shown in **Table 4.3**.

Table 4.3 Cyclic PLA-*b*-PEG conjugations

PEG	Linear PLA conjugation ^[e]		Cyclic PLA conjugation ^[f]	
	$M_n \text{ g.mol}^{-1}$ [g]	PDi ^[g]	$M_n \text{ g.mol}^{-1}$ [g]	PDi ^[g]
TEG HS-SH ^[a]	5,540	1.13	9,930	1.11
600 HS-SH ^[b]	11,460	1.08	10,120	1.14
2000 HS-SH ^[c]	12,780	1.07	11,580	1.12
2000 HS-Me ^[d]	7,580	1.13	9,240	1.16

^[a] Too small for analysis by GPC; ^[b] $M_n = 780 \text{ g.mol}^{-1}$, PDi = 1.16; ^[c] $M_n = 2140 \text{ g.mol}^{-1}$, PDi = 1.21; ^[d] $M_n = 2110 \text{ g.mol}^{-1}$, PDi = 1.14; ^[e] $M_n = 2,490 \text{ g.mol}^{-1}$, PDi = 1.24; ^[f] $M_n = 5,820 \text{ g.mol}^{-1}$, PDi = 1.18; ^[g] Determined by GPC analysis.

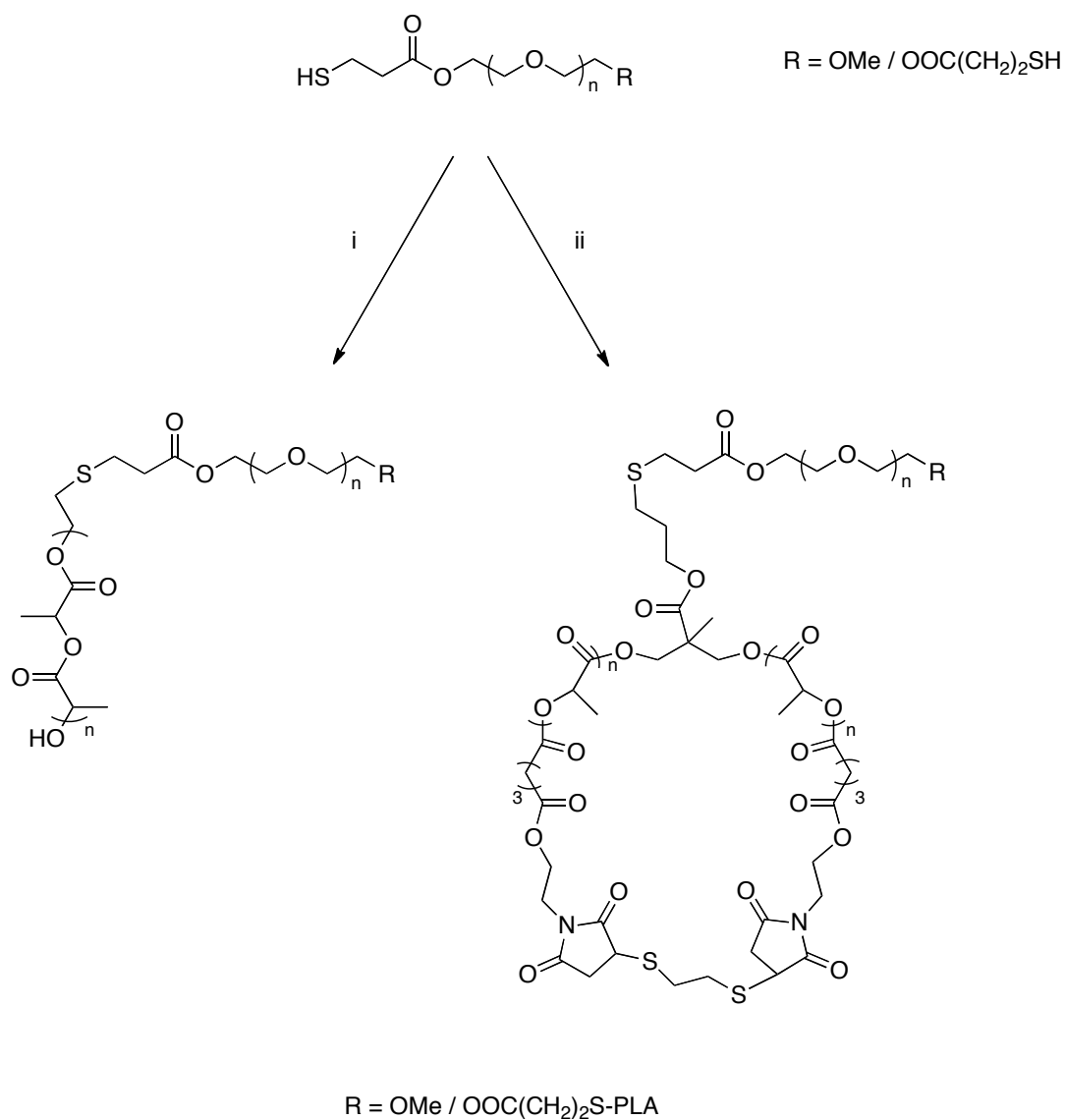


Figure 4.5.2.1 PEG-*b*-PLA linear and cyclic conjugations. i) linear PLA, **Figure 4.3.1**, DMPP, CH_2Cl_2 , 24 h; ii) cyclic PLA, **Figure 4.3.1**, DMPP, CH_2Cl_2 , 48 h.

It is important to note here that it was not possible to obtain MALDI-ToF MS analysis for any of the block copolymers synthesised due to the complexity of the

matrix-polymer system. A range of matrices were tried to aid ionisation, but the signal to noise ratio was never good enough to produce reliable data. Although individually, both polymers produce good results using the same matrix, when applied in a block copolymer it was not possible to obtain spectra with reliable molecular weight data. It was postulated that this might be because these polymer chains phase separate when applied to the MALDI-ToF plate due to the dilutions used. They do not therefore mix well with the matrix properly and poor spectra result. This is of particular interest as it suggests that the block copolymer would self-assemble under the right conditions, but it was not possible to examine this in further detail.

4.6 Poly(BLG-*co*-Cys) conjugations

Polymers for this conjugation were obtained from the research group of Dr. Andreas Heise. The polymers were poly(benzyl-*L*-glutamate-*co*-tertbutylmercapto-*L*-cysteine) and these could be deprotected, as has been reported in the literature, to poly(benzyl-*L*-glutamate-*co*-*L*-cysteine) **Figure 4.6.1**.¹⁸ This deprotection requires 5 days to reach completion, and thus requires carrying out in small batches that were stored under a nitrogen atmosphere and used within 1 - 2 days. It is

reasonable to assume that a small amount of thiol-thiol coupling may occur during this period but this should not be a significant amount under these conditions.

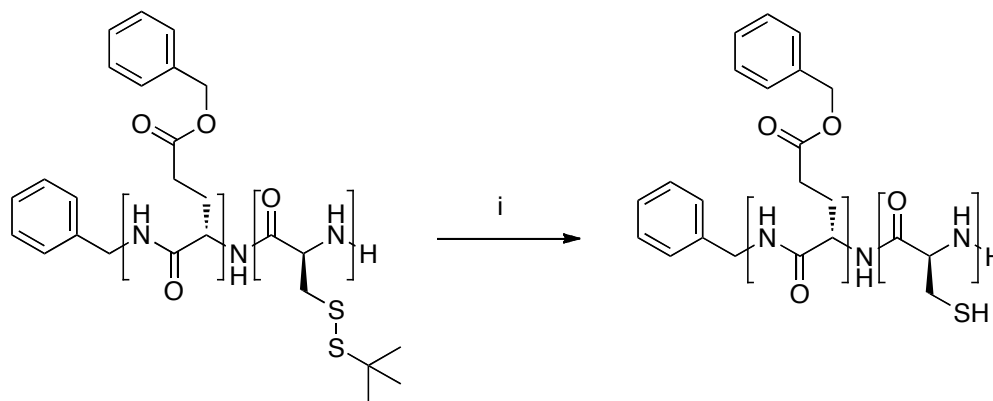


Figure 4.6.1 Deprotection of the poly(BLG-*co*-tBMLC) to poly(BLG-*co*-Cys). i) dithiothreitol, DMF, 60 °C, 5 days.

Three separate polymers were supplied for conjugation, with differing ratios of benzyl-*L*-glutamate to cysteine. These were BLG:Cys, 4:1, 2:1, and 1:1. This would allow the examination of the density that it was possible to conjugate to, with the intention that the higher this could be the more profound an impact it would have on physical and self-assembly properties. Once deprotection had been carried out all three polymers were subjected to conjugation reactions with both the linear and cyclic polymers previously used in this chapter, **Figure 4.6.2**. The GPC analysis of the resulting polymer is shown in **Table 4.4**.

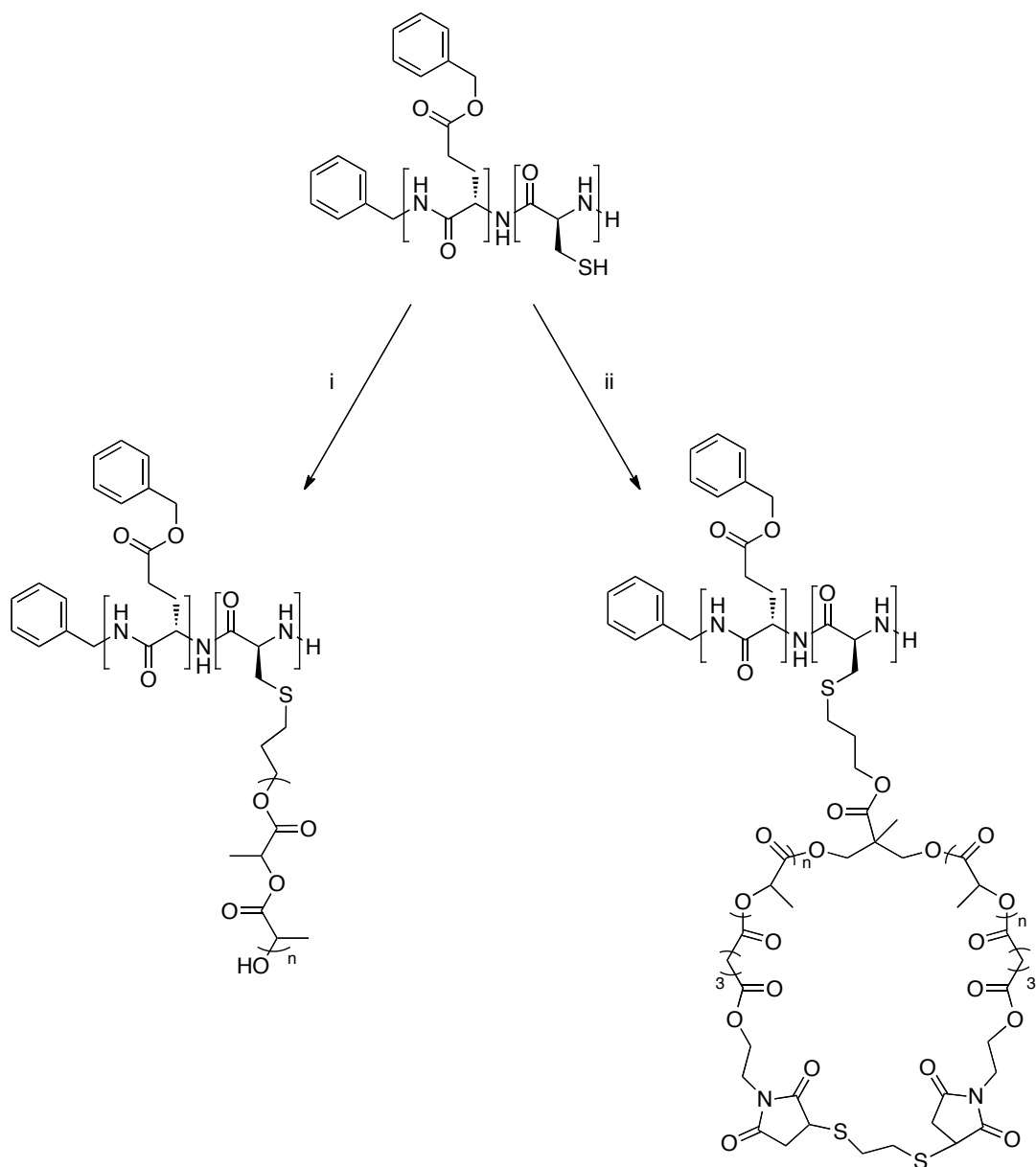


Figure 4.6.2 Conjugation of the linear and cyclic polymers to poly(BLG-*co*-Cys). i) linear PLA, **Figure 4.3.1**, DMPP, CH₂Cl₂, 48 h; ii) cyclic PLA, **Figure 4.3.1**, DMPP, CH₂Cl₂, 48 h.

Table 4.4 Poly(BLG-*co*-Cys)-*b*-PLA conjugations

	poly(BLG- <i>co</i> -Cys)		Linear Polymer ^[a]		Cyclic Polymer ^[b]	
	M_n g.mol ⁻¹ [c]	PDi ^[c]	M_n g.mol ⁻¹ [c]	PDi ^[c]	M_n g.mol ⁻¹ [c]	PDi ^[c]
4:1	2,730	1.18	75,230	1.34	63,280	1.36
2:1	3,040	1.16	95,340	1.38	73,430	1.47
1:1	2,570	1.33	-	-	-	-

^[a] $M_n = 2,490$ g.mol⁻¹, PDI = 1.24; ^[b] $M_n = 5,820$ g.mol⁻¹, PDI = 1.18; ^[c] Determined by GPC analysis.

MALDI-ToF MS analysis of the conjugated polymer yielded no usable data, and the solubility of the polymer in NMR solvents hampered analysis in this fashion also. Ideally it would have been possible to examine the conjugated products by AFM, as it would be expected that they were large enough to be seen. However, due to time constraints it was not possible to carry out this analysis.

GPC analysis reveals that conjugation is occurring, at least in the 4:1 and 2:1 polymers, and that there is a significant difference between the linear and cyclic polymer conjugations. This would be expected; the cyclic polymers may produce a much more rigid and compact structure that would have a short retention time in a GPC column, giving a much higher molecular weight than expected. Without

conclusive NMR data it is hard to determine the degree to which the conjugation has occurred, but with such a significant increase in the molecular weight being observed it is postulated that it is a high percentage.

Conjugation to the 1:1 polymer chain would certainly have occurred, although it would be reasonable to assume that due to the crowding complete conjugation does not occur, especially when we compare this to the 4-armed thiol conjugation carried out earlier in this chapter. However, it was not possible to record a GPC analysis for this polymer. It was postulated that this may be due to one of two reasons. Firstly, this polymer has the lowest solubility of any that were synthesised and it is possible that simply not enough polymer entered the DRI. However, the levels at which the polymer can be detected are very low so this is probably less likely. It is also possible the polymer has such a high molecular weight and broad PDI that the small amount that did pass into the GPC is just too spread out and dilute for me to detect from the baseline, certainly the GPC spectra of the 4:1 and 2:1 polymer chains were not particularly obvious.

This is an area that certainly requires further investigation but in principle the conjugation of both the linear and cyclic polymers onto the thiol bearing backbone is observed. This would prove interesting to observe under AFM as we would hope that the poly(lactide) chains would interact strongly when held in such close proximity. Indeed, with the cyclic polymer the ideal would be the formation of a nanotube like structure.

4.7 Conclusions

In conclusion, it has been shown that both the methodology that has been designed and the polymers that can be synthesised are versatile in both their application and in the synthesis of complex cyclical architectures. The facile control of thiol-ene ‘click’ chemistry has meant that an unprecedented number of architectures and range of chemical synthesis have been shown in the use of cyclic, stereoregular poly(lactide), including incorporation into a range of block copolymers.

Further research is required into the areas introduced in this chapter that unfortunately were not possible to investigate further due to time constraints. Paramount to this would be examining the physical properties of the new materials and look at the possibility of self-assembly and possible future applications. AFM analysis of the poly(benzyl-*L*-glutamate-co-*L*-cysteine) would be particularly interesting, with this complex example of polymer architecture.

4.8 References

- ¹ For a comprehensive examination of possible topologies see: Tezuka, Y.; Oike, H., *Prog. Polym. Sci.*, **2002**, 27, 1069.
- ² Oike, H.; Hamada, M.; Eguchi, S.; Danda, Y.; Tezuka, Y., *Macromolecules*, **2001**, 34, 2776
- ³ Tezuka, Y.; Fujiyama, K., *J. Am. Chem. Soc.*, **2005**, 127, 6266.
- ⁴ Pang, X.; Wang, G.; Jia, Z.; Liu, C.; Huang, J., *J. Polym. Sci. Part A: Polym. Chem.*, **2007**, 45, 5824.
- ⁵ Jia, Z.; Fu, Q.; Huang, J., *Macromolecules*, **2006**, 39, 5190.
- ⁶ e.g. a) Laurent, B.A.; Grayson, S.M., *J. Am. Chem. Soc.*, **2006**, 128, 4238. b) Bielawski, C.W.; Benitez, D.; Grubbs, R.H., *Science*, **2002**, 297, 2041.
- ⁷ e.g. Li, H.; Debuigne, A.; Jérôme, R.; Lecomte, P., *Angew. Chem. Int. ed.*, **2006**, 45, 2264.
- ⁸ e.g. Jia, Z.; Fu, Q.; Huang, J., *Macromolecules*, **2006**, 39, 5190.
- ⁹ e.g. Shi, G.-Y.; Pan, C.-Y., *J. Polym. Chem. Sci.: Part A: Polym. Chem.*, **2009**, 47, 2620.
- ¹⁰ e.g. Tezuka, Y.; Fujiyama, K., *J. Am. Chem. Soc.*, **2005**, 127, 6266.
- ¹¹ e.g. Oike, H.; Hamada, M.; Eguchi, S.; Danda, Y.; Tezuka, Y., *Macromolecules*, **2001**, 34, 2776.
- ¹² e.g. Tezuka, Y.; Oike, H., *Macromol. Rapid Commun.*, **2001**, 22, 1017.
- ¹³ e.g. Lepoittevin, B.; Dourges, M. A.; Masure, M.; Hermery, P.; Baran, K.; Cramail, H., *Macromolecules*, **2000**, 33, 8218.

¹⁴ No known examples of this architecture.

¹⁵ No known examples of this architecture.

¹⁶ e.g. a) Lepoittevin, B.; Hemery, P., *J. Polym. Chem. Sci.: Part A: Polym. Chem.*, **2001**, 39, 2723. b) Lepoittevin, B.; Dourges, M. A.; Masure, M.; Hermery, P.; Baran, K.; Cramail, H., *Macromolecules*, **2000**, 33, 8218.

¹⁷ Kricheldorf, H.R.; Langanke, D., *Macromol. Chem. Phys.*, **1999**, 200, 1183.

¹⁸ Habraken, G.J.M.; Koning, C.E.; Heuts, J.P.A.; Heise, A., *Chem. Commun.*, **2009**, 3612.

Chapter 5: Experimental

5.1 General experimental details

Materials. *rac*-Lactide (Aldrich) was purified by recrystallisation from dry dichloromethane and sublimation twice before use to remove any traces of water. Toluene for polymerisations was refluxed over sodium then distilled, degassed and stored under a nitrogen atmosphere. All alcohol initiators were dried over suitable drying agents, distilled and degassed. Acid chlorides were distilled from PCl_5 or SOCl_2 and stored over 4 Å molecular sieves. 4-(2-hydroxyethyl)-10-oxa-4-azatricyclo[5.2.1.0^{2,6}]dec-8-ene-3,5-dione,¹ Al salen complexes **1**, **2** and **3**,² and thiourea³ were synthesised as previously reported in the literature. All other chemicals and solvents were obtained from Aldrich and used as received unless otherwise stated.

General Considerations. All required manipulations were performed under moisture and oxygen free conditions either in a nitrogen filled glove box or by standard Schlenk techniques.

Polymer yields were quantitative in all syntheses, with mechanical losses from precipitation and purification being in the region of 5 - 10 %. Polymerisations of lactide were allowed to run to >95 % conversion in all cases.

5.1.1 Gel permeation chromatography (GPC)

GPC was used to determine the molecular weights and polydispersities of the synthesised polymers. The system comprised a Polymer Laboratories Midas autosampler and LC1120 HPLC pump equipped with a guard column (Polymer Laboratories PLGel 5 μ M, 50 \times 7.5 mm), two mixed D columns (Polymer Laboratories PLGel 5 μ M, 300 \times 7.5 mm) and a Polymer Laboratories ERC-7515A differential refractive index (DRI) detector (UV detector could also be connected when required). The mobile phase was chloroform/triethylamine (95/5) eluent at a flow rate of 1.0 mL.min⁻¹ and samples were calibrated against linear poly(styrene) standards (540 to 2.9 \times 10⁴ g.mol⁻¹) using Cirrus v3.0; elution time was standardised against that of toluene.

5.1.2 Nuclear magnetic resonance (NMR)

¹H and ¹³C NMR spectra were recorded on a Bruker DPX-300, DPX-400, AC400 or DRX-500 spectrometer at 293 K unless stated. Chemical shifts are reported as δ in parts per million (ppm) and referenced to the chemical shift of the residual solvent resonances (CDCl₃ ¹H: δ = 7.26 ppm; ¹³C δ = 77.16 ppm).

5.1.3 Matrix-assisted laser desorption and ionisation time-of-flight mass spectrometry (MALDI-ToF MS)

Mass spectra were acquired by MALDI-ToF mass spectrometry using a Bruker Daltonics Ultraflex II MALDI-ToF mass spectrometer, equipped with a nitrogen laser delivering 2 ns laser pulses at 337 nm with positive ion ToF detection performed using an accelerating voltage of 25 kV. Solutions of trans-2-[3-(4-*tert*butylphenyl)-2-methyl-2-propylidene]-malonitrile (DCTB) as matrix (0.3 μL of a 10 gL^{-1} acetone solution), sodium trifluoroacetate as cationisation agent (0.3 μL of a 10 gL^{-1} acetone solution) and analyte (0.3 μL of a 1 gL^{-1} CH_2Cl_2 solution) were applied sequentially to the target followed by solvent evaporation to prepare a thin matrix/analyte film.⁴ The samples were measured in reflectron ion mode and calibrated by comparison to 2×10^3 and 5×10^3 g.mol^{-1} poly(ethylene glycol) standards.

5.1.4 Other techniques

Elemental Analyses were performed by Warwick Analytical Services.

5.2 Experimental details for chapter 2

Preparation of functional poly(lactide)s. In a typical experiment, the chosen alcohol initiator (0.05 mmol) was added to an ampoule containing a solution of aluminum catalyst (**1**) (0.05 mmol) and *rac*-lactide (0.144 g, 1 mmol) in toluene (1.25 mL) under an atmosphere of nitrogen. The sealed ampoule was then heated to 70 °C for 4 hours before being cooled in ice for 10 minutes. The ampoule was then taken into a glove box whereupon the chosen acid chloride was added (0.5 mmol) before resealing the ampoule and heating at 70 °C for a further 120 hours. The resulting polymer was precipitated from CH₂Cl₂ in cold petroleum ether, collected by filtration and dried *in vacuo*.

Preparation of telechelic and star shaped poly(lactide)s. In a typical experiment, the chosen alcohol initiator (0.05 mmol) was added to an ampoule containing a solution of aluminum catalyst (**1**) (0.1 – 0.3 mmol) and *rac*-lactide (0.144 - 0.288 g, 1 - 2 mmol) in toluene (1.25 mL) under an atmosphere of nitrogen. Dipentaerythritol required stirring the alcohol with the aluminium complex for 16 hours at 70 °C prior to addition of lactide. The sealed ampoule was then heated to 70 °C for 4 hours before being cooled in ice for 10 minutes. The ampoule was then taken into a glove box whereupon the chosen acid chloride was added (1.0 – 3.0 mmol) before resealing the ampoule and heating at 70 °C for a further 120 hours.

The resulting polymers were precipitated from CH_2Cl_2 in cold petroleum ether, collected by filtration and dried *in vacuo*.

Dipentaerythritol initiated polymer (OH end group): ^1H NMR (CDCl_3 , 400.0 MHz): 5.20 – 5.00 (m, 60H, CCHOH); 3.34 (s, 12H, CCH_2OCO); 3.19 (s, 4H, CCH_2O); 1.3 – 1.1 (m, 120H, CH_3).

Synthesis of methoxypoly(ethyleneglycol)-4-chloro-4-oxobutanoate (Me-PEG-COCl). Prepared using a synthesis modified from the literature.⁵ Polyethylene glycol mono methyl ether (2.0 g, 3.6 mmol) was stirred under nitrogen with 10 equivalents of succinyl chloride (4.4 mL, 36 mmol). The excess acid chloride was removed by repeated washing with hexanes/diethyl ether (4:1 v:v). ^1H NMR (CDCl_3 , 400.0 MHz): 4.20 (t, 2H, $^3J_{\text{H-H}} = 5.7$ Hz, CH_2OCO); 3.64 - 3.65 (m, 2H, $\text{CH}_2\text{CH}_2\text{OCO}$); 3.5-3.6 (s, 42H, CH_2OCH_2); 3.48 (t, 2H, $^3J_{\text{H-H}} = 5.7$ Hz, $\text{CH}_2\text{OCH}_2\text{CH}_2\text{OCH}_3$); 3.31 (s, 3H, CH_3); 3.22 (s, 4H, $\text{OCOCH}_2\text{CH}_2\text{COCl}$); 3.16 (t, 2H, $\text{CH}_2\text{CH}_2\text{OCH}_3$); 2.64 (t, 2H, CH_2OCH_3).

Synthesis of 4-(chlorocarbonyl)benzyl dodecyl carbonotrithioate, 4. Prepared using a synthesis modified from the literature.⁶ K_3PO_4 (2.1 g, 10 mmol) was added to a stirred solution of dodecanethiol (2 g, 10 mmol) in 40 mL acetone at ambient temperature. The solution was allowed to stir for 1 hour before CS_2 (2.26 g, 30 mmol) was added. The now yellow solution was warmed to 40 °C and stirred for a further 1 hour. 4-(bromomethyl)benzoic acid (2.12g, 10 mmol) was added and the reaction stirred at 40 °C for 16 hours. The resultant solid was collected and partitioned between toluene (150 mL) and water (150 mL), the toluene was

collected and washed a further 3 times with water (150 mL) before the resulting yellow solid was washed twice with acetone (50 mL) and dried in a vacuum desiccator over P_2O_5 for 72 hours (3.1 g, 76 % yield). 1H NMR in $(CD_3)_2SO$ at 70 °C: δ 7.85 (d, 2H, $^3J_{H-H} = 7.3$ Hz, ArH); 7.38 (d, 2H, $^3J_{H-H} = 7.3$ Hz, ArH); 4.71 (s, 2H, ArCH₂S); 3.39 (t, 2H, $^3J_{H-H} = 7.2$ Hz, SCH₂CH₂); 1.67 (quintet, 2H, $^3J_{H-H} = 7.2$ Hz, SCH₂CH₂); 1.22-1.42 (m, 18H, C₉H₁₈); 0.88 (t, 3H, $^3J_{H-H} = 7.2$ Hz, CH₃). $^{13}C\{^1H\}$ NMR $(CD_3)_2SO$: 224.1 (CS₃); 167.9 (COOH); 138.8 (Ar); 131.8 (Ar); 129.8 (Ar); 129.1 (Ar); 68.1 (ArCH₂); 37.1 (SCH₂); 36.7, 31.7, 29.4, 29.3, 29.2, 29.1, 28.8, 28.6, 28.0, 22.4 (C₁₀H₂₂); 14.2 (CH₃).

Conversion to the acid chloride was carried out quantitatively in an excess of thionyl chloride under an atmosphere of nitrogen. 1H NMR (CDCl₃, 400.0 MHz): δ 8.06 (d, 2H, $^3J_{H-H} = 7.3$ Hz, ArH); 7.48 (d, 2H, $^3J_{H-H} = 7.3$ Hz, ArH); 4.68 (s, 2H, ArCH₂S); 3.36 (dd, 2H, SCH₂CH₂); 1.69 (quintet, 2H, $^3J_{H-H} = 7.1$ Hz, SCH₂CH₂); 1.22-1.40 (m, 18H, C₉H₁₈); 0.88 (t, 3H, $^3J_{H-H} = 7.1$ Hz, CH₃). $^{13}C\{^1H\}$ NMR $(CD_3)_2SO$: 222.0 (CS₃); 167.2 (COCl); 143.5 (Ar); 142.9 (Ar); 131.1 (Ar); 129.1 (Ar); 118.5 (ArCH₂); 41.9 (SCH₂); 40.1, 39.5, 36.8, 31.3, 29.0, 29.0, 28.9, 28.8, 22.1 (C₁₁H₂₂); 13.9 (CH₃).

Preparation of RAFT chain transfer agent functional PLA. PLA was prepared as previously described using **4** and the desired initiator. The ampoule was taken into a glove box whereupon 4-(chlorocarbonyl)benzyl dodecyl carbonotrithioate, **4**, was added before resealing the ampoule and heating at 70 °C for a further 120 hours.

The resulting polymer was precipitated from CH_2Cl_2 in cold petroleum ether, collected by filtration and dried *in vacuo*.

Preperation of PLA-PS block copolymers. RAFT CTA-functionalised PLA (0.01 mmol) was dissolved in a 200 μl toluene and 60 μl styrene. The solution was freeze, pump, thawed four times before being heated to 120 $^\circ\text{C}$ for 16 hours. The resulting block copolymer was precipitated in cold petroleum ether, collected by filtration and dried *in vacuo*.

Degradation of the PLA-PS block copolymers. PLA-PS was dissolved in a solution of toluene:methanol 90:10 before addition of 200 mol% TBD. The solution was stirred in a sealed ampoule at 100 $^\circ\text{C}$ for 48 h. The resulting polymer was precipitated in cold, acidified methanol, collected by filtration and dried *in vacuo*.

CuAAC click reactions. Highest conversion without seeing degradation of the polymer chain was achieved as follows. Alkyne functional PLA (100 mg) was stirred to form a suspension in THF. Azido triethylene glycol (10 eq.), Copper Iodide (1 eq.) and NEt_3 (5eq.) were added and the solution stirred at room temperature under a nitrogen atmosphere for 72 hours. The solution was filtered, and the THF removed under vacuum. The resulting solid was dissolved in CH_2Cl_2 and filtered before being precipitated in petroleum ether, collected by filtration and dried *in vacuo*.

Synthesis of pentanedioyl chloride mono-[2-(3,5-dioxo-10-oxa-4-azatricyclo[5.2.1.0^{2,6}]dec-8-en-4-yl)-ethyl] ester (maleimide-functional acid chloride),

6. Glutaric anhydride (1.87 g, 16.4 mmol), DMAP (0.40 g, 3.3 mmol) and NEt₃ (9.4 mL, 82 mmol) were added to a solution of 4-(2-hydroxyethyl)-10-oxa-4-azatricyclo[5.2.1.0^{2,6}]dec-8-ene-3,5-dione (3.42 g, 16.4 mmol) in CH₂Cl₂ (50 mL). The reaction was stirred at 30 °C for 16 h. The solution was poured onto 1 M HCl_(aq) (150 mL) and Et₂O (150 mL), the organic phase was collected and the aqueous phase extracted twice more with Et₂O (150 mL). The combined organic layers were dried over MgSO₄, filtered and solvent removed under vacuum to yield a white solid. Purification was carried out by repeated washing with hot toluene (3.34 g, 10.3 mmol, 63%). ¹H NMR (CDCl₃, 400.0 MHz): 10.48 (br s, 1H, COOH); 6.52 (s, 2H, CH_{vinyl}); 5.27 (s, 2H, CH_{vinyl}CH(OR)CH); 4.24 (t, 2H, ³J_{H-H} = 5.3 Hz, NCH₂CH₂O); 3.76 (t, 2H, ³J_{H-H} = 5.3 Hz, NCH₂CH₂O); 2.87 (s, 2H, CH_{vinyl}CH(OR)CH); 2.42 (t, 2H, ³J_{H-H} = 7.3 Hz, CH₂COOH); 2.36 (t, 2H, ³J_{H-H} = 7.3 Hz, CH₂CH₂CH₂COOH); 1.92 (p, 2H, ³J_{H-H} = 7.3 Hz, CH₂CH₂COOH). ¹³C{¹H} NMR (CDCl₃, 75.5 MHz): 178.5 (COOH); 176.1 (NC(O)CH); 172.5 (OC(O)CH₂); 136.4 (CH_{vinyl}); 80.8 (CH_{vinyl}CH(OR)CH); 60.6 (NCH₂CH₂O); 47.4 (CH_{vinyl}CH(OR)CH); 37.8 (NCH₂CH₂O); 32.8 (CH₂CH₂CH₂COOH); 19.4 (CH₂CH₂CH₂COOH). Anal. Calcd for C₁₅H₁₇NO₇: C 55.73; H 5.30; N 4.35. Found: C 55.53; H 5.31; N 4.34.

The maleimide functional carboxylic acid was quantitatively converted to the acid chloride using oxalyl chloride (5 eq.) in a CH₂Cl₂ solution under an atmosphere of nitrogen. The excess oxalyl chloride and CH₂Cl₂ were removed under vacuum

yielding the expected product as a white solid. ^1H NMR (CDCl_3 , 400.0 MHz): 6.52 (s, 2H, CH_{vinyl}); 5.26 (s, 2H, $\text{CH}_{\text{vinyl}}\text{CH}(\text{OR})\text{CH}$); 4.25 (t, 2H, $^3J_{\text{H-H}} = 5.3$ Hz, $\text{NCH}_2\text{CH}_2\text{O}$); 3.76 (t, 2H, $^3J_{\text{H-H}} = 5.3$ Hz, $\text{NCH}_2\text{CH}_2\text{O}$); 2.99 (t, 2H, $^3J_{\text{H-H}} = 7.3$ Hz, CH_2COCl); 2.87 (s, 2H, $\text{CH}_{\text{vinyl}}\text{CH}(\text{OR})\text{CH}$); 2.36 (t, 2H, $^3J_{\text{H-H}} = 7.3$ Hz, $\text{CH}_2\text{CH}_2\text{CH}_2\text{COCl}$); 1.98 (p, 2H, $^3J_{\text{H-H}} = 7.4$ Hz, $\text{CH}_2\text{CH}_2\text{COCl}$). $^{13}\text{C}\{^1\text{H}\}$ NMR (CDCl_3 , 75.5 MHz): 176.1 ($\text{NC}(\text{O})\text{CH}$); 172.1 ($\text{OC}(\text{O})\text{CH}_2$); 168.8 (COCl); 136.6 (CH_{vinyl}); 81.0 ($\text{CH}_{\text{vinyl}}\text{CH}(\text{OR})\text{CH}$); 60.9 ($\text{NCH}_2\text{CH}_2\text{O}$); 47.5 ($\text{CH}_{\text{vinyl}}\text{CH}(\text{OR})\text{CH}$); 37.8 ($\text{NCH}_2\text{CH}_2\text{O}$); 32.1 ($\text{CH}_2\text{CH}_2\text{CH}_2\text{COCl}$); 19.9 ($\text{CH}_2\text{CH}_2\text{CH}_2\text{COCl}$).

Procedure for thiophenol-maleimide conjugation reactions. Maleimide functionalized PLAs (0.003 mmol) were placed in a vial and sparged with N_2 . Solvent (1 mL) was added with stirring to dissolve the PLA. NEt_3 (2.6 μL , 0.03 mmol) and thiophenol (1.05 eq.) were added to the solution. The solution was stirred for the allotted time before the functionalized polymer was recovered by precipitation into petroleum ether (40-60 $^\circ\text{C}$) and dried under vacuum at 60 $^\circ\text{C}$ for 12 h.

5.3 Experimental details for chapter 3

General procedure for synthesis of α,ω -maleimide-functional poly(lactide)s. In a typical experiment, the chosen alcohol initiator (0.05 mmol) was added to an ampoule containing a solution of aluminum catalyst (**3**) (0.05 mmol) and *rac*-lactide (0.144 g, 1 mmol) in toluene (1.25 mL) under an atmosphere of nitrogen. The

sealed ampoule was then heated to 70 °C for 4 hours before being cooled in ice for 10 minutes. The ampoule was then taken into a glove box where upon the acid chloride (**2**) was added (0.5 mmol) before resealing the ampoule and heating at 70 °C for a further 120 hours. The resulting polymer was precipitated in cold petroleum ether, collected by filtration and dried *in vacuo* at 100 °C for 16 h to reveal a deprotected maleimide-functional polymer.

General procedure for polymer cyclisation. Maleimide functionalised PLAs (0.023 mmol) were placed in a vial and sparged with N₂. Degassed dichloromethane (10 mL) was added with stirring to dissolve the PLA and the solution was taken into a gas-tight 10 mL syringe. In a separate syringe, a degassed dichloromethane solution of 1,2-ethanedithiol (10 mL of a 2.25 mM solution, prepared by accurate measurement of dithiol using a micropipettor in a glove box) was prepared. Both solutions were injected (0.4 mL.h⁻¹) into a solution of NEt₃ (1.5 mL, 10.7 mmol) in dichloromethane (500 mL) saturated with Na₂S₂O₅ in a round bottom flask sealed with a septum. After complete addition, the solution was stirred for 3 h the functionalized polymer was recovered by filtration through a silica plug followed by removal of solvent under vacuum. The cyclic polymer was purified by precipitation from CH₂Cl₂ into petroleum ether (b.p. 40-60 °C) and was dried under vacuum at 60 °C for 12 h.

General procedure for dithiol bridge cleavage/in situ trapping reactions. PBu₃ (5.0 µL, 0.02 mmol) was added to a solution of polymer (0.003 mmol), NEt₃ (2.5 µL,

0.02 mmol) and *N*-methylmaleimide (0.5 mg, 0.005 mmol) or *N*-(1-pyrenyl)maleimide (1.5 mg, 0.005 mol) in dry, degassed THF (0.5 mL). After stirring for 3 h the polymer was precipitated into petroleum ether (40-60 °C) three times and was dried under vacuum at 60 °C for 12 h.

Synthesis of heat cleavable linker, 7. 9-Anthracenemethanol (0.5 g, 2.4 mmol, 1 eq.) and 2-(maleidmido)ethanol (0.34 g, 2.4 mmol, 1 eq.) were suspended in toluene. This solution was heated at reflux for 16 h and upon cooling white crystals of product form. Crystals collected by filtrations and no further purification required (0.61 g, 73 % yield). ¹H NMR (CDCl₃, 400.0 MHz): δ 7.56 (d, 1H, ³J_{H-H} = 7.6 Hz, ArH); 7.30 (d, 1H, ³J_{H-H} = 7.4 Hz, ArH); 7.25 (d, 1H, ³J_{H-H} = 7.4 Hz, ArH); 7.00-7.20 (m, 5H, ArH); 5.08 (m, 1H, ArCH₂OH); 4.88 (m, 1H, ArCH₂OH); 4.80 (s, 1H, ArCHAr); 3.32 (d, 1H, ³J_{H-H} = 7.2 Hz, NCOCHC); 3.24 (br s, 3H, CH₂CH₂OH and NCH₂); 3.02 (d, 2H, ³J_{H-H} = 7.4 Hz, CH₂CH₂OH); 2.88 (br s, 1H, CH₂OH); 1.17 (br s, 1H, CH₂CH₂OH).

General synthesis for diol initiators, 8, 9 and 10. i) Isopropylidene-2,2-bis(methoxy)propionic Acid was synthesised as reported in the literature.⁷ ii) Isopropylidene-2,2-bis(methoxy)propionic anhydride was then synthesised as reported in the literature.⁸ iii) Isopropylidene-2,2-bis(oxymethyl)propionic esters were then synthesised; alcohol (13 mmol, 1.0 eq.) and 4-(dimethylamino)pyridine (1.3g, 11mmol, 0.8 eq.) were dissolved in 40 mL of CH₂Cl₂ and 6 mL of pyridine was added. Isopropylidene-2,2-bis(methoxy)propionic anhydride (13g, 40mmol, 30

eq.) was added and the reaction mixture was stirred overnight at room temperature. 10 mL of a 1:1 mixture of pyridine and water was added and the mixture stirred for a further 16 h. 100 mL of CH_2Cl_2 was added and the organic layer was extracted with 1 M NaHSO_4 (3×60 mL), 10 % Na_2CO_3 solution (3×60 mL) and finally brine (1×60 mL). The organic phase was dried with MgSO_4 and reduced under vacuum to yield the desired ester (yield 60-80%). iv) Deprotection of the ester was carried out by stirring with DOWEX H^+ ion exchange resin, (~ 1.0 g) for 16 h, quantitatively yielding the expected diol. Purification was occasionally required by recrystallisation from an appropriate solvent.

Benzene bearing diol **8**: (83 % yield). ^1H NMR (CDCl_3 , 400.0 MHz): 7.2 - 7.35 (m, 5H, *Ar*); 4.56 (s, 2H, ArCH_2O); 3.80 (d, 2H, $^3J_{\text{H-H}} = 8.1$ Hz, CH_2OH); 3.24 (d, 2H, $^3J_{\text{H-H}} = 8.1$ Hz, CH_2OH); 2.48 (br s, *OH*); 1.12 (s, 3H, CH_3).

Alkene bearing diol, **9**: (78 % yield). ^1H NMR (CDCl_3 , 400.0 MHz): δ 5.85 (m, 1H, $\text{OCH}_2\text{CHCH}_2$); 5.21 (m, 2H, CHCH_2); 4.62 (d, 2H, $^3J_{\text{H-H}} = 4.1$ Hz, $\text{OCH}_2\text{CHCH}_2$); 3.88 (d, 2H, $^3J_{\text{H-H}} = 8.1$ Hz, CH_2OH); 3.16 (d, 2H, $^3J_{\text{H-H}} = 8.1$ Hz, CH_2OH); 2.70 (br s, *OH*); 1.02 (s, 3H, CH_3).

Alkyne bearing diol, **10**: (63 % yield). ^1H NMR (CDCl_3 , 400.0 MHz): δ 4.62 (d, 2H, $^3J_{\text{H-H}} = 3.2$ Hz, CH_2CCH); 3.68 (d, 2H, $^3J_{\text{H-H}} = 7.6$ Hz, CH_2OH); 3.52 (d, 2H, $^3J_{\text{H-H}} = 7.6$ Hz, CH_2OH); 2.76 (br s, *OH*); 2.44 (t, 1H, $^3J_{\text{H-H}} = 3.2$ Hz, CH_2CCH); 1.16 (s, 3H, CH_3).

General procedure for alkene/alkyne conjugations. Alkene/alkyne functionalised PLAs (~ 0.025 mmol) were placed in a vial and sparged with N_2 . Degassed CH_2Cl_2

(10 mL) was added with stirring to dissolve the PLA. To this a solution of dimethylphenylphosphine, DMPP (1 mL, 0.005 M), was added followed by the required thiol (10 eq. for alkene, 20 eq. for alkyne). The solution was stirred, sealed under N₂, for between 2 and 24 hours. The polymer was precipitated from the vial into petroleum ether (b.p. 40-60 °C), sometimes subsequent precipitations were required to remove excess thiol, and was dried under vacuum at 60 °C for 12 h.

Synthesis of maleimide-functional PLA via organic synthesis. 4-(2hydroxyethyl)-10-oxa-4-azatricyclo[5.2.1.0^{2,6}]dec-8-ene-3,5-dione, **5**, (0.36 g, 1.7 mmol), l-LA (5.00 g, 34.7 mmol) and 1-(3,5-bis(trifluoromethyl)phenyl)-3-cyclohexyl-thiourea (0.64 g, 1.7 mmol) were weighed into a vial. CH₂Cl₂ (50 mL) was added and the mixture stirred until the solution became clear. The polymerisation reaction was initiated by the addition of (-)-sparteine (0.19 mL, 0.9 mmol) and stirred for 30 mins. The reaction was quenched at >95 % conversion by precipitation in cold petroleum ether 40/60. Residual thiourea catalyst was removed by filtration through a silica plug, initially eluting with CH₂Cl₂/MeOH (100:1) then CH₂Cl₂/MeOH (100:5). The dried polymer was then stirred with 10 eq. of maleimide acid chloride, **6**, and 10 eq. NEt₃ in CH₂Cl₂ for 24 hours before precipitation in petroleum ether 40/60 resulted in the telechelic polymer in quantitative yield.

5.4 Experimental details for chapter 4

General procedure for one-pot spirocycles. Maleimide functionalised PLAs (0.023 mmol) were placed in a vial and sparged with N₂. Degassed dichloromethane (10 mL) was added with stirring to dissolve the PLA and the solution was taken into a gas-tight 10 mL syringe. In a separate syringe, a degassed dichloromethane solution of either trimethylolpropane tris-(3-mercaptopropionate) (10 mL of a 1.50 mM solution) or pentaerythritol tetrakis-(3-mercaptopropionate) (10 mL of a 1.13 mM solution) was prepared. Both solutions were injected (0.4 mL.h⁻¹) into a solution of NEt₃ (1.5 mL, 10.7 mmol) in dichloromethane (500 mL) saturated with Na₂S₂O₅ in a round bottom flask sealed with a septum. After complete addition, the solution was stirred for 3 h the functionalized polymer was recovered by filtration through a silica plug followed by removal of solvent under vacuum. The cyclic polymer was purified by precipitation from CH₂Cl₂ into petroleum ether (b.p. 40-60 °C) and was dried under vacuum at 60 °C for 12 h.

General procedure for alkene/alkyne conjugations with polymers. Alkene/alkyne functionalised PLAs (~0.025 mmol) were placed in a vial and sparged with N₂. Degassed CH₂Cl₂ (10 mL) was added with stirring to dissolve the PLA. To this a solution of dimethylphenylphosphine, DMPP (1 mL, 0.005 M), was added followed by the required thiol-bearing polymer (10 eq. for alkene, 20 eq. for alkyne where possible). The solution was stirred, sealed under N₂, for between 24 and 48 hours.

The polymer was precipitated from the vial into petroleum ether (b.p. 40-60 °C), sometimes subsequent precipitations were required to remove excess thiol, and was dried under vacuum at 60 °C for 12 h.

General procedure for the synthesis of thiol-bearing PEG. PEG polymers were dried using a toluene azeotrope (3 times) and overnight vacuum (2 times) before use. PEG polymers (~10 g) were suspended in 100 mL CH₂Cl₂ and stirred for 1 h to allow them to dissolve. A solution containing DCC (1.2 eq.), DMAP (0.2 eq.) and thiopropionic acid (2 eq.) in 50 mL of CH₂Cl₂ was added to the polymer and the resulting suspension stirred under N₂ for 24 h. A further solution containing DCC (1.2 eq.), DMAP (0.2 eq.) and thiopropionic acid (2 eq.) in 50 mL of CH₂Cl₂ was added and the solution stirred for another 24 h. The solution was filtered, and the solvent removed under vacuum. Recrystallisation from CH₂Cl₂ twice was required to yield the expected PEG thiol, yield ~35 %.

5.6 References

- ¹ Mantovani, G.; Lecolley, F.; Tao, L.; Haddleton, D. M.; Clerx, J.; Cornelissen, J.; Velonia, K., *J. Am. Chem. Soc.*, **2005**, *127*, 2966.
- ² a) Hormnirun, P.; Marshall, E. L.; Gibson, V. C.; White, A. J. P.; Williams, D. J., *J. Am. Chem. Soc.* **2004**, *126*, 2688. b) Hormnirun, P.; Marshall, E. L.; Gibson, V. C.; Pugh, R. I.; White, A. J. P., *Proc. Natl. Acad. Sci.*, **2006**, *103*, 15343.
- ³ Dove, A. P.; Pratt, R. C.; Lohmeijer, B. G. G.; Waymouth, R. M.; Hedrick, J. L., *J. Am. Chem. Soc.*, **2005**, *127*, 13798.
- ⁴ Nielen, M.W.F.; *Mass Spectrom. Rev.*, **1999**, *18*, 309.
- ⁵ Crisci, L.; Della Volpe, C.; Maglio, G.; Nese, G.; Palumbo, R.; Rachiero, G. P.; Vignola, M. C., *Macromol. Biosci.*, **2003**, *3*, 749.
- ⁶ Skey, J.; O'Reilly, R. K. *Chem. Commun.* **2008**, 4183.
- ⁷ Ihre, H; Holt, A; Frechet, J.M.J., *Macromolecules*, **1998**, *31*, 4061.
- ⁸ Gillies, E.R.; Frechet, J.M.J., *J. Am. Chem. Soc.*, **2002**, *124*, 14143.